UC Davis
UC Davis Electronic Theses and Dissertations

Title
Novel Autophagy Inhibitor for the Treatment of Pancreatic Cancer

Permalink
https://escholarship.org/uc/item/5057k76q

Author
Ramachandran, Mythili

Publication Date
2022

Peer reviewed|Thesis/dissertation

eScholarship.org Powered by the California Digital Library
University of California

Novel Autophagy Inhibitor for the Treatment of Pancreatic Cancer

By

MYTHILI RAMACHANDRAN

DISSERTATION

Submitted in partial satisfaction of the requirements for the degree of

DOCTOR OF PHILOSOPHY

in

Pharmacology and Toxicology

in the

OFFICE OF GRADUATE STUDIES

of the

UNIVERSITY OF CALIFORNIA

DAVIS

Approved:

Yuanpei Li, Chair

Kit Lam

Kermit Carraway

Committee in Charge

2022

Table of Contents

ABSTRACT

In Chapter 1, the introduction and literature review are provided for the basis of pancreatic cancer, its treatment options, and the current state of clinical trials. Autophagy as a process is discussed along with its relevance in cancer and particularly its role in pancreatic tumors is highlighted. Finally, cancer stem cells are reviewed with basic background, their relevance to pancreatic cancer and autophagy are again highlighted.

Chapter 2 discusses the current state of nanomaterials that can transform to adapt to each biological barrier present in tumors. Each stage of drug delivery is discussed to apply the relevant design ideas for new chemotherapeutics in the future.

In Chapter 3, the previous chapters are combined to illustrate the ability of the self-assembling nanoparticle, bisaminoquinolone derivative BAQ12O, that targets the cancer stem cell population in pancreatic tumor models.

Finally, a short conclusion summarizing the three chapters closes the dissertation.

CHAPTER 1

Introduction and Literature Review

Pancreatic Cancer

There is an urgent need for novel therapeutics to improve the treatment of pancreatic cancer as the five-year survival rate remains at a dismal 11.5 % according to the most recent Surveillance, Epidemiology, and End Results (SEER) data.[1] An estimated 60,430 new cases are expected this year in the United States and this cancer type is the third leading cause of cancer-related deaths.[1] Overall worldwide, the incidence of pancreatic cancer is rising and is the 13th most common cancer type and the 7th most common cause of cancer mortality.[2] Within the next decade, pancreatic cancer is projected to be the second leading cause of cancer associated mortality in the United States and Europe.[3] Most pancreatic cancer subtypes comprise of pancreatic ductal adenocarcinoma (PDAC) that arises from the exocrine pancreas.[2] This form is the most aggressive subtype and contributes to the very high mortality rate of the disease. The other underlying factor is that only 20% of patients are eligible for resectable surgery, making the drug regimens and clinical trials extremely vital to improve progression-free and overall survival.[4] While treating this cancer remains a challenge, there has been a lot of progress in recent years. The survival rate has improved due to improved perioperative care and more effective adjuvant therapies, reaching 30% for patients receiving a combination of a tumor resection and adjuvant therapy.[3]

Current Treatment Options

The current most effecitve treatment is surgical resection of the pancreas when possible (as evidenced by the highest survival rate). However, this option is not feasible for metastatic tumors. According to SEER statistics, approximately 52% of pancreatic

tumors upon diagnosis have already metastastized which contributes to the low survival rates in this disease. Even with surgical resection possible, adjuvant therapy was concurrently given to improve long term survival.[2] These adjuvant therapies include: FOLFIRNOX (fluoruracil, luecovorin, irinotecan, and oxaliplatin) and gemcitabine.[5] Gemcitabine is recommended in the cases with locally advanced or metastatic disease to minimize the toxicity associatied with the FOLFIRNOX treatment and serves as a reasonable first and second-line therapy.[5] In clinical trials currently gemcitabine is combined with numerous other potentially synergistic drugs. These list of drugs in combination with gemcitabine include: albumin-bound paclitaxel (Abraxane), cisplatin, capecitabine, and erlotinib.[5] Gemcitabine and erlotinib were approved even before the FOLFIRNOX regimen and MPACT (gemcitabine and albumin-bound paclitaxel) was approved for metastatic pancreatic cancer in 2013.[4] MPACT extended the median overall survival by 8.7 months.

Another category of drugs in clincal trials for pancreatic cancer is kinase inhibitors. Beginning with the original erlotinib, an oral epidermal growth factor receptor (EGFR) inhibitor, several recent papers have highlighted the benefit of the combining targeting the mitogen-activated protein kinase (MAPK) pathway.[6,7]

There has been significant improvement in pancreatic cancer treatment modalities compared to 20 years ago, especially in the field of surgical resection and post-operative care.[8] An unfortunate result of a study using data from 2006-2018 showed that only 4.9% of patients benefited from genome driven therapy for all types of metastatic or advanced stage cancers.[8] Indicating there is still a need for further understanding of the genetic drivers and expansion on drug biomarkers as well as novel

drug development methods need to be called upon to innovate new chemotherapeutics. More druggable targets and new pathways may hold some key insights.

Hydroxychloroquine in clinical trials

One of the drugs used in combination with the standard of care is the autophagy inhibitor, hydroxychloroquine (HCQ) as a systemic approach for treatment. HCQ is a known drug that has been approved by the FDA for multiple indications including rheumatoid arthritis and malaria and is derived from the parent drug chloroquine (CQ).[9] HCQ is more potent than CQ and is used more frequently in clinical trials. Initial safety studies of HCQ showed promising results with 800-1200 mg/day causing no serious adverse events in this trial period (NCT01273805). However, HCQ does induce retinopathy after prolonged use with a rate of 7.5% from 5 years of use and rising to 20% after 20 years of treatment.[10] In addition, the monotherapy showed insufficient autophagy inhibition at this dose.[11] HCQ is more commonly given as a combination treatment in other clinical trials including with gemcitabine, nab-paclitaxel, cisplatin and many of the other therapies listed previously for pancreatic cancer. The most recent study that has led to a Phase I/II clinical trial is the combination of tramentinib and hydroxychloroquine. Tramentinib is a MEK1/2 inhibitor which showed a promising 50% decrease in tumor (imaged using CT) when combined with HCQ therapy. This patient had been unrepsonsive to the standard FOLFIRINOX, and gemcitabine combinations with capecitabine as well as later nab-paclitaxel (abraxane) and cisplatin.[6] Based on this success and promising preclinical data, the THREAD study is ongoing and estimated to be completed by 2025. So far there is still work on autophagy inhibitors both in

evaluating biomarkers and developing more potent inhibitors. Unfortunately, there are no significant survival improvements in clinical trials in part due to these barriers.[12]

Autophagy

Background

Autophagy is a process of lysosomal degradation that allows for recycling of cellular components resulting in an adaptive metabolic reprogramming in response to stress. The discovery of this process in yeast earned Dr. Yoshinori Ohsumi the Nobel Laureate in Physiology and Medicine in 2016.[13] His work was based on the original findings of Christian de Duve who coined the term 'lysosome' in 1963 and subsequently earned the Nobel Prize in 1974 along with Albert Claude and George Palade.[14] The process is considered a "double-edged sword" as many tumors use this process during their initiation to prevent malignant growth however as the tumor is established and progressing, autophagy is used to fuel the tumor growth.[15] Autophagy is comprised of three main pathways which are divided into macroautophagy, microautophagy, and chaperone-mediated autophagy. Microautophagy involves directly degrading cargo into the lysosome through invaginations in the lysosomal membrane.[16] Chaperone mediated autophagy involves selective degradation of cargo using heat shock complex 70 (HSC70 or HSPA8) which binds to cargo and interacts with lysosome membrane protein 2A (LAMP2A) to degrade cargo directly in the lysosome.[17] Macroautophagy accounts for most autophagy in mammalian cells and will be hereafter synonymous with autophagy.

Autophagy is divided into four distinct steps which are initiation, nucleation, maturation, and degradation.[15] Initiation is the start of the phagophore formation and is begun by mechanistic target of rapamycin complex 1 (mTORC1) and Unc-51-like kinase (ULK1) complexed with Autophagy related gene 13 (ATG13). AMP-activated protein kinase (AMPK) and mTORC1 regulate the initiation start.[15] Nucleation begins with the phosphorylation of ULK1 complex which activates the second complex Beclin-1-VPS34 comprised of vacuolar protein sorting-associated protein (VPS), a phosphatidylinositol 3-kinase (PI3K), Beclin1, ATG14L, and other proteins.[15] At the point, the initiation and nucleation are beginning the phagophore formation and using the membrane from several possible subcellular candidates including the mitochondria, plasma membrane, or the endoplasmic reticulum.[15] Maturation involves the formation of the autophagosome with a myriad of ATG proteins. Among which the most ubiquitously used marker involves ATG7 and ATG3 conjugating to ATG8 or microtubule-associated protein light chain 3 (LC3) to the lipid phosphatidylethanolamine (PE).[18] ATG5-ATG12-ATG16L1 complex formed during this phase attaches to the PI3 phosphate from the VPS34 complex in the nucleation phase. LC3 is cleaved by ATG4 later and LC3-I, the soluble form is conjugated to PE.[15] After PE is conjugated, LC3-I is known as LC3-II and this ratio can be used to measure the amount of autophagosomes that have formed.[15,18,19] The other commonly used markers involve cargo receptors that can recognize LC3-I and allow the autophagic cargo to reach the autophagosome. These receptors are most commonly sequestosome-1 (SQSTM1/p62) or BRCA1 gene 1 protein (NBR1).[20] Maturation continues with the autophagosomes containing the cargo fusing to the lysosome for preparing for the degradation step. The autophagosome uses

microtubules to the lysosomes and are tethered to the lysosome with the help of syntaxin17 and a complex known as the homotypic fusion and protein sorting complex (HOPS).[21] Finally in degradation, the autophagosome and lysosome are fused into the autolysosome and lysosomal hydrolases degrade the internalized macromolecules. These degraded components are recycled to the cell by nutrient transporters which can then provide precursors to promote cell growth.

Autophagy in Cancer

In the context of cancer, autophagy plays a still contested role. It is thought to be a double-edged sword in the context of tumor treatment in that induction of autophagy prevents tumor formation in many cancer subtypes however autophagy is used to maintain the tumor growth and is hijacked to provide nutrients and as a method to deal with increased stress at a later stage of growth. There is a heterogeneity of autophagy dependence not only between various cancer types but between tumors in the same subtype. In autophagy dependent cancer types there is synergy between autophagy inhibitors and other drugs however in autophagy-independent tumors antagonism could result.[22] Many have shown that induction of autophagy is an antitumor mechanism through the use of genetic mouse models in which the Beclin 1 gene, *Becn 1* was knocked out resulting in spontaneous tumor formation in cancer models which have *Becn 1* deletions such as breast, ovarian and prostate cancers.[23] Beclin 1 was later shown to have additional oncogenic effects including affecting key genes like BRCA1[24] and p53[25] which are not associated with deletion of other autophagy genes. Another case for promoting autophagy induction is from the resulting increase in the known

autophagy marker, p62/SQSTM1. This cargo adaptor also has a dual role in tumor progression and suppression.[15] p62 was upregulated in the tumor cells and downregulated in the surrounding cancer associated fibroblast (CAF) that provides the nutrients for tumor progression.[26] There was also an increase in invasiveness of prostate tumor cells when p62 was inactivated in neighboring adipocytes.[27]

In the opposing side, autophagy inhibition is a viable strategy as autophagy is used as a prosurvival mechanism in the case of many cancers particularly with the genotypes containing mutants of rat sarcoma virus (RAS) , murine sarcoma viral oncogene homolog B (BRAF), tumor protein 53 (TP53), and liver kinase B1 (LKB1).[15] Many of these genotypes induce autophagy through various methods including DNA damage, ER stress, and general nutrient deficiencies.[15] In these cases, autophagy dependence is a key characteristic of the tumor and thus are more conducive to autophagy inhibition as a viable treatment method.

Current Autophagy Targeting Drugs

HCQ and CQ as previously discussed are the main drugs used in clinical trials to promote autophagy inhibition in various cancers. Along these lines, several more potent derivatives and autophagy inhibitors have been developed including the dimeric chloroquine compound, Lys05, formulated by the Amaravadi group. This group has also developed quinacrine derivatives DQ661 and DC661.[28,29] All of these drugs are currently in the preclinical stage and the current most potent CQ derivatives. Our lab has developed small molecule drugs based on the dimeric CQ structure as well that has the additional function of being able to self-assemble into nanoparticles allowing for the

benefits of both lysosomal targeting and nanoparticle delivery.[30] Late stage inhibitors such as these mentioned are potentially a more viable method of autophagy inhibition as the later stage allows for the benefit of increasing autophagosome production which in itself is toxic to the cell and targeting the lysosome allows for inhibition of other related scavenging or survival pathways. Other classes of earlier stage autophagy inhibitors include molecules that inhibit ULK1, VPS34, ATG4B, and phosphatidylinositol-3-phosphate 5-kinase type III (PIKFYVE).[15]

Autophagy in Pancreatic Cancer

In PDAC, it has been previously shown there is a high level of autophagic flux and that both pharmacological and genetic inhibition of autophagy prevents tumor growth.[31] The first study linking autophagy in PDAC was in 1981. In this study, hamsters were exposed to the carcinogen N-nitroso-bis(2-hydroxypropyl)amine (BHP) inducing cancer from the acinar region.[32] When monitoring the carcinogenesis of the acinar cells, autophagy was observed in the zymogen granules and granular ER.[32] Later, it was shown that neoplastic PDAC as higher compared to normal tissue when comparing rat premalignant and malignant cells after induction with carcinogen azaserine.[33] There is also a high level of inflammation in PDAC which is required for tumorigenesis as well as being a modulator of autophagy.[12] Autophagy is not only limited to the PDAC cells themselves, but the tumor microenvironment contains other cells that rely on autophagy to sustain the tumor. For example, the pancreatic CAFs which is the pancreatic stellate cell (PSC) are thought to use autophagy to supply nutrients to the tumor.[12] PSCs produce growth factors that can perform metabolic reprogramming of the tumor cells

and subsequently the tumor cells are also secreting exocrine signals to make the PSCs more malignant, as well.[34] The tumor microenvironment includes an immune component which autophagy and chloroquine have been used to modulate. This topic is very extensive and beyond the scope of the information presented here but further information can be found in the following reviews.[35,36] Overall, the context of autophagy is highly dependent on the stage of the tumor, the tumor microenvironment, and the genetic background of the tumor. Despite these conditions, it is evident that autophagy plays a major role in pancreatic cancer and its progression, and more studies will help elucidate its contribution.

Cancer Stem Cells

Background

Even within the same cancer subtype, the tumor contains a heterogeneous population of cells. Among these types of cells, there exists a small percentage that has the capability to propagate the tumor. This small population is known as cancer stem cells. Cancer stem cells have the properties of high tumorigenicity and metastatic potential, self-renewal, and the ability to differentiate into heterogeneous cells. Cancer stem cells were first discovered in acute myeloid leukemia[37,38] and have been confirmed in many other tumor subtypes later including breast cancer.[39] Pancreatic cancer stem cells were first identified in 2007 by the Simeone group who isolated $CD24^+$, $CD44^+$, $CD326^+$ triple positive cells from patient derived xenograft pancreatic tumors grown in immunocompromised mice.[40] These markers were first used in breast cancer stem cells

with the $CD326^{+}$, $CD44^{high}$, $CD24^{low}$ population showing the highest tumorigenic potential and stem cell regenerative properties. The triple positive population in pancreatic cancer showed similar qualities with an injection of just 100 cells being able to reform the histologically similar tumor when injected into NOD/SCID (Non-obese diabetic/severe-combined immunodeficient) mice.[40] This population was also 100-fold more tumorigenic than the population with the negative markers.[40] Subsequently, other stem cell populations have been found by other groups including $CD133^{+}$ population by Hermann et. al. They identified $CD133^{+}$ and $CXCR4^{+}$ as the particular subtype in the CD133 positive cells that determines metastatic potential while the triple positive population $CD24^{+}$, $CD44^{+}$, $CD326^{+}$ shown by Li et.al focused on tumor initiation and growth.[41] After these initial studies, several other markers have been identified including the extensive list of CD139, CD166, Aldehyde dehydrogenase 1 (Aldh1), leucine rich repeat containing G protein coupled receptor 5 (Lgr5), B-cell specific Moloney murine leukemia virus integration site 1 (Bmi1), and olfactomedin 4 (Olfm4). The combination of several markers increases the chance of purely isolated CSCs.[42]

One property of CSCs is that they are generally resistant to normal chemotherapy regimens. Most therapeutics target the actively proliferating cells and CSCs are quiescent allowing for tumor recurrence after treatment. With such high tumorigenic potential, allowing a few CSCs to survive would allow for eventual tumor regrowth and a potentially more resistant tumor that has more stem-like properties. Thus, targeting this population of cells is a viable strategy for improving the treatment options for many cancer types and particularly pancreatic cancer with its low survival rate.

Two main CSC models of development have been postulated to explain tumor origin and heterogeneity-the stochastic and hierarchical models. In the stochastic model all cancer cells are able to promote new tumor growth by conversion to a CSC phenotype especially in response to specific stimuli.[43] In the hierarchical, a set population of CSC exists which accounts for the tumor diversity through a combination of differentiated and quiescent tumor cells. Both models are likely responsible for a given tumor.[43]

Current CSC Targeting drugs

So far there is no specific CSC targeting drug approved by the FDA. Most drugs are still in the preclinical phase. The farthest drug in the approval process is currently Napabucasin (Napa), an oral STAT3 inhibitor which shows efficacy in colorectal and pancreatic cancer.[44] Signal transducer and activator of transcription 3 (STAT3) is overexpressed in many other cancer types including: breast, ovarian, hepatic and others.[44] STAT3 is a key regulator in stem cell maintenance with effects on CSC genes including c-Myc, NANOG, and β-catenin.[45,46] Napa similarly has been shown to affect stem cell maintenance including c-Myc, NANOG, β-catenin, Sox2 (sex-determining region Y-box protein 2).[46,47] In addition to stemness genes, Napa also inhibited stem cell function including tumorsphere formation as well as spleen and liver metastasis in vivo in mouse colon cancer models.[48] In spite of the success of the preclinical studies, Napa has been pulled out of many Phase III clinical trials due to toxicity or futility. Most recently CanStem111P (NCT02993731) trial combining Napa, Abraxane and Gemcitabine was discontinued to futility.[49] Additionally, the Phase III study of Napa and

paclitaxel for advanced gastric and gastroesophageal junction adenocarcinoma failed to reach the primary endpoint of overall survival (NCT02178956).[50] In combination with pembrolizumab (anti-PD-1 antibody) in metastatic colorectal cancer, there was acceptable toxicity and some antitumor activity, but the primary endpoint was also not met.[51] In short, there is still room for improvement for the state of CSC targeting drugs and particularly in pancreatic cancer it is a viable strategy for this aggressive tumor type.

CSC and Autophagy Dysregulation

Autophagy is a major process used by CSCs for various functions including plasticity, differentiation, migration/invasion and is involved in CSC resistance to normal chemotherapy.[8,43,52] The exact role of autophagy is still being investigated as the reality is that final answer is context dependent. However, there is extensive evidence that autophagy is a key regulator in many CSC characteristics. First in pluripotency, various pluripotency genes are regulated by autophagic flux. In a recent study by Sharif et.al, there was a marked decrease in stemness markers and increase in differentiation upon autophagy inhibition. Interestingly, the same effect was seen with autophagy induction with an increase of pluripotent genes so the autophagic homeostasis was the most important factor in human teratocarcinoma (cancer of embryonic stem cells) CSCs.[53] In addition, the tumor microenvironment which requires autophagy to promote survival in the hypoxic and acidic conditions. Autophagy is especially needed for providing nutrients in these harsh conditions.[52] Pancreatic cancer stem cells were shown to modulate HIF-1α to convert non-CSCs to CSCs mediated through autophagy

induction.[54] There was also a related study showing that pancreatic CSCs, hypoxic and autophagy markers were colocalized with immunohistochemistry of PDAC patient tissue.[55] Similarly, hepatocellular carcinoma CSCs showed response to autophagy inhibition as treatment because they relied on the same mechanism of autophagy induction in response to a hypoxic environment.[56] Mitophagy is another autophagy related process involving specific recycling of CSC mitochondria which is thought to be an important pathway in regulating cancer stemness.[43,57] Mitochondria are involved in stemness as plasticity often has significant differences in mitochondrial function, composition, and function.[58] Mitochondria are involved in the key aspect of CSC metabolic reprogramming. In general, due to the Warburg effect, tumor cells tend to rely on glycolysis for their excess nutrient requirements however CSCs have a higher reliance on oxidative phosphorylation (OXPHOS) and many different types of tumors including CSCs in pancreatic, glioblastoma, breast cancer, and lung cancer side population cells show an OXPHOS phenotype.[43] CSCs utilize OXPHOS as well as a higher antioxidant rate and as a result, mitophagy to regulate their stemness and tumorigenic potential.[43,59] With these methods reactive oxygen species (ROS) can be properly regulated and promote CSC survival. In summary, targeting autophagy/mitophagy provides a promising approach to target CSCs and stemness of tumors. Chloroquine has already been used to treat pancreatic CSCs in a study by the Heeschen group. However, it promoted death through the CXCL12/CXCR4 and Hedgehog pathways rather than through autophagy inhibition.[60] Chloroquine is a significantly less potent autophagy inhibitor and thus the main mechanism did not

involve autophagy inhibition in this scenario. More potent autophagy inhibitors could provide another unique method to target more CSCs and novel pathways.

Reference:

1. Siegel RL, Miller KD, Fuchs HE, Jemal A. Cancer Statistics, 2021. CA Cancer J Clin. 2021;71(1):7-33.
2. Torphy RJ, Fujiwara Y, Schulick RD. Pancreatic cancer treatment: better, but a long way to go. Surg Today. 2020;50(10):1117-25.
3. Neoptolemos JP, Kleeff J, Michl P, Costello E, Greenhalf W, Palmer DH. Therapeutic developments in pancreatic cancer: current and future perspectives. Nat Rev Gastroenterol Hepatol. 2018;15(6):333-48.
4. Zhang Z, Song J, Xie C, Pan J, Lu W, Liu M. Pancreatic Cancer: Recent Progress of Drugs in Clinical Trials. AAPS J. 2021;23(2):29.
5. Tempero MA, Malafa MP, Al-Hawary M, Behrman SW, Benson AB, Cardin DB, et al. Pancreatic Adenocarcinoma, Version 2.2021, NCCN Clinical Practice Guidelines in Oncology. J Natl Compr Canc Netw. 2021;19(4):439-57.
6. Kinsey CG, Camolotto SA, Boespflug AM, Guillen KP, Foth M, Truong A, et al. Protective autophagy elicited by RAF→MEK→ERK inhibition suggests a treatment strategy for RAS-driven cancers. Nat Med. 2019;25(4):620-7.
7. Bryant KL, Stalnecker CA, Zeitouni D, Klomp JE, Peng S, Tikunov AP, et al. Combination of ERK and autophagy inhibition as a treatment approach for pancreatic cancer. Nat Med. 2019;25(4):628-40.
8. Leonhardt CS, Traub B, Hackert T, Klaiber U, Strobel O, Büchler MW, et al. Adjuvant and neoadjuvant chemotherapy in pancreatic ductal adenocarcinoma. Journal of Pancreatology. 2020;3(1):1-11.

9. Ferreira PMP, Sousa RWR, Ferreira JRO, Militão GCG, Bezerra DP. Chloroquine and hydroxychloroquine in antitumor therapies based on autophagy-related mechanisms. Pharmacol Res. 2021;168:105582.
10. Yusuf IH, Sharma S, Luqmani R, Downes SM. Hydroxychloroquine retinopathy. Eye. 2017;31(6):828-45.
11. Wolpin BM, Rubinson DA, Wang X, Chan JA, Cleary JM, Enzinger PC, et al. Phase II and Pharmacodynamic Study of Autophagy Inhibition Using Hydroxychloroquine in Patients With Metastatic Pancreatic Adenocarcinoma. The Oncologist. 2014;19(6):637-8.
12. Görgülü K, Diakopoulos KN, Kaya-Aksoy E, Ciecielski KJ, Ai J, Lesina M, et al. The Role of Autophagy in Pancreatic Cancer: From Bench to the Dark Bedside. Cells. 2020;9(4).
13. Levine B, Klionsky DJ. Autophagy wins the 2016 Nobel Prize in Physiology or Medicine: breakthroughs in baker's yeast fuel advances in biomedical research. Proc Natl Acad Sci USA 2017;114:201–5.
14. Li X, He S, Ma B. Autophagy and autophagy-related proteins in cancer. Mol Cancer. 2020;19(1):12.
15. Amaravadi RK, Kimmelman AC, Debnath J. Targeting Autophagy in Cancer: Recent Advances and Future Directions. Cancer Discov. 2019;9(9):1167-81.
16. Oku M, Sakai Y. Three Distinct Types of Microautophagy Based on Membrane Dynamics and Molecular Machineries. Bioessays. 2018;40(6):e1800008.
17. Kaushik S, Cuervo AM. The coming of age of chaperone-mediated autophagy. Nat Rev Mol Cell Biol. 2018;19(6):365-81.

18. Walczak M, Martens S. Dissecting the role of the Atg12-Atg5-Atg16 complex during autophagosome formation. Autophagy. 2013;9:424–425
19. Levy JMM, Towers CG, Thorburn A. Targeting autophagy in cancer. Nat Rev Cancer. 2017;17(9):528-42.
20. Lamark T, Kirkin V, Dikic I, Johansen T. NBR1 and p62 as cargo receptors for selective autophagy of ubiquitinated targets. Cell Cycle. 2009;8:1986–1990.
21. Takats S, Pircs K, Nagy P, et al. Interaction of the HOPS complex with Syntaxin 17 mediates autophagosome clearance in Drosophila. Mol Biol Cell. 2014;25:1338–1354.
22. Chmurska A, Matczak K, Marczak A. Two Faces of Autophagy in the Struggle against Cancer. International Journal of Molecular Sciences. 2021;22(6):2981.
23. Qu X, Yu J, Bhagat G, Furuya N, Hibshoosh H, Troxel A, et al. Promotion of tumorigenesis by heterozygous disruption of the beclin 1 autophagy gene. J Clin Invest 2003;112:1809–20.
24. Laddha SV, Ganesan S, Chan CS, White E. Mutational landscape of the essential autophagy gene BECN1 in human cancers. Mol Cancer Res 2014;12:485–90
25. Beer LA, Wang H, Tang HY, Cao Z, Chang-Wong T, Tanyi JL, et al. Identification of multiple novel protein biomarkers shed by human serous ovarian tumors into the blood of immunocompromised mice and verified in patient sera. PLoS One 2013;8:e60129.
26. Valencia T, Kim JY, Abu-Baker S, Moscat-Pardos J, Ahn CS, Reina-Campos M, et al. Metabolic reprogramming of stromal fibroblasts through p62-mTORC1 signaling promotes inflammation and tumorigenesis. Cancer Cell 2014;26:121–35.

27. Huang J, Duran A, Reina-Campos M, Valencia T, Castilla EA, Muller TD, et al. Adipocyte p62/SQSTM1 suppresses tumorigenesis through opposite regulations of metabolism in adipose tissue and tumor. Cancer Cell 2018;33:770–84
28. McAfee Q, Zhang Z, Samanta A, Levi SM, Ma X-H, Piao S, et al. Autophagy inhibitor Lys05 has single-agent antitumor activity and reproduces the phenotype of a genetic autophagy deficiency. Proceedings of the National Academy of Sciences of the United States of America. 2012;109(21):8253-8.
29. Rebecca VW, Nicastri MC, Fennelly C, Chude CI, Barber-Rotenberg JS, Ronghe A, et al. PPT1 Promotes Tumor Growth and Is the Molecular Target of Chloroquine Derivatives in Cancer. Cancer Discovery. 2019;9(2):220-9.
30. Ma Z, Li J, Lin K, Ramachandran M, Zhang D, Showalter M, et al. Pharmacophore hybridisation and nanoscale assembly to discover self-delivering lysosomotropic new-chemical entities for cancer therapy. Nat Commun. 2020;11(1):4615.
31. Yang S, Wang X, Contino G, Liesa M, Sahin E, Ying H, et al. Pancreatic cancers require autophagy for tumor growth. Genes & development. 2011;25(7):717-29.
32. Flaks B, Moore MA, Flaks A. Ultrastructural analysis of pancreatic carcinogenesis. IV. Pseudoductular transformation of acini in the hamster pancreas during N-nitroso-bis(2-hydroxypropyl)amine carcinogenesis. Carcinogenesis. 1981;2(12):1241-53.
33. Réz G, Tóth S, Pálfia Z. Cellular autophagic capacity is highly increased in azaserine-induced premalignant atypical acinar nodule cells. Carcinogenesis. 1999;20(10):1893-8.
34. Halbrook C.J., Lyssiotis C.A. Employing Metabolism to Improve the Diagnosis and

Treatment of Pancreatic Cancer. Cancer Cell. 2017;31:5–19.

35. Jiang G-M, Tan Y, Wang H, Peng L, Chen H-T, Meng X-J, et al. The relationship between autophagy and the immune system and its applications for tumor immunotherapy. Molecular Cancer. 2019;18(1).
36. Luo X, Qiu Y, Dinesh P, Gong W, Jiang L, Feng X, et al. The functions of autophagy at the tumour-immune interface. Journal of Cellular and Molecular Medicine. 2021;25(5):2333-41.
37. Bonnet D, Dick JE. Human acute myeloid leukemia is organized as a hierarchy that originates from a primitive hematopoietic cell. Nat Med 1997;3:730–7.
38. Lapidot T, Sirard C, Vormoor J, et al. A cell initiating human acute myeloid leukemia after transplantation into SCID mice. Nature 1994;17:645–8.
39. Al-Hajj M, Wicha MS, Benito-Hernandez A, Morrison SJ, Clarke MF. Prospective identification of tumorigenic breast cancer cells. Proc Natl Acad Sci U S A 2003;100: 3983–8.
40. Li C, Heidt DG, Dalerba P, Burant CF, Zhang L, Adsay V, et al. Identification of Pancreatic Cancer Stem Cells. Cancer Research. 2007;67(3):1030-7.
41. Hermann PC, Huber SL, Herrler T, Aicher A, Ellwart JW, Guba M, et al. Distinct Populations of Cancer Stem Cells Determine Tumor Growth and Metastatic Activity in Human Pancreatic Cancer. Cell Stem Cell. 2007;1(3):313-23.
42. Li Y, Kong D, Ahmad A, Bao B, Sarkar FH. Pancreatic cancer stem cells: emerging target for designing novel therapy. Cancer Lett. 2013;338(1):94-100.

43. Nazio F, Bordi M, Cianfanelli V, Locatelli F, Cecconi F. Autophagy and cancer stem cells: molecular mechanisms and therapeutic applications. Cell Death & Differentiation. 2019;26(4):690-702.
44. Hubbard JM, Grothey A. Napabucasin: An Update on the First-in-Class Cancer Stemness Inhibitor. Drugs. 2017;77(10):1091-103.
45. Zhang F, Li C, Halfter H, Liu J. Delineating an oncostatin M-activated STAT3 signaling pathway that coordinates the expression of genes involved in cell cycle regulation and extra- cellular matrix deposition of MCF-7 cells. Oncogene. 2003;22:894–905.
46. Lee TK, Castilho A, Cheung VC, et al. CD24(+) liver tumor- initiating cells drive self-renewal and tumor initiation through STAT3-mediated NANOG regulation. Cell Stem Cell. 2011;9(1):50–63.
47. Bromberg J, Darnell JE Jr. The role of STATs in transcriptional control and their impact on cellular function. Oncogene. 2000;19(21):2468–73.
48. Li, Y., et al., Pancreatic cancer stem cells: emerging target for designing novel therapy. Cancer Lett, 2013. 338(1): p. 94-100.
49. Sonbol MB, Ahn DH, Goldstein D, Okusaka T, Tabernero J, Macarulla T, et al. CanStem111P trial: a Phase III study of napabucasin plus nab-paclitaxel with gemcitabine. Future Oncol 2019;15:1295-302biting cancer stemness. Proc Natl Acad Sci USA. 2015;112(6):1839–44.
50. Sonbol MB, Bekaii-Saab T. A clinical trial protocol paper discussing the BRIGHTER study. Future Oncol 2018;14:901-6

51. Kawazoe A, Kuboki Y, Shinozaki E, Hara H, Nishina T, Komatsu Y, et al. Multicenter Phase I/II Trial of Napabucasin and Pembrolizumab in Patients with Metastatic Colorectal Cancer (EPOC1503/SCOOP Trial). Clin Cancer Res 2020;26:5887-94
52. Yang X, Ye F, Jing Y, Wei L. Autophagy and Tumour Stem Cells. Adv Exp Med Biol. 2020;1207:301-13.
53. Sharif T, Martell E, Dai C, Kennedy BE, Murphy P, Clements DR, et al. Autophagic homeostasis is required for the pluripotency of cancer stem cells. Autophagy. 2017;13(2):264-84.
54. Zhu H, Wang D, Liu Y, Su Z, Zhang L, Chen F, et al. Role of the Hypoxia-inducible factor-1 alpha induced autophagy in the conversion of non-stem pancreatic cancer cells into CD133+ pancreatic cancer stem-like cells. Cancer Cell International. 2013;13(1):119.
55. Rausch V, Liu L, Apel A, Rettig T, Gladkich J, Labsch S, et al. Autophagy mediates survival of pancreatic tumour-initiating cells in a hypoxic microenvironment. The Journal of Pathology. 2012;227(3):325-35.
56. Song YJ, Zhang SS, Guo XL, Sun K, Han ZP, Li R, et al. Autophagy contributes to the survival of CD133+ liver cancer stem cells in the hypoxic and nutrient-deprived tumor microenvironment. Cancer Lett. 2013;339(1):70-81.
57. Wang X, Lee J, Xie C. Autophagy Regulation on Cancer Stem Cell Maintenance, Metastasis, and Therapy Resistance. Cancers (Basel). 2022;14(2).
58. Vazquez-Martin A, Van den Haute C, Cufí S, Corominas-Faja B, Cuyàs E, Lopez-Bonet E, et al. Mitophagy-driven mitochondrial rejuvenation regulates stem cell fate.

Aging (Albany NY). 2016;8(7):1330-52.

59. Snyder V, Reed-Newman TC, Arnold L, Thomas SM, Anant S. Cancer stem cell metabolism and potential therapeutic targets. Front Oncol. 2018;8:1–9.

60. Balic A, Sørensen MD, Trabulo SM, Sainz B, Cioffi M, Vieira CR, et al. Chloroquine Targets Pancreatic Cancer Stem Cells via Inhibition of CXCR4 and Hedgehog Signaling. Molecular Cancer Therapeutics. 2014;13(7):1758-71.

CHAPTER 2

Transformable Nanoparticles to Bypass Biological Barriers in Cancer Treatment

Abstract

Nanomedicine based drug delivery platforms provide an interesting avenue to explore for the future of cancer treatment. Here we discuss the barriers for drug delivery in cancer therapeutics and how nanomaterials have been designed to bypass these blockades through stimuli responsive transformation in the most recent update. Nanomaterials that consider the challenges of each step provide a promising solution for new cancer therapeutics.

Introduction

Cancer remains one of the leading causes of mortality in the world despite significant advances in medicine and emerging treatment options.[1] Current treatment methods include surgery, radiotherapy and chemotherapy. Chemotherapy is the current preferred treatment when the tumor is not resectable and for preventing metastasis. Many chemotherapeutic agents are small molecules that have widespread systemic toxicity from nonspecific interactions affecting healthy tissue, poor solubility and narrow therapeutic indexes. To address these challenges, the use of nanomaterials is a method to improve existing chemotherapeutics with enhanced drug delivery to the tumor site along with imaging and detecting disease progression using a theranostic approach. Nanomedicine, referring to drugs approximately in the 1-100 nm range have the ability to be more easily functionalized, including their size, charge and surface properties, making them promising new generation chemotherapeutics.

Strategic design of nanoparticles to overcome each barrier for effective cancer treatment is necessary to improve current treatment options. The biological barriers include initial circulation in blood in which the shear stress and interactions with blood proteins must be avoided. Next, targeting the tumor and avoiding healthy cells, along with extravasation of the blood vessel and reach the tumor tissue. The drug must then penetrate dense extracellular matrix formed around tumors and enter the cell. Finally, the drug must remain in the cell long enough to exert an effect (Figure 1). Nanomedicine provides many advantages to address these barriers.[2] Initially, the enhanced permeability and retention (EPR) effect was the original explanation used to describe the superior capabilities of nanoparticles in tumor therapies. Nanoparticles preferentially enter the tumor due to the leakier vasculature surrounding the tumor and are retained by the lower lymphatic clearance.[2] Recent reports have suggested additional mechanisms to explain nanoparticle uptake especially in desmoplastic tumors, namely transcytosis.[3,4] Transcytosis involves the use of a receptor mediated process to move the nanoparticle across the cell membrane. In the case of nab-paclitaxel, albumin bound paclitaxel facilitates transcytosis in the dense stroma of pancreatic cancer.[5,6]

Additionally, the size paradox that exists for nanoparticles needs to be accounted for when creating an optimal therapeutic agent. Smaller nanoparticles can easily traverse the bloodstream and be internalized by the tumor quickly. However, a smaller size results in quick clearance by the reticuloendothelial system (RES) and kidney.[2] Larger nanoparticles avoid premature clearance and are retained for longer durations but cannot penetrate the tumor as efficiently.[7] To overcome this paradox,

transformability is a key method that could combine the advantages of both small and large nanoparticles to promote transcytosis in addition to the inherent EPR effect that makes nanoparticles attractive therapeutics.

Every transformable attribute should be unique and specific to a certain step in the cascade of drug delivery. The cascade has recently been coined CAPIR for circulation, accumulation, penetration, internalization, and release of the drug.[7] The variation in tumor and patient type makes it very difficult to synthesize a nanoparticle that includes all the factors in the tumor uptake cascade without some form of stimuli responsive transformation at critical steps, as many favorable properties at one stage are adverse in another. Thus, the strategy of transformable nanoparticles holds promise for the next advances in chemotherapeutics to tackle the barriers in cancer drug delivery.

Blood Circulation

Nanoparticle circulation is a pharmacokinetic barrier faced by all types of therapeutics.[8] The shape and size of the nanoparticles largely dictate their chemical properties and their interactions in blood. Every nanoparticle and drug must have some degree of hydrophilicity to traverse the bloodstream. Nanoparticles also bind to plasma proteins and form a corona which can alter the size and properties of the drug.[8] One such property is surface charge. Both positively charged nanoparticles are cleared very quickly by the mononuclear phagocytic (MPS) system as well as very highly negative charged zeta potentials.[7,8]

The circulation time of the nanoparticle must be adjusted for each tumor type and

case. For example, extended circulation time is not necessarily a favorable factor if the nanoparticle can't penetrate the tumor with poor biodistribution. In solid tumors, an excessively long plasma half-life could increase the potential of toxicity.[8] However, in leukemia and other blood tumors as well in delivering chemotherapies, this serves as an advantage to have a longer circulation.[9,10] To modulate the circulation time, the surface charge of the nanoparticle can be adjusted as previously mentioned. Several modification ligands and functional groups have been used for this purpose. Amines and imines are commonly functional groups as their pK_as are near physiological conditions and they subsequently are protonated in more acidic environments. Zwitterionic ligands such as carboxy- or sulfobetaines have both positive and negatively charged groups which can be used to modify charge.[11]

Stability is a critical issue at this stage to prevent premature release of the encapsulated drug before reaching the tumor site. Our group and others have utilized a boronate ester cross-linkage between boronic acid and diols to improve nanoparticle stability until exposed to a lower pH in the target location.[12,13] Another strategy for stability is the use of disulfide cross-linkages, such as in the core of micelles, which can withstand the shear stress in blood and improve circulation and delivery of the drug cargo.[14-16]

Stealth is another factor to include in the transformability of nanoparticles. To avoid immune clearance by the MPS system there are a variety of methods that have been developed. Most commonly a coating with polyethylene glycol (PEG)[17,18] is used to avoid clearance with concurrent stabilization of the nanomaterial. After

the success of Doxil, PEGylated doxorubicin (DOX), many materials have followed suit in using this polymer and its derivatives. For example, we have previously demonstrated that PEG_{2000} which was used to create cross-linked nanoparticles that promote stability until their interaction with acidic tumor microenvironment. This PEGylation provided increased circulation time and shielded the effect of the positively charged nanoparticles in oral cancer mouse models.[17] In addition to PEG, many other hydrophilic polymers have been used to improve stability and evasion from the immune system such as PLGA [poly(lactic-co-glycolic acid)], POx [poly(2-oxazoline)] and other poly zwitterions.[8]

Alternatively, cell membranes can be used as a coating for nanomaterials to provide stealth in the blood.[18] Several different types of cell membranes have been used to promote diverse functions. To avoid immune clearance, red blood cell (RBC) membranes are used to coat nanoparticles.[18-22] Cell membranes are collected to form vesicles and loaded with the nanomaterial. Along with RBCs, platelets have also been used to avoid MPS and are easy to fractionize due to the lack of nuclei in both cell types.[17] Additionally, nanoparticles can be camouflaged using exosomes, small extracellular vesicles that are secreted by cells.[23] A recent study used exosomes from tumor cells exposed to DOX loaded silicon nanoparticles as carriers allowing for better tumor accumulation and more extravasation from blood vessels.[24]

The protein corona effect is another phenomenon facing nanoparticles when in circulation. As the nanoparticle enters the bloodstream, plasma proteins accumulate on the surface of the nanoparticle and affect the zeta potential as well as size of the

nanoparticle.[25] One example, Abraxane, albumin-bound paclitaxel, utilizes human serum albumin to facilitate entry of the drug into tumor and many other examples have followed its lead in utilization of serum proteins. A study by Zhang et. al. showed utilizing the protein corona properties for nanoparticle targeting.[26] Liposomes were functionalized with a peptide that interacts with apolipoproteins. These liposomes allowed the receptor binding domain of the apolipoprotein to be exposed and deliver DOX for glioma treatment.[26] Hijacking the protein corona for delivery is a useful method to prevent the pitfalls of inactivation of nanoparticles before they can deliver their target.[25]

Tumor Targeting and Extravasation

Targeting the tumor involves the use of ligands specific to tumor cells or tumor microenvironments. Many of the common targeting ligands have sensitivity to pH[27], enzyme reactivity[25], temperature[28], and other biomarkers.

One such example of nanotheranostics response to stimuli is reaction to glutathione (GSH). In our group, we developed a probe for magnetic resonance imaging (MRI) which was able to disassemble upon exposure to reduced glutathione which is present in excessive amounts in the tumor (Figure 2).[29] Others have also utilized the biomarker for tumor targeting and transformation in treatment.[10,30] Another condition that can be used for tumor targeting is the hypoxia often found in tumor microenvironments. Shen et. al. have utilized all-trans retinoic acid (ATRA) encapsulated in a nitroimidazole-modified hylauroinic acid-oxalate-camptothecin (CPT) conjugate to target the cancer stem cell niche in tumors. In hypoxic

conditions the ATRA is released causing differentiation of the cancer stem cells and exposing them to the chemotherapeutic loaded in the nanoparticle, CPT.[31]

In the case of brain tumors, the added targeting barrier to bypass is the blood brain-barrier (BBB). This barrier is composed of pericytes, astrocytes, and endothelial cells forming tight junctions which regulate the substances that can enter and exit the brain.[32] In our lab, we have utilized a transcytosis method to navigate this barrier for brain tumor therapeutics. Two functional moieties were used to ensure BBB entry and transformation at the tumor site. First, Maltobionic acid, a glucose derivative, was used to facilitate GLUT1 transcytosis past the BBB and second, 4-carboxyphenylboronic acid to target sialic acid that is overexpressed in brain tumor cells (Figure 3).[33] Clark et.al. has used transferrin for transcytosis across the BBB also with an acid cleavable link between the transferrin and the nanoparticle core to facilitate nanoparticle uptake in the brain parenchyma.[34]

Tumor Penetration and Uptake

Regarding nanoparticle tumor penetration, the current consensus is that the EPR effect is responsible for the superior efficacy of nanoparticles for drug delivery to the tumor. The EPR effect cannot account for excessive extracellular matrix (ECM) that surrounds many of the tumor types in which nanomaterials are effective.[24,35] The overall pathway includes perfusion into the intratumoral vessels, extravasation then penetration into the tumor mass.[36] In the previous step, PEGylation provided the stealth needed for circulation. However, at this stage, entry into the tumor is limited by high PEG density.[36] Transcytosis can be used at this step to facilitate tumor

uptake by modifying materials with tumor targeting.

Within the tumor, high interstitial pressure is an added barrier preventing tumor penetration. To bypass this issue, many nanoparticles include anti-angiogenic factors to normalize the vasculature. Recently, Li et. al. developed a stimuli responsive nanoparticle that utilizes thrombin loaded nanomaterials that also simultaneously deplete tumor-associated platelets to deplete abnormal angiogenesis.[37] They showed nanomaterials composed of poly(etherimide)-poly(lactic-*co*-glycolic acid)$_2$ (PEI-PLGA$_2$) copolymer for DOX encapsulation and an antibody R300 against platelets was functionalized on the surface through electrostatic interactions, allowing the final nanoparticle to release R300 and DOX at their targeted location to target platelets and tumor biomarkers.[37] In addition to the standard anti-angiogenic drugs, nitric oxide (NO) can be delivered which can not only modulate angiogenesis but also promotes vascular homeostasis and endothelial cell functions.[38] Sung et. al made a NO delivery nanoparticle using a dinitrosyl iron complex [Fe(μ-SEt)$_2$(NO)$_4$] as the NO donor and poly-lactic glutamic acid (PLGA) as the method of controlled release of NO which showed efficacy in hepatocellular carcinoma models.[38] Another method to decrease the higher interstitial pressure is to target the ECM proteins in the tumor microenvironment. The composition of the ECM is highly tumor dependent but generally include collagen and fibrinogen.[7] A collagen targeting material was made by Yao and colleagues in the form of a nanoenzyme capsule containing collagenase nanocapsules with heavy-chain ferritin nanocages containing DOX. Once the nanozyme capsule complex reached the mildly acidic tumor environment, the

collagenase capsule was degraded, and collagenase could be activated to degrade collagen. The ferritin nanocage also promoted tumor penetration along with having a tumor targeting ability. This nanoparticle also alleviated the hypoxic tumor environment with these components.[39] Another hypoxia stimuli responsive material recently made is by Chen et. al who used a one-step method to combine paclitaxel, catalase, human serum albumin, and chlorine e6 (Ce6) into HAS-Ce6-Cat-PTX nanoparticles. These nanoparticles started at 100 nm for optimal blood circulation and upon reaching the tumor became small protein-drug complexes of 20 nm. The catalase responded to the endogenous H_2O_2 to form oxygen and alleviate the hypoxic environment.[40]

Size transformation is another strategy to improve tumor penetration and uptake. Many studies have utilized the properties of large to small transformation at the tumor site to prolong circulation as well as increase uptake at the tumor site. The main strategies include detachment of small vesicles from hybrid large-small nanoparticles or some degradation of the hybrid particle, a shell coating which detaches upon target location, and finally a self-shrinkage.[41] There are several different methods used to achieve these mechanisms. First, the use of pH will allow for transformation at the specific acidic tumor microenvironment. One ligand used was the amphiphilic copolymer $PDPA_{30}$-*b*-$PAMA_{15}$ which is hydrophobic in physiological pH and becomes hydrophilic in acidic pH resulting in a decrease from 35 to 10 nm.[42] A more dramatic size decrease was seen with the use of 2,3-Dimethylmaleicanhydride (DMA) which reacts in acidic conditions to amine groups and causes decomposition of a PCL-CDM-PAMAM/Pt system along with a charge

reversal in a 100 nm to 5 nm size reduction.[43]

Another facet of drug uptake includes uptake to the target location. Due to the size of many nanoparticles, uptake into the cell requires endocytosis and subsequent trapping in the endosome and lysosome. One strategy to overcome this phenomenon is direct targeting of the lysosome. Lysosomal targeting is a viable strategy due to the dysregulation of lysosomal pathways when managing the higher metabolic requirements needed by tumor cells or to provide a method other than apoptosis for conventional chemotherapy-resistant cells. Our group has previously developed a lysosome targeting small molecule that self assembles into a nanoparticle. Lysosome targeting caused disruption of its membrane combined with autophagy inhibition leading to potent efficacy in autophagy-dependent tumors. (Figure 4).[44] Other nanomaterials developed ways to avoid endosomal trapping through three main mechanisms, cell penetrating peptides (CPPs) or polymer-based nanomaterials that can create pores in the endosome or lipid-based vehicles that can fuse with the endosome membrane to escape.[45] Liposomes functionalized with an ionizable cationic lipid in their outer membrane can become protonated in the endosome and escape or disrupt the endosomal membrane.[46] Some recent studies with CPPs include the development of a TAT analog conjugated with methoxy PEG (MPEG)-poly(ε-caprolactone) (PCL) diblock copolymer which was unable to complex with DNA without the TAT CPP.[47]

Tumor Retention

In relation to tumor retention, the EPR effect is again called upon to describe the

superior ability of nanoparticles to be retained in the tumor.[2] The retention is seen through the limited lymphatic clearance present in tumors.

Retention can be favored by transformation into various shapes apart from the general spherical vesicles that allow for decreased efflux of the drug. Nanoparticles in fiber conformations are more favorable for decreased tumor efflux while spherical particles are more favorable for circulation and tumor penetration[41] as well as intravenous injection[48]. Our group and others have developed transformable nanoparticles that prolong the drug at the tumor site by transformation into a nanofiber shape as a result of targeting receptor stimuli.[49-51] or pH in the target location.[52,53] Two such examples of nanofibers and nanofibril transformation are illustrated in Figure 5. A recent study by Borkowska et al. showed accumulation of mixed charged nanoparticles that upon reaching the lysosome would aggregate into nanocrystals and be retained in the lysosome.[54]

One other method for tumor retention is to use small to large nanoparticle transformation. Aggregation of small nanoparticles at the site of the tumor prolongs the retention of the drug and improves efficacy. Additionally, nanoparticles can be optimized to include advantageous optical properties that allow for measurement of aggregation through emission or quenching of fluorescence[55,56] or other measurable signals. Smaller size nanoparticles allow for easier tumor penetration but are also more likely to be cleared faster. For optimal tumor retention, aggregates of smaller particles can utilize the advantages of the smaller size without premature clearance. A stimuli response at the tumor site will allow for selective aggregation and prevent nonspecific interactions. Methods for this

transformation include a click reaction, electrostatic interaction, phase transitioning, swelling or self-assembling to transform into larger sizes and aggregate.[41] One recent study by Hu et.al. has used a nanogel shell surface made of hyaluronic acid along with the enzyme, transglutaminase (TG). Upon tumor entry, TG catalyzed a peptide bond between lysine and glutamine allowing for 10 nm particles to aggregate into 120 nm in breast cancer models.[57]

Finally, tumor retention should be balanced with clearance of the drug to prevent systemic toxicity. An ideal nanoparticle should be retained long enough at the tumor to exert its effect. A technique to ensure timely clearance particularly at nonspecific locations was used by Wang et. al. which they entitled new tumor selective cascade activated self-retention system (TCASS). Their nanofiber underwent self-assembly at the tumor site while showing small molecule clearance in normal organs as the fibers were monomers.[58]

Discussion/Conclusion/Perspective

The ability of nanomedicine to reach clinical translation requires more study into the pharmacokinetics and pharmacodynamics of nanomaterials. The heterogenous nature of tumors and patients is a challenge that should be addressed with adaptable nanomaterials specific to each case. New drug candidates along with improving preclinical models will allow for a more promising outlook for new chemotherapeutics. As seen in the discussion of these barriers, there are often contradictory conditions that promote increased efficacy at points of the delivery cascade. Additionally in the case of current personalized medicine, the patient and

tumor type should be considered to provide maximum overall efficiency and most effective clinical translation. To summarize, blood circulation should be long enough to reach the target location while being concealed by the RES and MPS system and stable enough to prevent premature drug release. Next, the nanoparticle should be able to penetrate the tumor and still be able to be internalized by the cell in the often-harsh tumor microenvironment. Finally, there should be tumor retention along with a timely clearance to prevent excessive toxicity. Stimuli-response allows nanoparticles to maximize effectiveness and provides the best outcome for a clinically relevant therapeutic. Novel treatments that account for tumor barriers and can adapt to tumor stimuli have the potential to revolutionize cancer therapy.

Figure 1

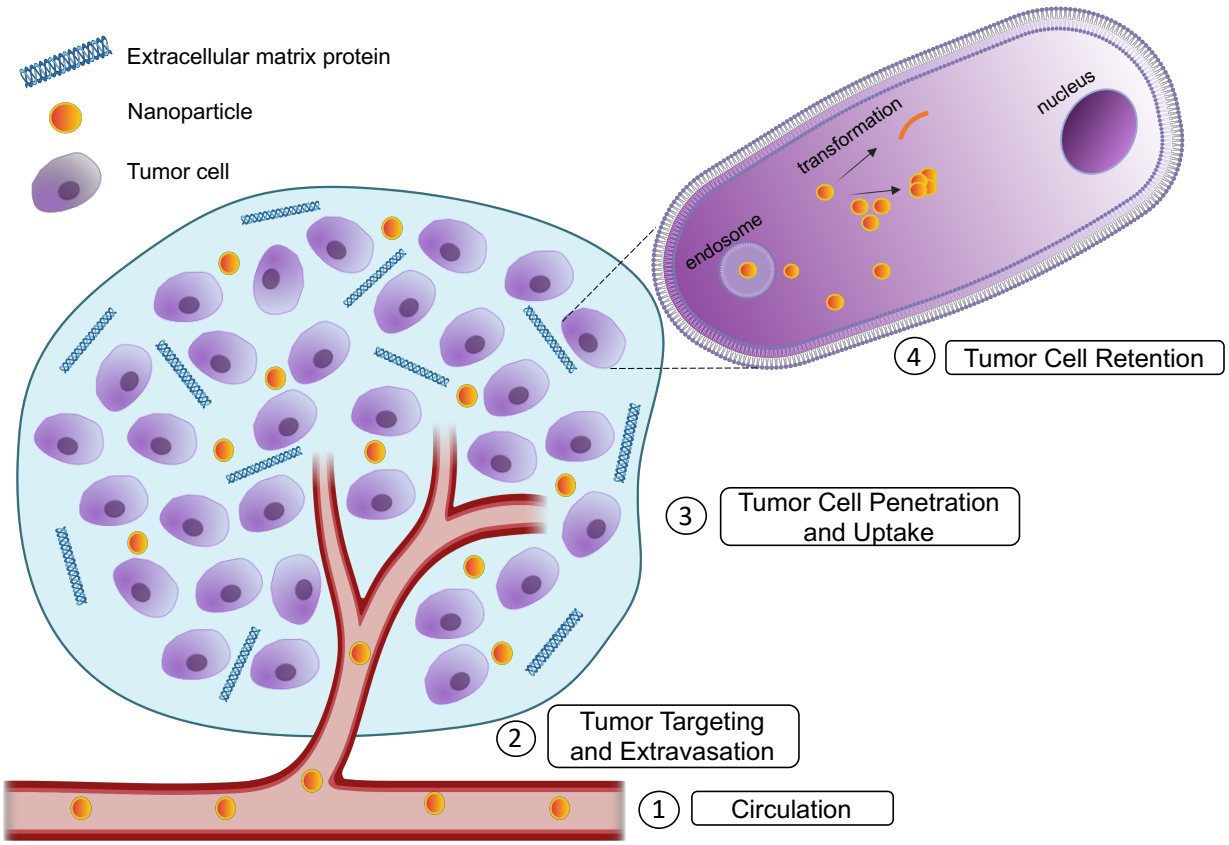

Figure 1: Biological Barriers in Drug Delivery to Tumors

Several barriers preclude drug delivery to tumors. These include severe destabilizing conditions during circulation, targeting the tumor location and extravasation into the tumor blood vessel. Next, the drug must penetrate the excess extracellular matrix (ECM) proteins and reach the tumor cells and finally, the drug must be retained in the tumor cells and avoid premature efflux. Made using Biorender.com.

Figure 2

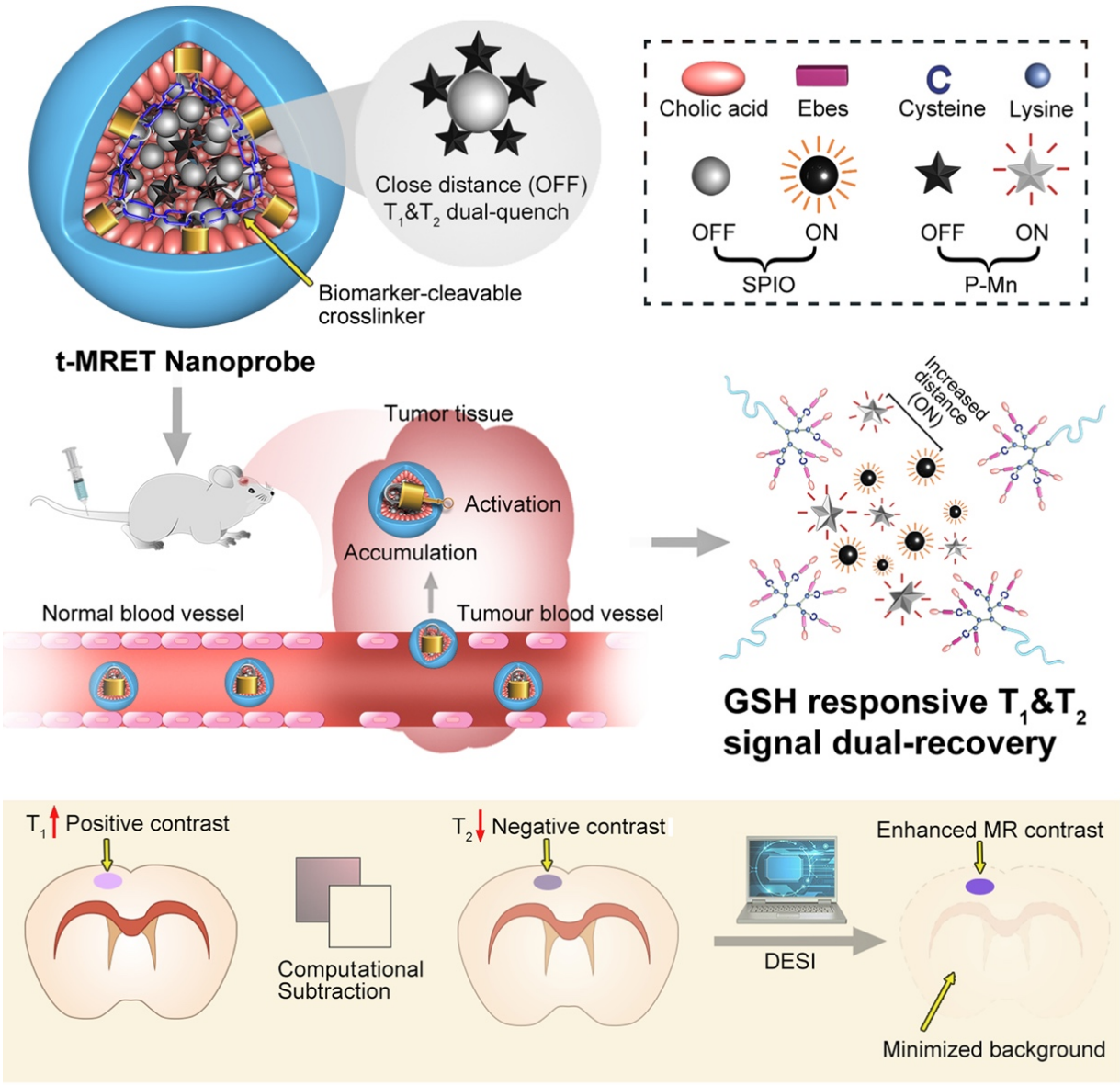

Dual-contrast Enhanced Subtraction Imaging (DESI)

Figure 2: Schematic illustration of the TMRET nanotechnology and DESI utilizing GSH responsive transformation. Mn^{2+} conjugated to pheophorbide a serves as both an 'enhancer' in the T1 MRI signal and a 'quencher' in the T2 MRI signal, whereas the SPIO nanoparticle acts as an 'enhancer' in the T2 MRI signal and a 'quencher' in the T1 MRI signal. P-Mn and SPIO were coloaded into a disulfide crosslinked micelle to form TMRET nanoparticles. Upon interaction with reduced GSH (glutathione) the disulfide bond is cleaved allowing for signal measurement. Reproduced with permission from (29).

Figure 3:

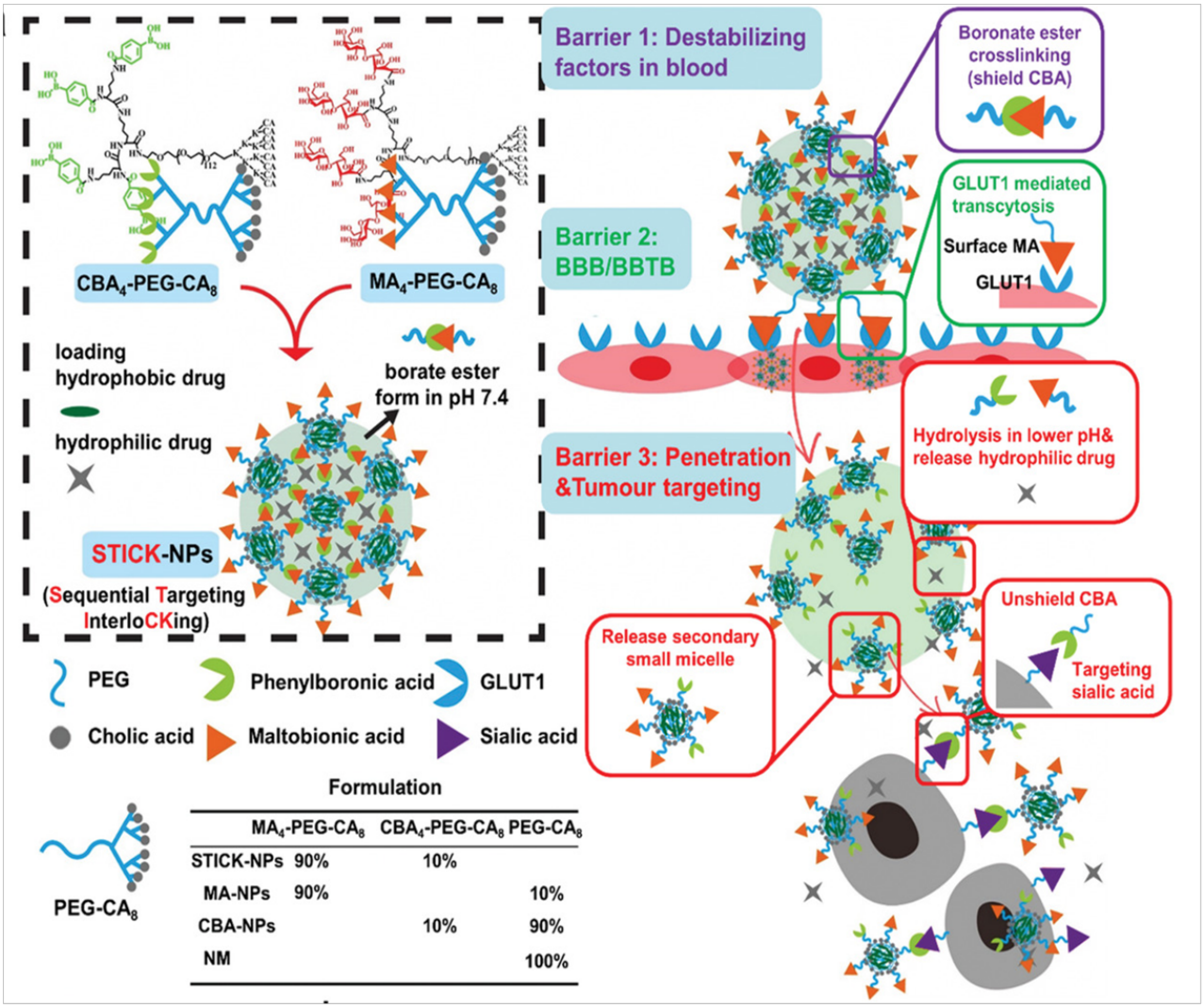

Formulation

	MA_4-PEG-CA_8	CBA_4-PEG-CA_8	PEG-CA_8
STICK-NPs	90%	10%	
MA-NPs	90%		10%
CBA-NPs		10%	90%
NM			100%

Figure 3: Design of transformable STICK-NPs and detailed multibarrier tackling mechanisms to brain tumors. The pair of targeting moieties selected to form sequential targeting in crosslinking (STICK) were maltobionic acid (MA), a glucose derivative, and carboxyphenylboronic acid (CBA), one type of boronic acid, and were built into our well-characterized self-assembled micelle formulations (PEG–CA8). STICK-NPs were assembled by a pair of MA4–PEG–CA8 and CBA4–PEG–CA8 with the molar ratio of 9:1 while intermicelle boronate crosslinkages, STICK, formed between MA and CBA resulting in larger nanoparticle size. Excess MA moieties were on the surface of the nanoparticles, while CBA moieties were first shielded inside the STICK to avoid nonspecific bindings. Hydrophobic drugs were loaded in the hydrophobic cores of secondary small micelles, while hydrophilic agents were trapped in the hydrophilic space between small micelles. In the following studies, we included several control micelle formulations including NM (no targeting), MA–NPs (single BBB targeting), and CBA–NPs (single sialic acid tumor targeting) nanoparticles (inserted table). In detail, STICK-NPs could overcome Barrier 1 (destabilizing condition in the blood) by intermicellar crosslinking strategy, Barrier 2 (BBB/BBTB) by active GLUT1 mediated transcytosis through brain endothelial cells, and Barrier 3 (penetration & tumor cell uptake) by transformation into secondary smaller micelles and reveal of secondary active targeting moiety (CBA) against sialic acid overexpressed on tumor cells in response of acidic extracellular pH in solid tumors. Reproduced with permission from (33).

Figure 4:

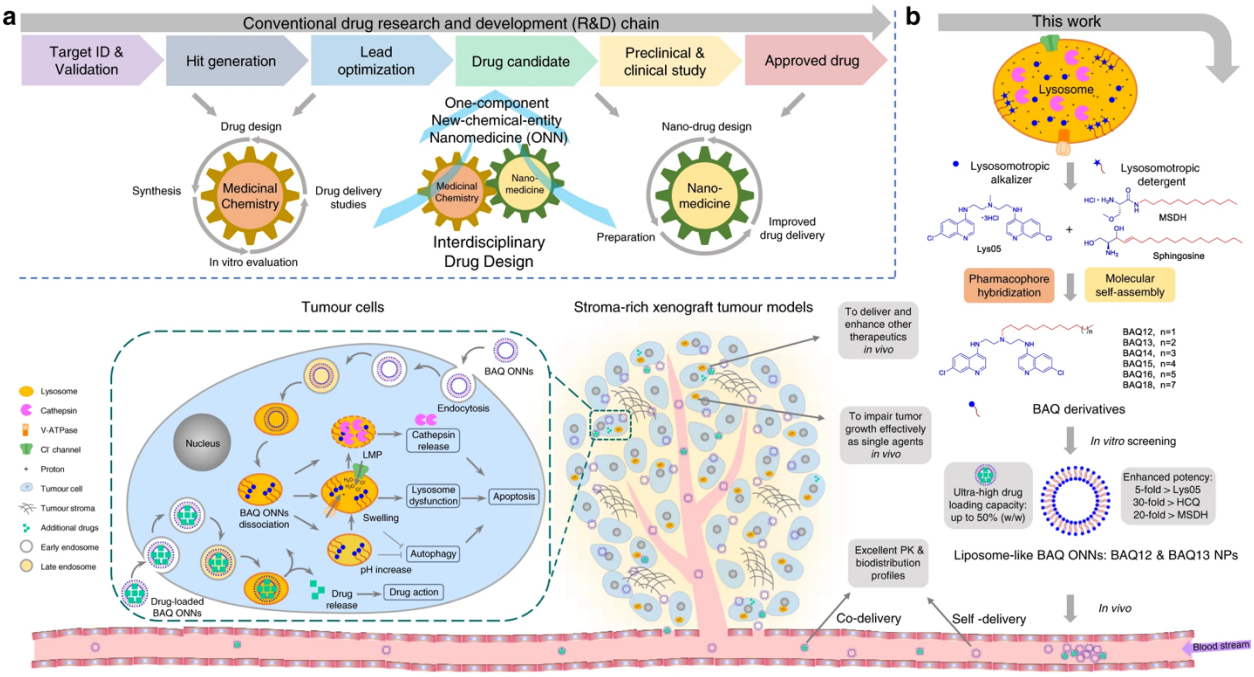

Figure 4: Tumor Targeting with BAQ ONNs. a) An interdisciplinary drug design strategy is proposed to integrate the conventional fields of medicinal chemistry and nanomedicine. Drugs are named as one-component new-chemical-entity nanomedicines (ONNs), which are designed according to the strategies of conventional drug design and molecular self-assembly so that they could acquire the advantages from the perspectives of both drug discovery and drug delivery. b) The proof-of-concept experiment in this work: discovery of self-delivering lysosomotropic bisaminoquinoline (BAQ) derivatives for cancer therapy. The BAQ derivatives, generated from the hybridisation of lysosomotropic detergents and the BAQ-based autophagy inhibitor, can self-assemble into BAQ ONNs that show enhanced functions in vitro, excellent delivery profiles and significant in vivo therapeutic effects as single agents. Moreover, they also possess high drug-loading efficiency to deliver the additional drug into tumour sites, thus generating a promising application of combination therapy. Reproduced from (44).

Figure 5:

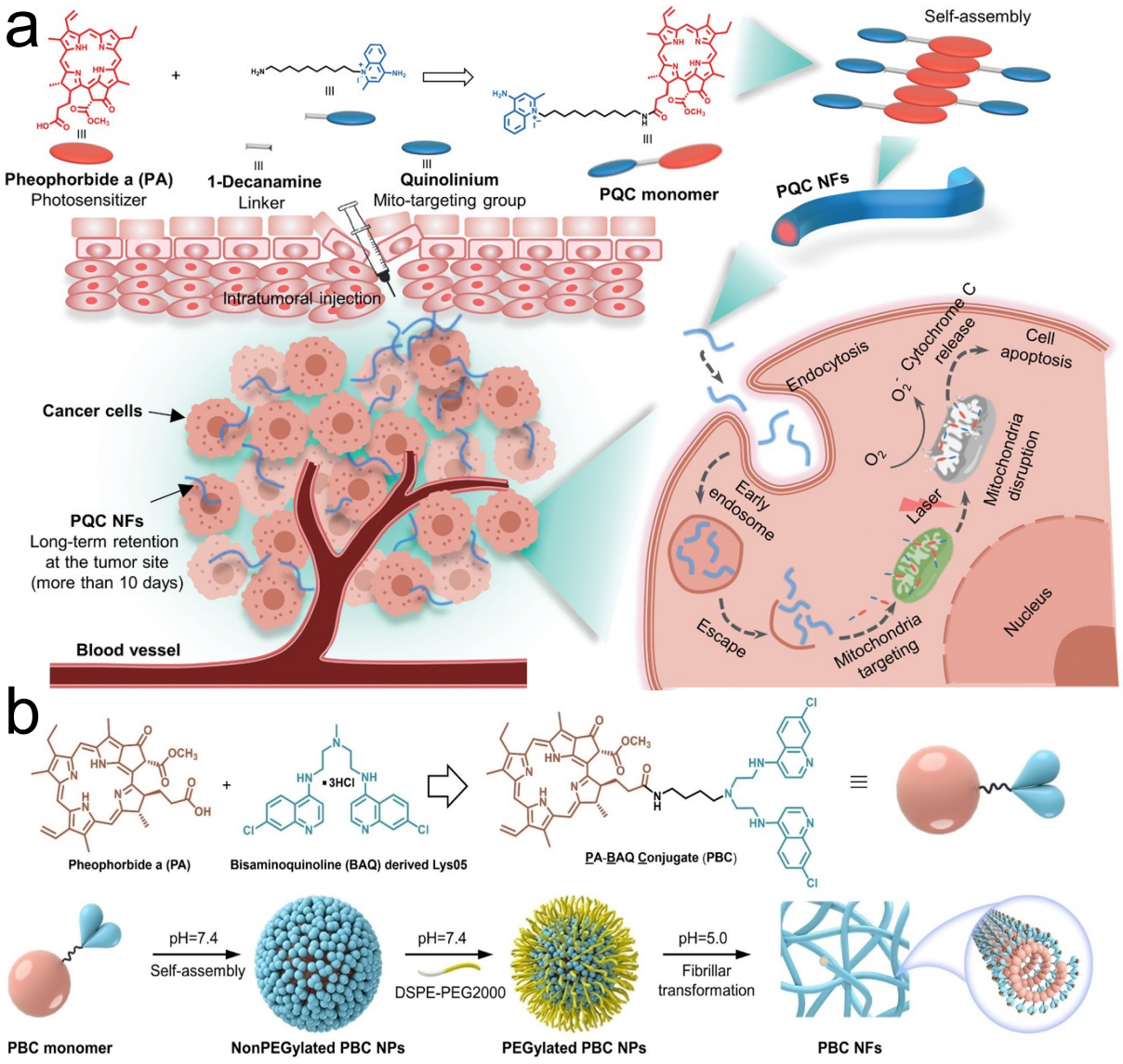
a
Pheophorbide a (PA)
Photosensitizer
1-Decanamine
Linker
Quinolinium
Mito-targeting group
PQC monomer
Self-assembly
PQC NFs
Intratumoral injection
Cancer cells
PQC NFs
Long-term retention
at the tumor site
(more than 10 days)
Blood vessel
Endocytosis
Early endosome
Escape
Mitochondria targeting
Laser
Cytochrome C release
Cell apoptosis
Mitochondria disruption
Nucleus
b
Pheophorbide a (PA)
Bisaminoquinoline (BAQ) derived Lys05
PA-BAQ Conjugate (PBC)
PBC monomer
pH=7.4
Self-assembly
NonPEGylated PBC NPs
pH=7.4
DSPE-PEG2000
PEGylated PBC NPs
pH=5.0
Fibrillar transformation
PBC NFs

Figure 5: Tumor Retention through transformation into nanofibers and nanofibrils. A) Synthesis of single small molecule-assembled mitochondria targeting nanofibers (PQC NFs). The PQC monomer is a conjugate of PA and quinolinium. PQC NFs exhibited nanomolar cytotoxicity by mediating mitochondria-targeting phototherapy and were retained long-term at the tumor site. With these advantages, PQC NFs achieved robust anticancer effects in vivo with a 100% complete cure rate after the administration of only a single dose.

B) Chemical structure of PBC monomer containing pheophorbide a (PA) and bisaminoquinolone derived Lys05. Self-assembling and transformation behaviors of PBC at pH 7.4 and pH 5.0. PBC transformation into nanofibrils allowed for long term retention in the tumor site in oral cancer xenograft models. Reproduced with permission from (51) and (52).

Reference:

1. Siegel RL, Miller KD, Fuchs HE, Jemal A. Cancer statistics, 2022. CA Cancer J Clin. 2022;72(1):7-33.
2. Kobayashi H, Watanabe R, Choyke PL. Improving conventional enhanced permeability and retention (EPR) effects; what is the appropriate target? Theranostics. 2013;4(1):81-9.
3. Liu X, Jiang J, Meng H. Transcytosis - An effective targeting strategy that is complementary to "EPR effect" for pancreatic cancer nano drug delivery. Theranostics. 2019;9(26):8018-25.
4. Sindhwani S, Syed AM, Ngai J, Kingston BR, Maiorino L, Rothschild J, et al. The entry of nanoparticles into solid tumours. Nat Mater. 2020;19(5):566-75.
5. Iglesias J. nab-Paclitaxel (Abraxane®): an albumin-bound cytotoxic exploiting natural delivery mechanisms into tumors. Breast Cancer Res. 2009;11(Suppl 1):S21.
6. Von Hoff DD, Ervin T, Arena FP, Chiorean EG, Infante J, Moore M, et al. Increased survival in pancreatic cancer with nab-paclitaxel plus gemcitabine. N Engl J Med. 2013;369(18):1691-703.
7. Sun Q, Zhou Z, Qiu N, Shen Y. Rational Design of Cancer Nanomedicine: Nanoproperty Integration and Synchronization. Adv Mater. 2017;29(14).
8. Fam SY, Chee CF, Yong CY, Ho KL, Mariatulqabtiah AR, Tan WS. Stealth Coating of Nanoparticles in Drug-Delivery Systems. Nanomaterials (Basel). 2020;10(4).
9. Yadav KS, Jacob S, Sachdeva G, Chuttani K, Mishra AK, Sawant KK. Long

circulating PEGylated PLGA nanoparticles of cytarabine for targeting leukemia. Journal of Microencapsulation. Journal of Microencapsulation; 2011;28(8):729–42.

10. Qiu J, Cheng R, Zhang J, Sun H, Deng C, Meng F, et al.. Glutathione-Sensitive Hyaluronic Acid-Mercaptopurine Prodrug Linked via Carbonyl Vinyl Sulfide: A Robust and CD44-Targeted Nanomedicine for Leukemia. Biomacromolecules. Biomacromolecules; 2017;18(10):3207–14.
11. Sanità G, Carrese B, Lamberti A. Nanoparticle Surface Functionalization: How to Improve Biocompatibility and Cellular Internalization. Front Mol Biosci. 2020;7:587012.
12. Li Y, Xiao W, Xiao K, Berti L, Luo J, Tseng HP, et al. Well-defined, reversible boronate crosslinked nanocarriers for targeted drug delivery in response to acidic pH values and cis-diols. Angew Chem Int Ed Engl. 2012;51(12):2864-9.
13. M. Nakahata, S. Sakai. Cross-Linking Building Blocks Using a “Boronate Bridge” to Build Functional Hybrid Materials. ChemNanoMat 2019;5(141).
14. Li Y, Xiao K, Luo J, Xiao W, Lee JS, Gonik AM, et al. Well-defined, reversible disulfide cross-linked micelles for on-demand paclitaxel delivery. Biomaterials. 2011;32(27):6633-45.
15. Xiao K, Liu Q, Al Awwad N, Zhang H, Lai L, Luo Y, et al. Reversibly disulfide cross-linked micelles improve the pharmacokinetics and facilitate the targeted, on-demand delivery of doxorubicin in the treatment of B-cell lymphoma. Nanoscale. 2018;10(17):8207-16.
16. Zhang L, Jing D, Wang L, Sun Y, Li JJ, Hill B, et al. Unique Photochemo-

Immuno-Nanoplatform against Orthotopic Xenograft Oral Cancer and Metastatic Syngeneic Breast Cancer. Nano Lett. 2018;18(11):7092-103

17. Xue X, Huang Y, Bo R, Jia B, Wu H, Yuan Y, et al. Trojan Horse nanotheranostics with dual transformability and multifunctionality for highly effective cancer treatment. Nat Commun. 2018;9(1):3653.
18. Zhen X, Cheng P, Pu K. Recent Advances in Cell Membrane-Camouflaged Nanoparticles for Cancer Phototherapy. Small. 2019;15(1):e1804105.
19. Hu CM, Zhang L, Aryal S, Cheung C, Fang RH. Erythrocyte membrane-camouflaged polymeric nanoparticles as a biomimetic delivery platform. Proc Natl Acad Sci U S A. 2011;108(27):10980-5.
20. Xu X, Yang G, Xue X, Lu H, Wu H, Huang Y, et al.. A polymer-free, biomimicry drug self-delivery system fabricated via synergistic combination of bottom-up and top-down approaches. Journal of Materials Chemistry B 2018;6(47):7842–53.
21. Liang H, Huang K, Su T, Li Z, Hu S, Dinh PU, et al. Mesenchymal Stem Cell/Red Blood Cell-Inspired Nanoparticle Therapy in Mice with Carbon Tetrachloride-Induced Acute Liver Failure. ACS Nano. 2018;12(7):6536-44.
22. Pei Q, Hu X, Zheng X, Liu S, Li Y, Jing X, et al. Light-Activatable Red Blood Cell Membrane-Camouflaged Dimeric Prodrug Nanoparticles for Synergistic Photodynamic/Chemotherapy. ACS Nano. 2018;12(2):1630-41.
23. Carney RP, Hazari S, Rojalin T, Knudson A, Gao T, Tang Y, et al. Targeting Tumor-Associated Exosomes with Integrin-Binding Peptides. Adv Biosyst. 2017;1(5).
24. Yong T, Zhang X, Bie N, Zhang H, Li F, Hakeem A, et al. Tumor exosome-based

nanoparticles are efficient drug carriers for chemotherapy. Nat Commun. 2019;10(1):3838.

25. de Lázaro I, Mooney DJ. Obstacles and opportunities in a forward vision for cancer nanomedicine. Nat Mater. 2021;20(11):1469-79.
26. Zhang Z, Guan J, Jiang Z, Yang Y, Liu J, Hua W, et al. Brain-targeted drug delivery by manipulating protein corona functions. Nat Commun. 2019;10(1):3561.
27. Liu M, Huang L, Zhang W, Wang X, Geng Y, Zhang Y, et al. A transistor-like pH-sensitive nanodetergent for selective cancer therapy. Nat Nanotechnol. 2022.
28. Borys N, Dewhirst MW. Drug development of lyso-thermosensitive liposomal doxorubicin: Combining hyperthermia and thermosensitive drug delivery. Adv Drug Deliv Rev. 2021;178:113985.
29. Wang Z, Xue X, Lu H, He Y, Lu Z, Chen Z, et al. Two-way magnetic resonance tuning and enhanced subtraction imaging for non-invasive and quantitative biological imaging. Nat Nanotechnol. 2020;15(6):482-90.
30. Xiao K, Liu Q, Suby N, Xiao W, Agrawal R, Vu M, et al. LHRH-Targeted Redox-Responsive Crosslinked Micelles Impart Selective Drug Delivery and Effective Chemotherapy in Triple-Negative Breast Cancer. Adv Healthc Mater. 2021;10(3):e2001196.
31. Shen S, Xu X, Lin S, Zhang Y, Liu H, Zhang C, et al. A nanotherapeutic strategy to overcome chemotherapeutic resistance of cancer stem-like cells. Nat Nanotechnol. 2021;16(1):104-13.
32. Tang W, Fan W, Lau J, Deng L, Shen Z, Chen X. Emerging blood-brain-barrier-

crossing nanotechnology for brain cancer theranostics. Chem Soc Rev. 2019;48(11):2967-3014.

33. Wu H, Lu H, Xiao W, Yang J, Du H, Shen Y, et al. Sequential Targeting in Crosslinking Nanotheranostics for Tackling the Multibarriers of Brain Tumors. Adv Mater. 2020;32(14):e1903759.
34. Clark AJ, Davis ME. Increased brain uptake of targeted nanoparticles by adding an acid-cleavable linkage between transferrin and the nanoparticle core. Proc Natl Acad Sci U S A. 2015;112(40):12486-91.
35. Liu Y, Huo Y, Yao L, Xu Y, Meng F, Li H, et al. Transcytosis of Nanomedicine for Tumor Penetration. Nano Lett. 2019;19(11):8010-20.
36. Zhou Q, Dong C, Fan W, Jiang H, Xiang J, Qiu N, et al. Tumor extravasation and infiltration as barriers of nanomedicine for high efficacy: The current status and transcytosis strategy. Biomaterials. 2020;240:119902.
37. Li Z, Di C, Li S, Yang X, Nie G. Smart Nanotherapeutic Targeting of Tumor Vasculature. Acc Chem Res. 2019;52(9):2703-12.
38. Sung YC, Jin PR, Chu LA, Hsu FF, Wang MR, Chang CC, et al. Delivery of nitric oxide with a nanocarrier promotes tumour vessel normalization and potentiates anti-cancer therapies. Nat Nanotechnol. 2019;14(12):1160-9
39. Yao H, Guo X, Zhou H, Ren J, Li Y, Duan S, et al. Mild Acid-Responsive "Nanoenzyme Capsule" Remodeling of the Tumor Microenvironment to Increase Tumor Penetration. ACS Appl Mater Interfaces. 2020;12(18):20214-27.
40. Chen Q, Chen J, Liang C, Feng L, Dong Z, Song X, et al. Drug-induced co-assembly of albumin/catalase as smart nano-theranostics for deep intra-tumoral

penetration, hypoxia relieve, and synergistic combination therapy. J Control Release. 2017;263:79-89.

41. Chen, J., et al., Smart transformable nanoparticles for enhanced tumor theranostics. Applied Physics Reviews, 2021;8(4):p.041321.
42. Yu W, Liu R, Zhou Y, Gao H. Size-Tunable Strategies for a Tumor Targeted Drug Delivery System. ACS Cent Sci. 2020;6(2):100-16.
43. Li HJ, Du JZ, Du XJ, Xu CF, Sun CY, Wang HX, et al. Stimuli-responsive clustered nanoparticles for improved tumor penetration and therapeutic efficacy. Proc Natl Acad Sci U S A. 2016;113(15):4164-9.
44. Ma Z, Li J, Lin K, Ramachandran M, Zhang D, Showalter M, et al. Pharmacophore hybridisation and nanoscale assembly to discover self-delivering lysosomotropic new-chemical entities for cancer therapy. Nat Commun. 2020;11(1):4615.
45. Xu E, Saltzman WM, Piotrowski-Daspit AS. Escaping the endosome: assessing cellular trafficking mechanisms of non-viral vehicles. J Control Release. 2021;335:465-80.
46. Schlich M, Palomba R, Costabile G, Mizrahy S, Pannuzzo M, Peer D, et al. Cytosolic delivery of nucleic acids: The case of ionizable lipid nanoparticles. Bioeng Transl Med. 2021:e10213.
47. Tanaka K, Kanazawa T, Shibata Y, Suda Y, Fukuda T, Takashima Y, et al. Development of cell-penetrating peptide-modified MPEG-PCL diblock copolymeric nanoparticles for systemic gene delivery. Int J Pharm. 2010;396(1-2):229-38.

48. Tang M, Lin K, Ramachandran M, Li L, Zou H, Zheng H, et al. A mitochondria-targeting lipid-small molecule hybrid nanoparticle for imaging and therapy in an orthotopic glioma model. Acta Pharm Sin B. 2022;12(6):2672-82.
49. Zhang L, Wu Y, Yin X, Zhu Z, Rojalin T, Xiao W, et al. Tumor Receptor-Mediated In Vivo Modulation of the Morphology, Phototherapeutic Properties, and Pharmacokinetics of Smart Nanomaterials. ACS Nano. 2021;15(1):468-79.
50. Sun C, Wang Z, Yang K, Yue L, Cheng Q, Ma YL, et al. Polyamine-Responsive Morphological Transformation of a Supramolecular Peptide for Specific Drug Accumulation and Retention in Cancer Cells. Small. 2021;17(43):e2101139.
51. Zhang L, Jing D, Jiang N, Rojalin T, Baehr CM, Zhang D, et al. Transformable peptide nanoparticles arrest HER2 signalling and cause cancer cell death in vivo. Nat Nanotechnol. 2020;15(2):145-53.
52. Lin K, Ma Z, Li J, Tang M, Lindstrom A, Ramachandran M, et al. Single Small Molecule-Assembled Mitochondria Targeting Nanofibers for Enhanced Photodynamic Cancer Therapy In Vivo. Advanced Functional Materials. 2021;31(10):2008460.
53. Ma Z, Lin K, Tang M, Ramachandran M, Qiu R, Li J, et al. A pH-Driven Small-Molecule Nanotransformer Hijacks Lysosomes and Overcomes Autophagy-Induced Resistance in Cancer. Angew Chem Int Ed Engl. 2022.
54. Borkowska M, Siek M, Kolygina DV, Sobolev YI, Lach S, Kumar S, et al. Targeted crystallization of mixed-charge nanoparticles in lysosomes induces selective death of cancer cells. Nat Nanotechnol. 2020;15(4):331-41.
55. Xue X, Huang Y, Wang X, Wang Z, Carney RP, Li X, et al. Self-indicating, fully

active pharmaceutical ingredients nanoparticles (FAPIN) for multimodal imaging guided trimodality cancer therapy. Biomaterials. 2018;161:203-15.

56. Wu, H., et al., Rotatable Aggregation-Induced-Emission/Aggregation-Caused-Quenching Ratio Strategy for Real-Time Tracking Nanoparticle Dynamics. Advanced Functional Materials, 2020;30(15):1910348.
57. Hu Q, Sun W, Lu Y, Bomba HN, Ye Y, Jiang T, et al. Tumor Microenvironment-Mediated Construction and Deconstruction of Extracellular Drug-Delivery Depots. Nano Lett. 2016;16(2):1118-26.
58. An HW, Li LL, Wang Y, Wang Z, Hou D, Lin YX, et al. A tumour-selective cascade activatable self-detained system for drug delivery and cancer imaging. Nat Commun. 2019;10(1):4861.

CHAPTER 3

Small molecule self-assembled micelle inhibits autophagy and leads to ferroptosis induction in pancreatic cancer stem cells

ABSTRACT

Pancreatic cancer is one of the most lethal cancer subtypes in part due to the presence of a small subset of cells known as cancer stem cells (CSCs). This population is a portion of the tumor that is thought to cause tumor heterogeneity from their ability to differentiate into various tumor cells and cause tumor resurgence. In this study, we characterize a drug in a series of small molecules that self-assemble into nanoparticles. A bisaminoquinoline derivative containing a nitric oxide bond, BAQ 12O, showed the ability to self-assemble into a micelle and had selective potency in pancreatic CSCs. A notable decrease in CSC function was also seen including decreased tumorigenesis and pluripotency. BAQ 12O is derived from a bisaminoquinolone chloroquine derivative and showed an inhibition in autophagy. The inhibition in autophagy caused by BAQ 12O resulted in ferroptosis related death in CSCs. BAQ 12O showed promising in vivo efficacy in a patient derived pancreatic CSC model combined with the standard of care drug, gemcitabine along with an excellent safety profile in both mice and rats. The study also contributes showing the dependence of autophagy and ferroptosis in CSCs.

INTRODUCTION

Pancreatic Cancer is one of the most lethal cancer subtypes with a 11.5% five-year survival rate[1]. There are limited options for treatments and many of the current options are not effective. One reason for this high mortality in this cancer subtype is the presence of cancer stem cells (CSCs), a portion of the tumor that retains stem-like abilities and is responsible for tumorigenesis and tumor resurgence.[2] CSCs also are thought to account for the heterogeneity in a tumor due to their ability to differentiate into a variety of cells.[2] There are no clinically available drugs targeting this population currently which could provide a novel strategy to combat the aggressive nature of this cancer.

A strategy to target CSCs is through inhibition of autophagy. Autophagy is a lysosome-mediated catabolic process in which macromolecules are recycled to provide nutrients used to fuel tumor growth.[3] Pan tumor types, autophagy is considered a double-edged sword, as autophagy is used both to recycle nutrients and remove damaged organelles to promote cell growth as well as a being a canonical death pathway in which essential organelles are degraded. In the cancer subtext, inhibiting autophagy at an early stage could promote tumor growth whereas inhibiting autophagy in the tumor maintenance stage results in tumor ablation.[2, 3] Nevertheless, the tumor context and subtype plays and important role in determining effectiveness of autophagy targeted treatment. Specifically in the case of pancreatic cancer, there is a high autophagic flux and a reliance on autophagy for both growth and maintenance of the tumor.[4] In addition to pancreatic tumors, autophagy flux is thought to be dysregulated

in cancer stem cell populations which require high levels of autophagy to maintain their pluripotent ability, metastatic potential, and differentiation abilities.[2] Currently, many clinical trials for pancreatic cancer are utilizing chloroquine (CQ) and more commonly its safer derivative, hydroxychloroquine (HCQ), in combination with the standard of care chemotherapy, gemcitabine.[5, 6] However, HCQ and CQ are not very potent and the concentration needed to inhibit autophagy are not clinically feasible.[7]

To address these problems, we employed the use of our previously described one component new chemical entity nanomedicine (ONN) series.[8-11] This series has been developed from the divalent chloroquine derivative, Lys05, one of the current most potent chloroquine derivatives.[7] Lys05 is a bisaminoquinolone (BAQ) derivative that we further functionalized with the lysomotropic detergent MSDH to promote self-assembly in our previous work to form the lead compounds, BAQ12 and BAQ13.[8] These ONNs combined the advantages of small molecule drug design and the delivery advantages of nanomaterials to provide very potent lysosome targeting nanoparticles that inhibited autophagy. Here we expand on this work to include a new ONN generation with BAQ N-oxide 12O (BAQ12O). BAQ12O like the previous generations can self-assemble into a nanoparticle, however some notable differences are present between the two generations. First, BAQ12 and 13 form liposomes while BAQ12O self assembles into a micelle-like particle, so there are intrinsic differences in size, functionality and load-carrying capabilities.[12] Next, we noticed the phenomenon that BAQ12O is selectively more potent in the CSC line our lab previously developed from a pancreatic ductal adenocarcinoma (PDAC) patient tumor.[8] We employed fluorescent assisted cytometric sorting (FACS) for known CSC markers CD326, CD24, and CD44, which were the first

set of markers used to identify the CSC population in pancreatic tumors.[13] This model allowed us to explore the lysosome targeting and autophagy inhibition properties of BAQ12O in CSCs. We further found another difference in that BAQ12O autophagy inhibition led to ferroptosis induction in the CSCs.

Ferroptosis is the iron-mediated, non-apoptotic death process characterized by Dixon et. al. in 2012.[14] Excess iron ultimately causes lipid peroxidation and leads to an oxidative stress related death. We identified this pathway after BAQ12O treatment in CSCs using two sequencing methods, both in the mRNA level and proteomic pathway analysis, after noticing the lack of standard apoptotic morphology and marker activation. Further studies showed that BAQ12O treatment resulted in excess reactive oxygen species, increased labile iron levels, decreased glutathione and notable lipid peroxidation. The relationship between autophagy and ferroptosis is well established, however there is still debate on how they modulate each other.[15, 16] Ferroptosis is also a promising strategy for CSC targeting which often require non-conventional chemotherapeutics to be completely eradicated.[16] BAQ12O combines this unique strategy to target CSCs in pancreatic tumors through the duality of autophagy inhibition and ferroptosis induction as well as the functionalities of both small molecules and nanomedicine for drug delivery. This study shows that BAQ12O had excellent safety profiles, potent autophagy inhibition leading to ferroptosis induction in CSCs, and high efficacy in mouse CSC xenograft models. There was also synergy with the current standard of care for pancreatic cancer, gemcitabine, making BAQ12O a promising translational drug candidate.

MATERIALS AND METHODS

Bisaminoquinolone nitric oxide (BAQ12O) Synthesis

Characterization and Synthesis of BAQ12O can be found in Supplementary Figure 1.

Preparation and Characterization of BAQ 12O Nanoparticle

BAQ12O was dissolved with DSPE-PEG_{2000} in a 4:1 ratio in methanol. This solution was added dropwise into DI H_2O and allowed to mix for 5 minutes in a 1:10 volume. Next the solution underwent rotary evaporation (40 °C, 20 min), followed by the characterization with Zetasizer Nano ZS (Malvern) for dynamic light scattering measurement (DLS) and zeta potential. The TEM samples were prepared by dropping 0.5 mM NPs on carbon square mesh and dried naturally, which were then observed under the Talos L120C TEM (FEI) at an accelerating voltage of 80 kV. Fluorescence of BAQ12O NP and BAQ12O that was not formulated was completed on the

Pharmacokinetic Study

Three female Sprague Dawley rats (Envigo) were administered BAQ12O intravenously through the jugular vein catheter. Blood was collected at the shown timepoints, and serum was collected after blood was allowed to clot for 1 hour. Fluorescence of BAQ12O was used to determine drug concentrations in each sample. Pharmacokinetic parameters were determined using a two-compartment model.

Cell Culture/CSC Culture

MIA-PaCa2 and Panc1 were cultured in DMEM (Corning) supplemented with 10% FBS (Sigma) and 1% Penicillin/Streptomycin (Sigma). ASPC-1 and BXPC3 were cultured in RPMI-1640 (Corning) with the same additives. CSCs were sorted from tumor cells as previously described.[8] Plates were coated with 1% Vitronectin (Gibco A14700) for 3 hours for CSC culture. Media (Gibco A2858501) was changed every 2 days and cells were passaged using gentle cell dissociation reagent (Stem Cell Technologies 07174). A549 cells stably transduced with LC3B-GFP were kindly given by Professor Priya Shah's lab. All cells were grown in 37°C at 5% CO_2.

Cytotoxicity assays

Cytotoxicity was determined using CellTiterGlo assay (Promega). Three replicate wells were used for each condition and six wells for untreated control was used as 100% viability.

3D Culture

Growth-Factor reduced Matrigel (Corning, 354230) at 5 mg/mL was used to coat a 24 well plate Pancreatic cancer cells or CSCs were seeded at 3000 cells/well suspended in 3:2 ratio of Matrigel: Cell suspension. All cells were cultured in serum free stem cell growth media (Gibco A2858501). After 24h of adherence, wells were subjected to their respective drug treatments and imaged 9 days after seeding. Imaging was completed with confocal microscopy (Zeiss LSM 800). All image analysis was done using ImageJ.

Western blot

Tissue or cell lysates were harvested using RIPA buffer supplemented with protease inhibitors. Lysates were resolved on a 12% SDS-PAGE gel and transferred to PVDF membranes. Membranes were blocked for 1 hour in 5% milk in TBST and incubated overnight with antibodies (Cell Signaling Technologies) at 4°C and probed with secondary-HRP conjugated antibody for 1 hour at RT. Membranes were developed using enhanced chemiluminescence substrate (National Diagnostics) and detected using ChemiDoc system (Bio-Rad).

Tumor xenograft studies

NOD-*Rag1*^{null} *IL2rg*^{null} (NRG) mice were purchased from Jackson Laboratory (4-6 weeks old). All experiments involving mice were performed in accordance with the Institutional Animal Care and Use of Committee policy, University of California-Davis. Animals were housed in 12-hour light/dark cycle with controlled temperature and humidity facility. Tumor volume (mm^3) was measured using calipers and calculated using length*width/2.

Tumorigenesis Study:

Male NRG mice were injected with 10^4 CSCs in a 1:1 Matrigel (Corning) solution in both the right and left flank. Treatment began 1 day after injection and continued twice a week with the following treatment groups: Lys05 (50 mg/kg) IP; BAQ12O administered IV (50 mg/kg) and orally (100 mg/kg) until palpable tumors formed in the majority of the saline treated control for a total time of 35 days.

Quantitative Real Time PCR (qPCR)

RNA was collected using TRIzol reagent (Invitrogen). Reverse transcriptase PCR was performed with 1 µg of RNA using High-Capacity RNA-to-cDNA kit (AppliedBiosystems). cDNA was diluted to 1:5 and 2 µL of sample was used for a total reaction volume of 15 µL with SYBR green Master Mix reagent (Applied Biosystems). Reaction was run on BioRad CFX96 Real-Time PCR Detection System. All data was normalized to GAPDH amplification.

Endocytosis Study

$3*10^5$ CSCs were allowed to attach overnight in 6 well plates. Cells were exposed to conditions either temperature or endocytosis inhibitor listed for 30 minutes and then washed. Drug was added for 6h and Lysates were collected using DMSO containing 0.1% Triton X. Lysates were placed in a fluorescent 96 well plate and read at BAQ12O fluorescence (385/506λ).

LC3B-GFP-RFP

$3*10^4$ CSCs were plated in 8 chamber slides (Ibidi) and allowed to attach. Premo LC3B-GFP-RFP (Thermofischer Scientific) was added to CSCs and 12h later drugs were added for 16h. Cells were fixed after treatment in 4% paraformaldehyde to prevent increased signal during imaging. Images were taken on 63x objective using confocal microscope (Zeiss). Puncta were quantified using ImageJ using the Otsu model for thresholding.

DQ-BSA Vacuoles

CSCs or A549 transduced with LC3B-GFP were plated in 4 chamber slide (Lab Tek II) and given 10 µg/mL before drug treatment. After 6h to allow the dye to enter the cell drugs were treated for 16h with 3 µM of listed treatments. After treatment, cells were stained with Hoescht 33342 1:2000 for 20 min and fixed in 4% Paraformaldehyde. Imaging was completed using Zeiss confocal microscopy at 63x oil objective and quantified using Image J. Vacuoles were thresholded using Otsu model and quantified.

Proteomics (Data independent Acquisition-Label Free Quantitation (DIA-LFQ))

CSCs were exposed 24h to BAQ12O 6 µM after allowing adherence for 1 day and lysates were collected as previously mentioned using RIPA buffer containing protease and phosphatase inhibitors. Lysates were concentrated using Acetone overnight in -20°C and given to the UC Davis Proteomics Core Facility.

Measurement of ROS

5000 CSCs were seeded in a 96 well plate and allowed to adhere overnight. Drugs concentrations listed were dosed and ROS level was determined after washing cells and adding DCFDA dye (10µM) for 30 minutes at 37°C. After dye, cells were washed 3x and read at fluorescence 485/535 nm on Spectramax iD5.

FerroOrange Labile Fe^{2+} detection

FerroOrange dye was added to CSCs plated in a 96 well plate. Drugs were incubated for 24h at the listed concentrations and washed in PBS. 1 μM of dye was added to well for 30 minutes and detected at (507/547λ) using Spectramax fluoresecence plate reader.

Measurement of Glutathione and Oxidized Glutathione (GSH/GSSG)

5000 CSCs were seeded in 96 well plates and allowed to attach overnight. Drugs were added for 24h and GSH/GSSG was measured according to the manufacturer's instructions (Promega). Luminescence was measured using Spectramax iD5 plate reader.

Measurement of Lipid Peroxidation

$2.5*10^4$ cells were seeded into 4 chamber slide plates (Lab Tek II) and allowed to attach overnight. Drug treatments were added as noted for 16h and BODIPY 665/676 dye (20 μM) was stained for 30 min along with Hoescht 33342 1:2000 for 20 min. Cells were fixed with 4% Paraformaldehyde and washed 3x in PBS before drying and attaching coverslips. Imaging was performed using confocal microscopy (Zeiss LSM 800). All image analysis was done using ImageJ. For flow cytometric evaluation, $3*10^5$ cells were attached overnight in 6 well plates. Drug was added similarly and the same BODIPY dye staining conditions were applied. Propidium Iodide (final 1μg/mL) was used as viability marker and samples were analyzed on a Becton Dickinson FACS Canto I Analytical Cytometer.

Combination Index

Combenefit software was used to graph combination index. Combination Index (CI) was also calculated by (IC_{50} Drug 1 in combination/ IC_{50} Drug 1 alone) + (IC_{50} Drug 2 in combination/ IC_{50} Drug 2 alone) where CI <1 was considered synergistic.

Combination Study

Female NRG mice were subcutaneously injected with 10^4 CSCs in a 1:1 Matrigel (Corning) solution in both the right and left flank. Tumors were allowed to grow to 100-150 mm^3 and grouped to normalize average tumor weight. Each group was randomly assigned to a treatment (n=6). The groups were as follows: vehicle control; Gemcitabine 50 mg/kg IP once a week; Gemcitabine 50 mg/kg IP once a week + BAQ12O 50 mg/kg IV every 2 days. The treatment period was a total of 43 days. Tumors were collected for immunohistochemical and western blot analysis.

Maintenance Study

Female NRG mice were subcutaneously injected with 10^4 CSCs in a 1:1 matrigel (Corning) solution in both the right and left flank. Tumors were allowed to grow to 100-150 mm^3 and grouped to normalize average tumor weight. Treatment groups were assigned randomly (n=6). All mice were given Gemcitabine 50 mg/kg IP twice a week then separated into one group receiving BAQ12O 50 mg/kg IV every 3 days and the other receiving vehicle. The total treatment period was 52 days. Tumors were collected for immunohistochemical and western blot analysis.

Immunohistochemistry

Tumors were collected from each mouse and fixed 24h in 10% formalin. The next day tissue was transferred to 70% Ethanol and sent for paraffin embedding. Sections are 4 μm. Primary antibodies were incubated 2 h rt and overnight then detected.

Statistics

Unpaired, two-sided t test, χ^2, 2-way ANOVA and survival analysis were performed using Graphpad Prism 6.

RESULTS

BAQ12O Nanoparticle Characterization

We previously characterized a series of bisaminoquinolone derivatives for lysosomal targeting drugs. We have modified these lead compounds to find the current most promising candidate showing cancer stem cells selectivity, BAQ12O. This compound is similar to BAQ12 but includes a nitric oxide bond shown in Figure 1a. BAQ12O shows the same property of self-assembly but forms a micelle instead of a liposome seen by BAQ12 or BAQ13 self-assembly. The micelle was further stabilized by addition of DSPE-PEG_{2000} promoting both stability of micelle and the property of blood circulation stability *in vivo* characteristic of pegylation.[17] Both dynamic light scattering and transmission electron microscope images confirmed the formation of BAQ12O nanoparticle (NP) into a micelle of around 130 nm (Figure 1c,d). Another property of BAQ12O not seen in the previous generation of BAQ12 and BAQ13 is its fluorescent

properties (Figure 1e) resulting from the additional nitric oxide bond[18], allowing for easy monitoring of the drug in both in vitro and in vivo systems. The addition of PEG also showed BAQ12O stability in FBS as well (Figure 1f). The critical aggregation concentration of BAQ12O was shown to be very low at 0.08 μM indicated a quicker micelle formation (Figure 1g). Finally, pharmacokinetic parameters were calculated after IV administration of BAQ12O nanoparticle in catheterized rats. BAQ12O showed very quick uptake into tissue after administration which we later confirmed to be tumor retention in subsequent biodistribution studies in mouse xenograft models (Figure 5b). Additionally, BAQ12O NP toxicity was characterized in mouse and rat models showing no obvious body weight changes after repeated administration of 120 mg/kg and 50-75 mg/kg respectively (Supplemental Figure 2a,b). There was also no apparent organ toxicity nor any significant changes in hematological analysis of serum or complete blood count compared to animals treated with PBS (Supplemental Figure 2c,d). In cell lines, BAQ12O had much higher IC_{50} in normal noncancerous cells including normal human donor mesenchymal stem cells (MSCs) compared to CSCs. (Supplemental Figure 2e).

BAQ12O Shows Selectivity for CSCs and Inhibits CSC Pluripotency and Tumorigenesis

Some of the key characteristics of CSCs include their self-renewal and their tumorigenic potential. BAQ12O has been shown to inhibit both functions. First, potency was noted in the CSC line compared to bulk pancreatic tumor cell lines (Figure 2a) and also in comparison to the current most potent chloroquine derivatives tested in CSCs

(Supplementary Figure 3a). Very interestingly, BAQ12O showed more potency than oxidized Lys05 (Lys05-O) and BAQ12 in CSCs as well as Lys05 itself (see structures in Supplementary Figure 3a). In fact, Lys05-O did not show any cell killing or autophagic inhibition (Supplementary 3a,b) which highlights the advantage of BAQ12O micelle formation for lysosome targeting. Another noteworthy point is that BAQ12 showed consistent toxicity in bulk and stem cell populations according to our previous work[8] while BAQ12O is far more selective to CSCs. To further this point, a direct comparison with the stem cell population was performed using two different methods in various cell lines. CSCs were differentiated with FBS[18] and Panc1 CSC population was selected by promoting stemness in tumorsphere conditions.[19] In direct comparison to CSCs and differentiated CSCs BAQ12O was a little over 5 times more potent in CSCs and in Panc1 tumorsphere cells, BAQ12O showed similar 4-fold potency compared to the whole population (Figure 2b). A similar effect was seen in other pancreatic tumor cell lines also selected for tumorsphere cells (Supplementary Figure 3c). It is also notable that this selectivity is not serum dependent, so the media interaction as seen with varying degrees of serum (10, 2.5 and 0) did not affect the IC_{50} value in MIA-PaCa2 cells normally cultured in 10% serum media (Supplementary Figure 3d) combined with the stability of BAQ12O NP in FBS (Figure 1f) shows there is an alternate explanation for BAQ12O selectivity. To verify whether BAQ12O specifically targets CSCs and tumorigenesis *in vivo*, a treatment regimen was performed to target the cells before they differentiated and formed the tumor bulk.[20] Autophagy is thought to provide a role in tumorigenesis by providing pre-malignant cells the ability to escape various stressors (e.g. metabolic, inflammatory, and genotoxic) that could prevent tumor growth,

especially in pancreatic tumors.[2, 4] CSCs were injected and allowed to graft in the mouse for one day before treatment began and continued every 3 days until palpable tumors began to form in the vehicle treated group (35 days of treatment). The groups were as follows: (i) vehicle (ii) Lys05 50 mg/kg IP (iii) BAQ12O 50 mg/kg IV (iv) BAQ12O 100 mg/kg oral administration. Lys05 was not tolerated by tail vein injection at 50 mg/kg and thus was given through intraperitoneal injection as the original authors utilized in their *in vivo* mouse models.[7] The results indicate that BAQ12O significantly impeded tumor development and had a dose response effect with the various routes of administration (IV vs. PO). After treatment ceased with palpable tumors in the vehicle group, no tumors had formed in either of the BAQ12O groups compared to 75% of tumors in the Lys05 treatment group. After allowing 2 weeks of monitoring without treatment, tumors arose in the BAQ12O groups but still with a significantly better survival outcome than the Lys05 treatment (Figure 2c). A similar result was seen *in vitro* tumorigenesis with 3D tumorsphere formation. CSCs were seeded onto Matrigel and treated with 3 mM of either BAQ12O or the precursors. Treatment with BAQ12O prevented sphere formation not only in CSC but also in two other established pancreatic cell lines. There were no spheres formed in the BAQ12O treatment while other drugs failed to prevent sphere formation that was significantly different from the group treated with vehicle (Figure 2d,e). Very interestingly, the same effect was not seen in Lys05-O or BAQ12 which failed to prevent tumor formation in the same three cell lines. Along with preventing CSC function, BAQ12O also had an effect on stem cell pluripotency markers. Pluripotency is a defining characteristic of stem cells in which certain genes participate in maintaining the characteristic undifferentiated stem cell state of CSCs.[21]

Upon quantitative analysis of mRNA, Sox2, Nanog and Oct3/4 genes were markedly decreased compared to vehicle treated CSCs. In addition, BAQ12O treatment significantly decreased expression of Sox2 protein while the precursors did not (Figure 2f,g).

BAQ12O enters CSCs through Clathrin-Mediated Endocytosis, Targets the Lysosome and causes Autophagic Dysfunction.

To verify the mechanism of BAQ12O NP uptake into the CSC we performed an endocytosis pathway study. First, CSCs were incubated in 4°C for 30 minutes and compared to 37°C conditions to determine whether drug entry was energy mediated (Figure 3a). After seeing a noticeable decrease in BAQ12O signal we then incubated cells with various endocytosis inhibitors and compared drug uptake signal. There was no significant decrease with Genistein pretreatment showing little influence of caveolae-mediated endocytosis. Macropinocytosis may account for a small percentage of uptake of BAQ12O, as there was slight decrease with amiloride pretreatment. However, this decrease was not significant. Chloropromazine showed the most significant decrease in uptake which likely indicates the higher BAQ12O dependence on clathrin-mediated endocytosis (CME). This result matches the findings of other nanoparticles which have a size around 100 nm[23] (Figure 3a). After entering the CSC through an endosome, BAQ12O reaches the lysosome within 2h (Figure 3c). Autophagic inhibition was observed with an increase in the microtubule associated light chain protein B (LC3B I and II) and Sequestosome (p62) protein markers with the divalent chloroquine derivative, Lys05, as a control (Figure 3b). Furthermore, transmission electron

microscope (TEM) images showed an increase of autophagosomes upon BAQ12O treatment as well as the presence of autophagic vacuole-like vesicles arising from lysosomal dysfunction. BAQ12O showed a prominent increase in this type of morphology particularly compared to the precursors (Figure 3d). These two experiments indicate late stage autophagic inhibition. The increase of LC3B was further evaluated by transfecting the LC3B-GFP-RFP plasmid into CSCs. This demonstrated the precise late stage of autophagy inhibition. Two main controls were used, chloroquine, which will alter the pH of the lysosome result in higher GFP and RFP signal from increased LC3B while Leupeptin does not change alter the pH by targeting lysosomal proteases and consequently shows decreased GFP signal comparatively, which is more susceptible to acidic degradation.[24] BAQ12O showed more similarity to Leupeptin while Lys05 and 12 showed more similarity to chloroquine and caused increased yellow puncta (Figure 3e,f). Finally, BAQ12O showed CSC lysosomal dysregulation by increased signal of DQ-BSA (a commercial BODIPY labeled bovine serum albumin fluorescent marker) which was unique to BAQ12O and not seen in the previous generation compounds (Figure 3g,h), matching the TEM images showing vacuole like vesicles arising from BAQ12O treatment (Figure 3d). This phenomenon is selective to the CSCs as seen by the increased LC3B signal in stably transduced LC3B-GFP-A549 cells but no DQ-BSA signal after a comparatively higher dose of BAQ12O was given (Supplementary Figure 2e).

BAQ12O Eliminates CSCs through Ferroptosis related death

Ferroptosis is a non-apoptotic form of death that was characterized by Dixon et.al. in 2012. Many papers have shown there is a close relationship between autophagy and ferroptosis and the two processes highly regulate each other. Initial interest in this pathway came from the proteomic analysis of CSCs treated with BAQ12O which were compared to untreated CSCs. In enrichment analysis, ferroptosis and associated processes showed significance in the top ten enriched pathways (Figure 4a). We also evaluated classical death pathways and saw no change in apoptosis proteins Caspase 3 or PARP cleavage or in activation of necroptosis proteins RIP3, MLKL, or HMGB1 levels (Supplementary Figure 6). To further evaluate ROS production was measured in comparison to known ferroptosis inducers, Erastin and RSL3. BAQ12O showed more significant ROS increase in CSCs and a dose dependent increase (Figure 4b). To measure the redox effect, the reduced and oxidized glutathione were measured by the GSH/GSSG ratio (GSH-reduced glutathione to GSSG-oxidized). This process is mediated by GPX4 so the ferroptosis inducer RSL3 was used as the more direct comparison.[14]BAQ12O showed again a dose dependent decrease in GSH/GSSG ratio portraying an oxidative stress profile seen in ferroptosis (Figure 4d). Labile iron was labeled with FerroOrange dye that selectively binds Fe^{2+} and produces fluorescence, compared to untreated, the amount of Fe^{2+} showed an increase with BAQ12O treatment in CSCs (Figure 4c). The main markers of ferroptosis include the resulting lipid peroxidation leading to cell death. Lipid peroxidation was seen in confocal analysis with a dose dependent increase in peroxidated lipid droplets in confocal analysis (Figure 4f) and in flow cytometric analysis using BODIPY 665/676 dye (Figure 4e). Ferroptosis genes which showed upregulation in the proteomic analysis were confirmed with qPCR

and there was significant increase in ferritin proteins (FTL, FTH1, ferritin light and heavy chain respectively) as well as in HMOX (heme oxygenase 1), another marker of oxidative stress and a marker of excess iron in pancreatic β-cells[24] (Figure 4g). The qPCR analysis also validated findings from bulk RNA sequencing performed on CSCs treated with BAQ12O. HMOX, FTL, and FTH1 all increased and many other ferroptosis associated genes (Supplementary Figure 8). Finally, Figure 4h shows increase in transferrin receptor 1 (TrF1) in CSCs, a marker of ferroptosis induction which is confirmed by the positive control RSL3 increase in TrF1 levels. BAQ12O showed more increase in CSC TrF1 compared to RSL3 treatment.

BAQ12O shows Efficacy in Combination with Current Chemotherapy and as a Maintenance Therapy to Prevent Tumor Resurgence

One important aspect of clinically relevant novel drugs is their ability to synergize with existing chemotherapeutics. Particularly in the case of cancer stem cell targeting drugs, combination is a viable strategy to target the small subset of CSCs and the bulk of the tumor simultaneously.[27] Currently, the autophagy inhibitors, HCQ and CQ, are also in clinical trials in combination with several chemotherapeutics.[3] Most recently, the addition of HCQ in combination with gemcitabine and nab-Paclitaxel even failed to improve survival outcomes.[5] Unfortunately, from clinical data, HCQ shows insufficient autophagy inhibition and moreover has notable retinopathy toxicity rate after long term use. In two separate experiments, BAQ12O showed synergy with a current standard of care drug for pancreatic cancer, gemcitabine [28] (Figure 5a). Along with synergy, BAQ12O has favorable biodistribution with selective tumor retention in mice bearing

CSC implanted tumors (Figure 5b). There was significant tumor retention that was maintained from an early stage after drug administration and low signal in other organs matching the results seen from the previous pharmacokinetic and toxicity studies (Figures 1h and Supplementary Figure 2).BAQ12O was additionally evaluated in two different treatment regimens, traditional combination chemotherapy and maintenance therapy. Maintenance therapy begins with an induction phase consisting of chemotherapeutic only which is then is substituted with another drug.[29] It has been previously shown to be a promising strategy to alleviate the toxicities of chemotherapy and promote a longer overall and progression-free survival in several types of cancers.[29, 30] In the following studies mice were subjected to one of the following treatment schedules (Figure 5c, Supplementary Figure 7). In the maintenance therapy, all groups received an induction of gemcitabine and were then separated into two groups with one receiving BAQ12O maintenance and the others receiving the vehicle control. After these treatments, a significant reduction in tumor volume was seen in the BAQ12O treated groups compared with gemcitabine treated only in all treatment regimens (Figure 5c). Upon histological analysis, there was a marked decrease in Ki67 in BAQ12O treated groups compared to gemcitabine matching the H&E staining of less viable nuclei (Figure 5d). Autophagic markers were also evaluated showing a marked increase in p62 and LC3. Both markers were evaluated to ensure autophagic inhibition as LC3 increase is also a marker of autophagic induction.[24] Western blot analysis of three tumors from each group showed autophagy inhibition and ferroptosis induction with increase of transferrin receptor as comparable to the CSC cell line result. (Figure 5e).

This result is a promising for pancreatic cancer treatment. Although the combination of HCQ with gemcitabine and nab-paclitaxel has failed, there was no analysis of the effect of autophagy inhibition in this trial. In a clinical study examining the effects of HCQ as adjuvant therapy with gemcitabine, the patients who showed a greater than 51% increase in the LC3B-II levels in their peripheral blood mononuclear cells showed improvement in disease-free survival and overall survival.[6] The drug BAQ12O we have described here is far more potent than the current most potent HCQ and CQ derivative which holds some promise for clinical translation.

Discussion

Here we have synthesized and characterized another molecule in our previously defined first-in-class series of self-assembling small molecules combining nanomedicine and medicinal chemistry properties in the ONN strategy. BAQ12O showed the ability to self-assemble into a micelle that we have further stabilized using DSPE-PEG_{2000}. TEM and DLS characterization show the BAQ12O NP micelle forms a size of approximate 130 nm. The micelle had a low critical aggregation concentration of 0.08 μM and is stable even in FBS for a week. BAQ12O NP also showed fluorescent properties that allowed for ease of imaging and due to its ability to form a NP, BAQ12O has the ability to load dyes for imaging needing a longer wavelength or to manage tissue penetration issues. BAQ12O NP also showed no obvious toxicity with a maximum tolerated dose above 120 mg/kg in mice and no obvious systemic toxicity in major organs and hematological complete blood counts and serum proteins (Supplementary Figure 2). The other notable phenomenon is that BAQ12O had a higher selectivity for CSCs

compared to normal stem cells (human MSCs) which even share 1 common marker (CD44). A future toxicity study to complete would be to compare long term usage of the drug to ensure there is no retinopathy similar to the toxicity profile seen in some patients receiving long term HCQ therapy.[5]

BAQ12O showed not only low toxicity but a selectivity for the population of the pancreatic tumor cell population, CSCs, that are often left untreated and lead to tumorigenesis and tumor recurrence. Not only did BAQ12O target this population it also effected their functions including tumorigenesis both *in vivo* and *in vitro* and pluripotency markers that determine CSC self-renewing capabilities. In these cells, BAQ12O also showed lysosomal dysfunction leading to late-stage autophagy inhibition. BAQ12O produced more vacuoles measured by DQ-BSA analysis compared to the previous generation compounds and had subsequently more potent autophagy inhibition shown by increased levels of LC3B and p62 autophagy markers compared to the same previous generation compounds. We attribute these as autolysosomes based on their ability to degrade GFP in the LC3B-GFP-RFP transfected CSCs.

This study also sheds light on the role of ferroptosis in both stem cell processes and in relation to autophagy. There is currently much debate on whether autophagy induction or inhibition induces ferroptosis. In the original characterization of ferroptosis by Dixon et.al, autophagy inhibition and ferroptosis could occur together. However, some recent reports by Mancias et. al showed that autophagy induction led to ferritinophagy in which the autophagic carrier $NCOA_4$ (nuclear receptor Coactivator 4) responsible for degrading ferritin, the iron transporter is activated causing ferritin degradation, increased iron and thus induction of ferroptosis. Further studies showed that RSL3, the

GPX4 inhibitor causing ferroptosis bypasses ferritinophagy[31] which agrees with our results. The likely method in this case is oxidative stress resulting from inability to manage ROS and labile Fe levels as well as a decline in oxidative stress response systems including glutathione. In any case, our study looking at pancreatic CSCs provides a novel targeting strategy of both inhibiting autophagy and inducing ferroptosis provides a promising perspective for CSC targeting drugs.[16] Future studies can involve precisely which autophagic marker is causing the ferroptosis induction ruling out ferritinophagy.

Finally, this mechanism provided potent *in vivo* efficacy in mouse engrafted with CSC tumors. Particularly, the ability to work synergistically with the current standard of care for pancreatic cancer, gemcitabine. These results combined with its excellent safety profile and biodistribution showing tumor targeting and retention indicate there is a promising translational application of this drug to clinic. Future studies not completed in this work include evaluating BAQ12O in orthotopic and immune competent tumor models which will be required for future translation. Autophagy has already been shown to be an important process for immune cell evasion of pancreatic cancer.[32] Currently, there is no specific clinical drug against CSCs. Additionally, HCQ and CQ are approved for use as autophagy inhibitors but show inconsistent autophagy inhibition in clinic. The drug we have designed in this project tackles these issues by showing a more potent autophagy inhibition than the current most potent chloroquine derivatives as well as targeting CSCs. There is also currently no ferroptosis inducer available for clinical use. Thus, BAQ12O provides several unique advantages to address the highly lethal nature of pancreatic cancer. In addition, its ability to self-deliver and ease of scale

up make it a promising translational compound. Its nanoparticle qualities make functionalization and load carrying capabilities make its application in drug delivery feasible and relevant to more autophagy-dependent tumor subtypes.

Figure 1: BAQ12O Nanoparticle Characterization

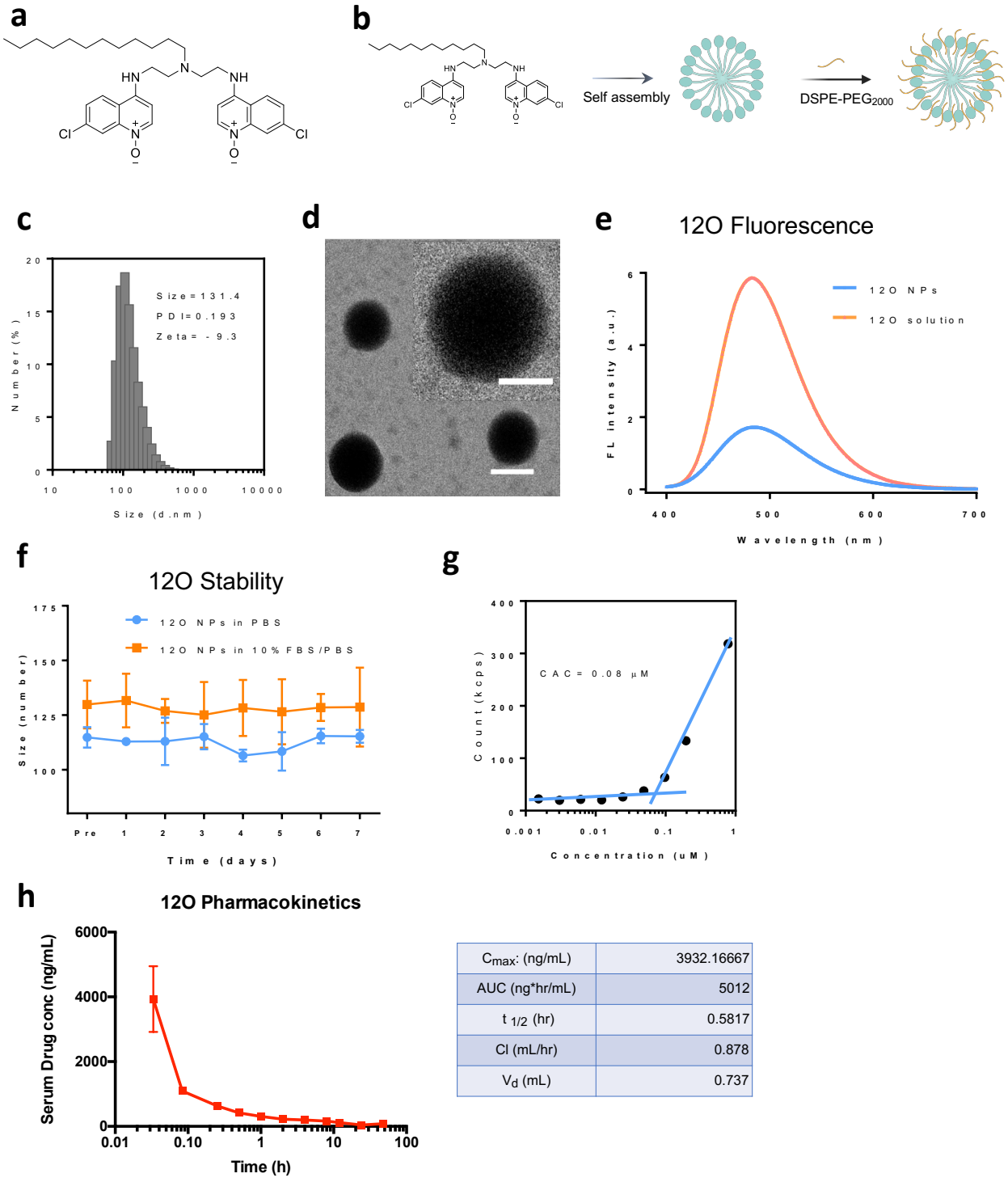

C_{max}: (ng/mL)	3932.16667
AUC (ng*hr/mL)	5012
$t_{1/2}$ (hr)	0.5817
Cl (mL/hr)	0.878
V_d (mL)	0.737

FIGURE 1: BAQ 12O Nanoparticle Characterization

a Structure of bisaminoquinolone nitric oxide BAQ12O **b** Scheme to self-assemble BAQ12O into nanoparticle and pegylation with DSPE-PEG2000 for added stability. **c** Dynamic Light scattering of BAQ12O showing nanoparticle size of 131 nm. Zeta potential was also measured at -9.3 ζ. **d** Transmission Electron Microscopy image of BAQ12O showing micelle formation and size of 130 nm. Zoom in on top right. Scale bar is 100 nm. **e** Fluorescence intensity of BAQ12O in nanoparticle form as well as in solution. BAQ12O showed an excitation/emission of 385/506 λ **f** Stability of BAQ12O nanoparticle in FBS vs. PBS solution. **g** Critical aggregation concentration of BAQ12O NP is 0.08 μM. **h** Serum blood concentration of BAQ12O in Pharmacokinetic study of rats given BAQ12O IV injection. Average of n=3. Parameters calculated from a 2-compartment model.

Figure 2: BAQ12O shows selectivity for CSCs and inhibits CSC Pluripotency and Tumorigenesis

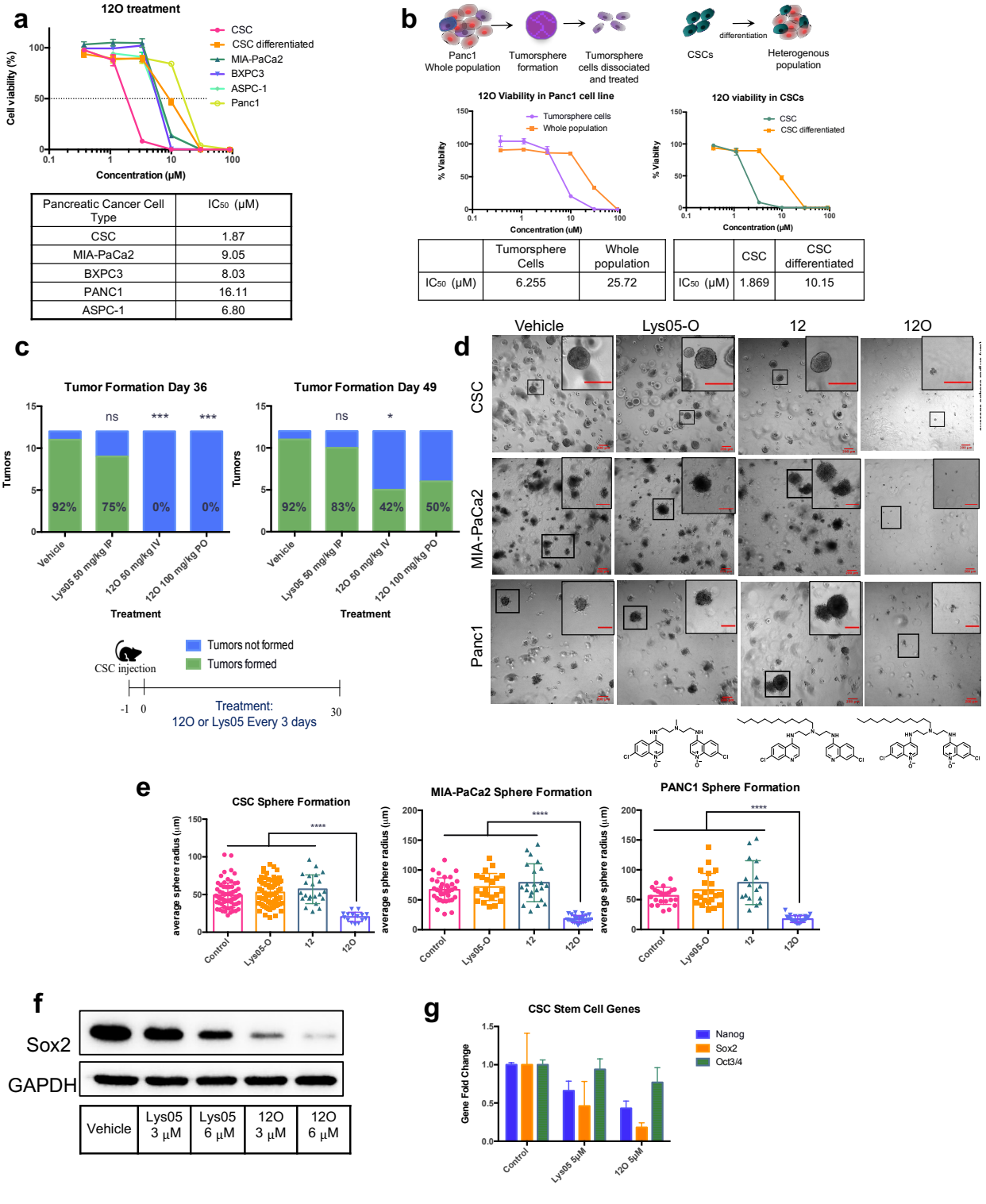

Pancreatic Cancer Cell Type	IC_{50} (μM)
CSC	1.87
MIA-PaCa2	9.05
BXPC3	8.03
PANC1	16.11
ASPC-1	6.80

	Tumorsphere Cells	Whole population
IC_{50} (μM)	6.255	25.72

	CSC	CSC differentiated
IC_{50} (μM)	1.869	10.15

Figure 2: BAQ12O shows selectivity for CSCs and inhibits CSC Pluripotency and Tumorigenesis

a IC_{50} screen of BAQ12O in various pancreatic cell lines. **b** IC_{50} screen of tumorsphere cells collected from Panc1 cells grown in nonadherent conditions and differentiated CSC cells shown in the scheme above. BAQ12O is more potent in the population with more stem-like characteristics. **c** Tumorigenesis in vivo shown in treatment schedule below, tumor formation was evaluated after drug treatment finished at the indicated time points. Tumors formed and compared to number of tumors injected in mice. Treatment began after CSC implantation. Statistics were calculated using χ^2 analysis. **d** Tumorigenesis evaluated in vitro measuring tumorsphere production after seeding cells (CSCs, MIA-PaCa2, and Panc1) in matrigel. Structures of drugs shown below of precursors and previous generation compounds. Scale bar of whole and zoomed in window are 200 μm. **e** Quantification of sphere or cells. Student's t test was used to calculate p value. **f** Western blot analysis of stem cell marker Sox2 in treated CSCs. **g** Decrease in stem cell markers of CSCs in qPCR analysis.

Figure 3: BAQ12O enters CSCs through clathrin-mediated endocytosis, targets the lysosome and causes autophagic dysfunction.

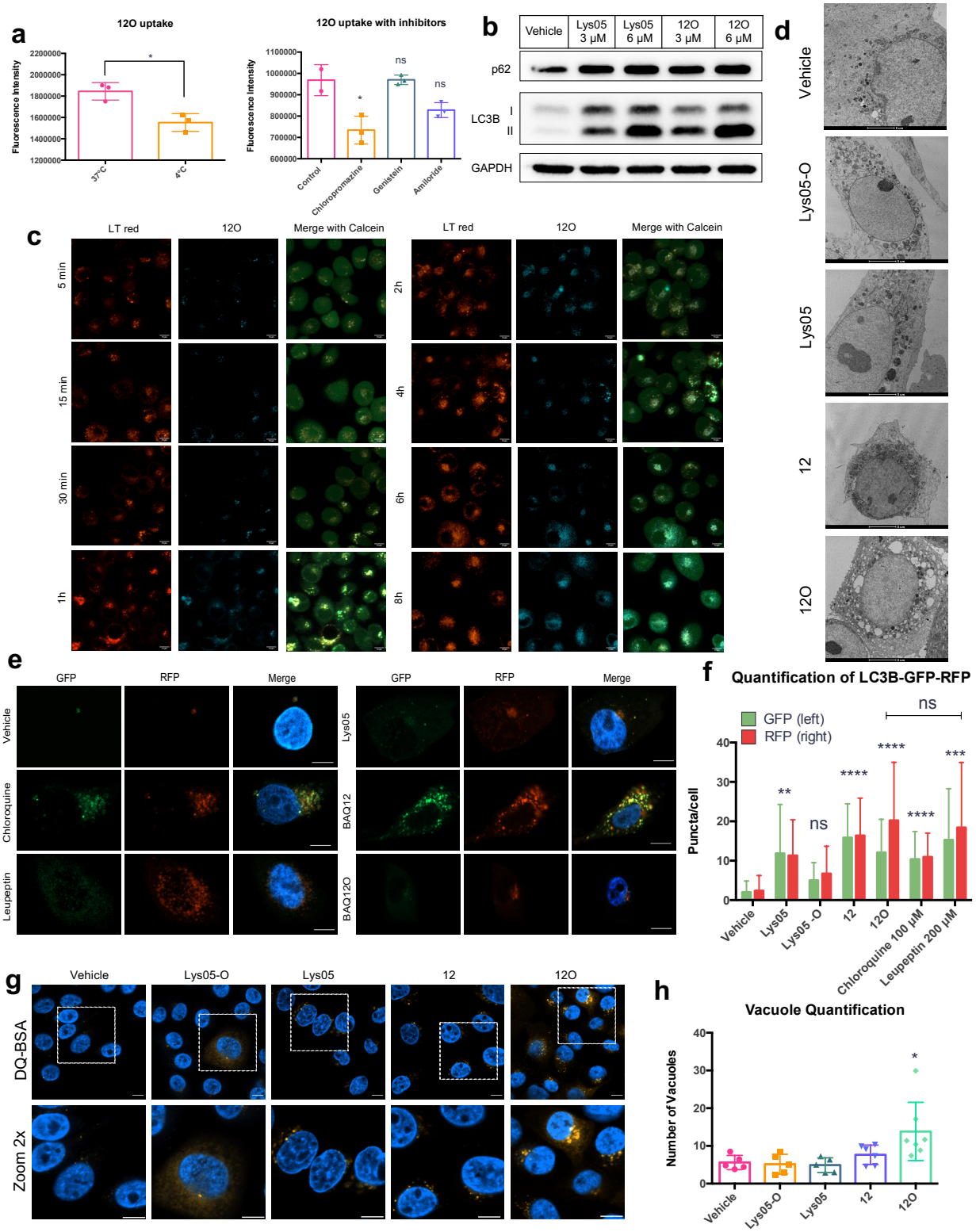

Figure 3: BAQ12O enters CSCs through clathrin-mediated endocytosis, targets the lysosome and causes autophagic dysfunction.

a BAQ12O signal after treatment with the indicated temperatures or inhibitors in CSCs. Student's t test was used to calculate p value. **b** Immunoblotting of autophagy proteins p62 and LC3B after 24h treatment at the indicated doses in CSCs. **c** time course of BAQ12O uptake into CSC with lysotracker red staining, drug fluorescence and Calcein as a viable cell maker. **d** TEM image of BAQ12O treated CSCs compared to Lys05, Lys05-O, 12 and vehicle treated CSCs. More vacuolization is seen in 12O treated CSCs. Scale bar=5 μm **e** Transfected CSCs with LC3B-GFP-RFP along with indicated drug treatments Lys05, 12, 12O at 3μM and controls Chloroquine 100 μM, Leupeptin A 200 μM for 16h. Hoechst 33342 used to stain nucleus. Pictures have been edited to focus on 1 representative cell from each group. Scale bar=10μm **f** Quantification of GFP and RFP puncta. p value from Student's t test. **g** Vacuoles shown DQ-BSA after 16h treatment in CSCs. Pictures were zoomed in 2x to show vacuoles. Scale bar=10μm. **h** DQ-BSA vacuoles quantified. p value from Student's t test.

Figure 4: BAQ12O Eliminates CSCs through Ferroptosis related Death

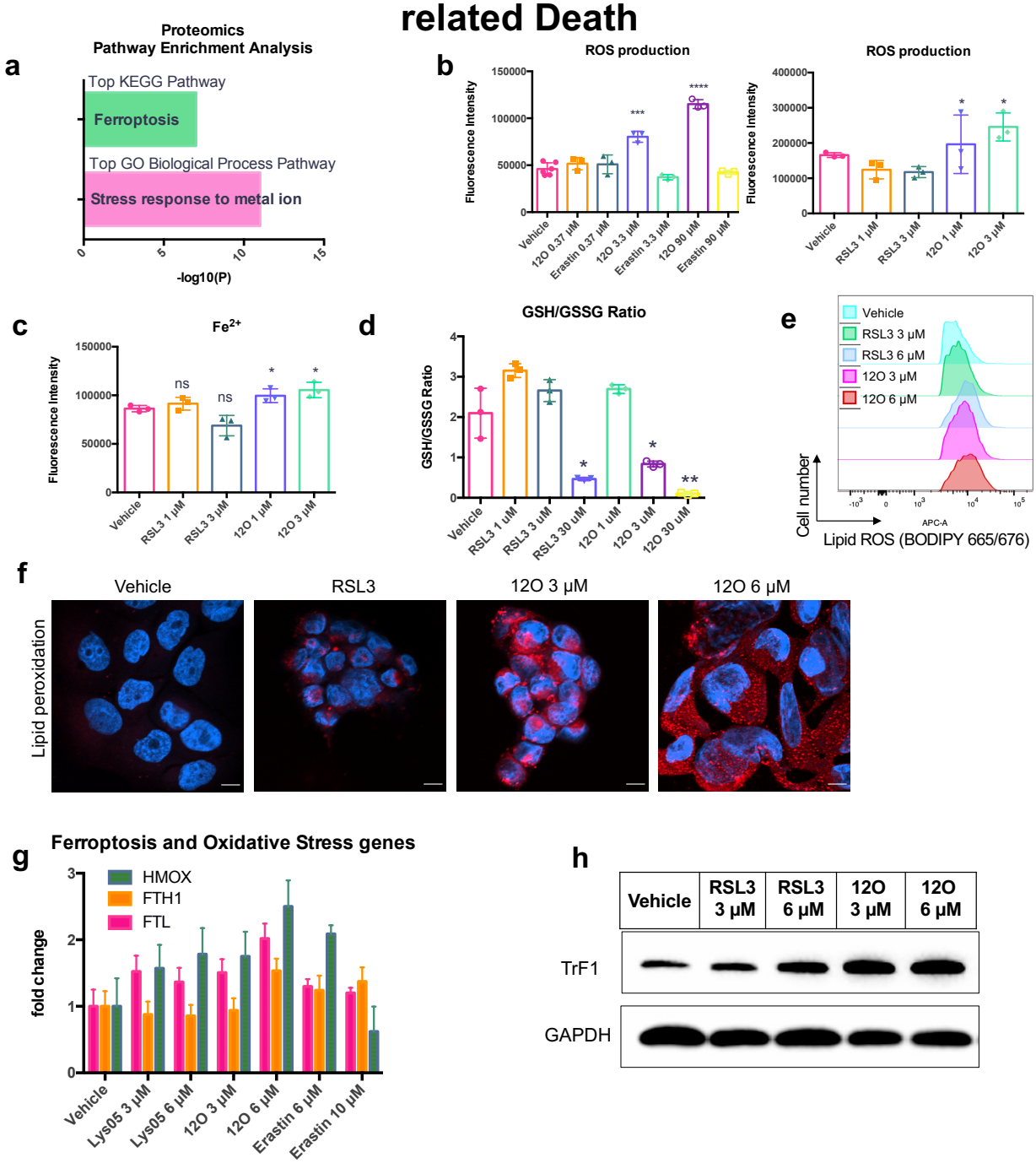

Figure 4: BAQ12O Eliminates CSCs through Ferroptosis related Death

a Pathway enrichment analysis from proteomic analysis of CSCs treated with BAQ12O and vehicle treated cells. Ferroptosis and related pathways highly significant among all proteins showing a significant change between vehicle treated and BAQ12O treated CSCs. The top pathways from GO Biological Pathways and KEGG databases are shown **b** ROS production measured by DCF-DA fluorescence signal showing increased ROS production with BAQ12O treatment with two ferroptosis inducers, Erastin and RSL3 in CSCs. p value calculated using Student's t test. **c** Labile Fe signal measured with FerroOrange dye after drug treatment for 24h in CSCs. p value calculated using Student's t test. **d** Oxidized glutathione ratio measured 24h after the noted concentration of drug. More potent decrease of glutathione redox potential with BAQ12O treatment in CSCs. **e** Flow cytometry analysis of CSCs stained with BODIPY 665/676 dye after 24h of indicated drug treatment. **f** Lipid peroxide staining using BODIPY 665/676 dye in CSC after indicated drug treatment (RSL3 = 6μM). Increased lipid droplets with peroxidation with treatment. Representative pictures shown with 10 μm scale bar. **g** qPCR of ferroptosis and oxidative stress genes after treatment for the indicated doses for 24h. **h** Western blot analysis of Fe transporter transferrin receptor in CSC lysates collected after 24h drug treatments.

Figure 5: BAQ12O shows tumor targeting and efficacy in combination with current chemotherapy and as a maintenance therapy to prevent tumor resurgence

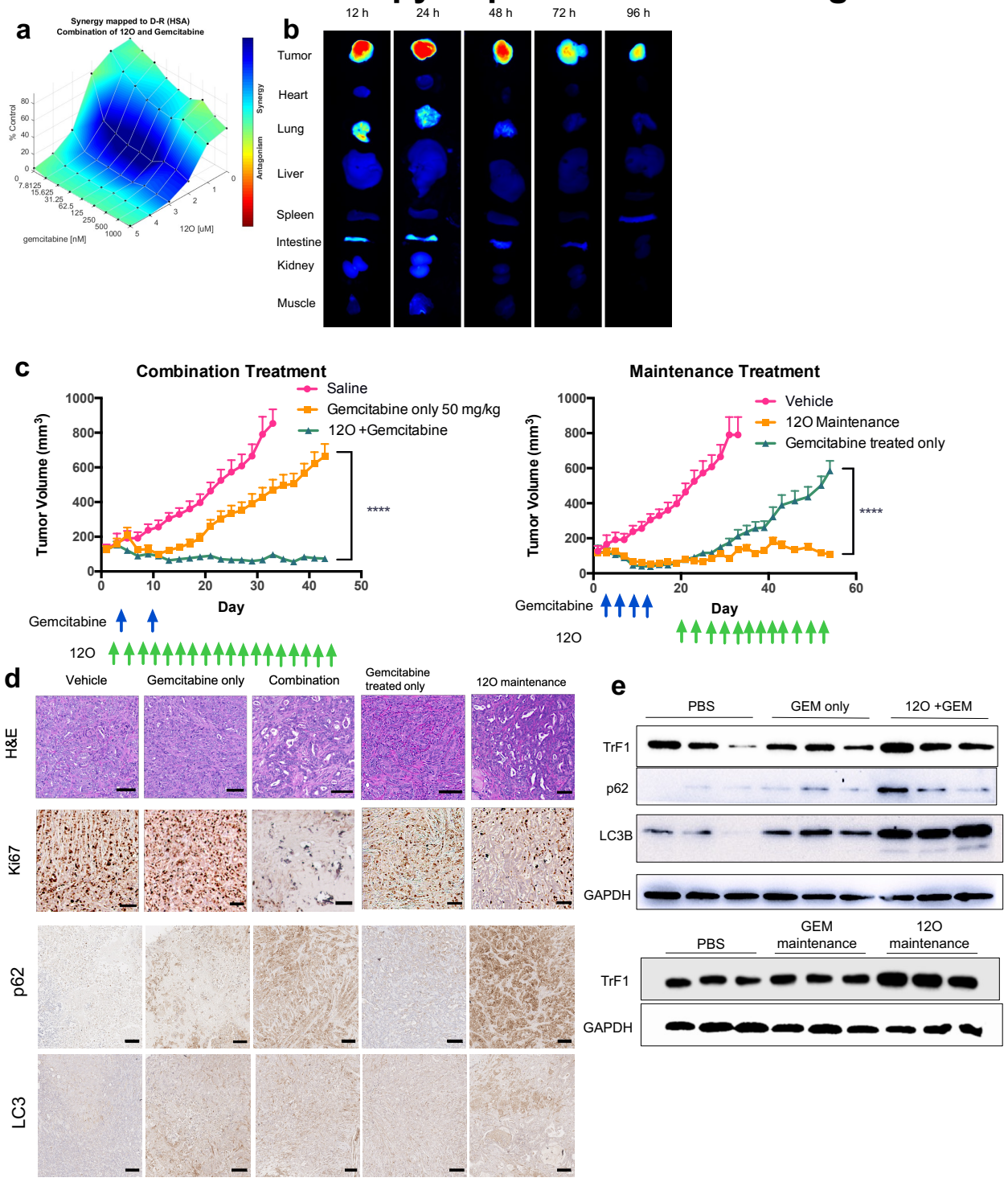

Figure 5: BAQ12O shows Tumor Targeting and Efficacy in Combination with Current Chemotherapy and as a Maintenance Therapy to prevent Tumor Resurgence

a Combination synergy between Gemcitabine and 12O. Calculated from n=3 independent replicates. **b** Ex-vivo Biodistribution of 12O in CSC tumor mouse models. **c** Tumor volumes for combination and maintenance treatment regimens. Gemcitabine was given 50 mg/kg IP either once or twice/week and 12O was given 50 mg/kg IV either 2 or 3 times/week for the indicated period. **d** Representative histological analysis of tumors from both treatment regimens along with immunohistological staining of Ki67, p62 and LC3. Scale bar is 100μm. **e** Western blot analysis of individual tumor samples from each group for ferroptosis markers and autophagy markers.

SUPPLEMENTARY FIGURES

Supplementary Figure 1: Chemical Characterization of BAQ12O

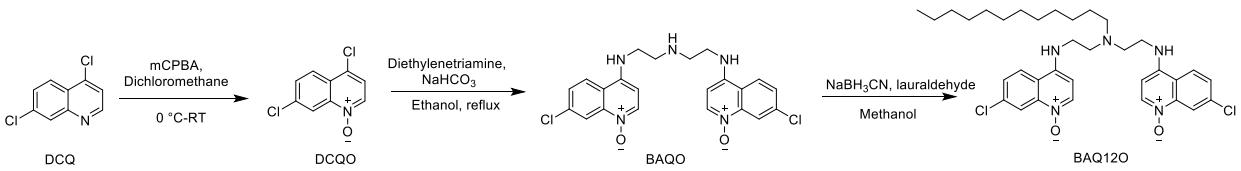

Chemical synthesis of BAQ12O

1. Synthesis of DCQO. 4,7-dichloroquinoline (2 g, 10 mmol) was dissolved in 50 mL and was vigorously stirred (500 rpm) on an ice-water bath for 15 min. mCPBA (2.7 g, 12 mmol) was added carefully in bath (4 times) to the reaction solution. The resulting reaction mixture was allowed to stir (500 rpm) at room temperature for 12 hr. TLC indicated complete conversion of starting materials to one major spot. Dichloromethane (100 mL) and potassium carbonate (4.1 g, 30 mmol) were added to the reaction solution, which was stirred (300 rpm) for 1 hr at room temperature. The mixture was poured into a 500 mL beaker containing 200 mL water and stirred (300 rpm) for another 1 hr. (The organic phase was collected, washed with saturated sodium carbonate (75 mL×3), water (75 mL×3), brine (75 mL×3), respectively, and dried with anhydrous sodium sulfate overnight. After filtration, solvent was evaporated under reduced pressure, and the resulting crude material was recrystallized with 80 mL acetonitrile. The resulting solid product was filtered for collection, and then was dried under vacuum to afford 1.8 g DCQO as white solid. ^{1}HNMR (600 MHz, $CDCl_3$) δ 8.79 (d, J=1.8 Hz, 2 H), 8.44 (d, J=6.6 Hz, 2 H), 8.44 (d, J=8.4 Hz, 2 H), 7.71 (d, J_1=9.0 Hz, J_2=2.4 Hz, 2 H), 7.38 (d, J=6.0 Hz, 2 H). HRMS (ESI): m/z calculated for $C_9H_6Cl_2NO$ $[M+H]^+$ 213.9821, found 213.9834.

Supplementary Figure 1a: H^1NMR spectra of DCQO in $CDCl_3$.

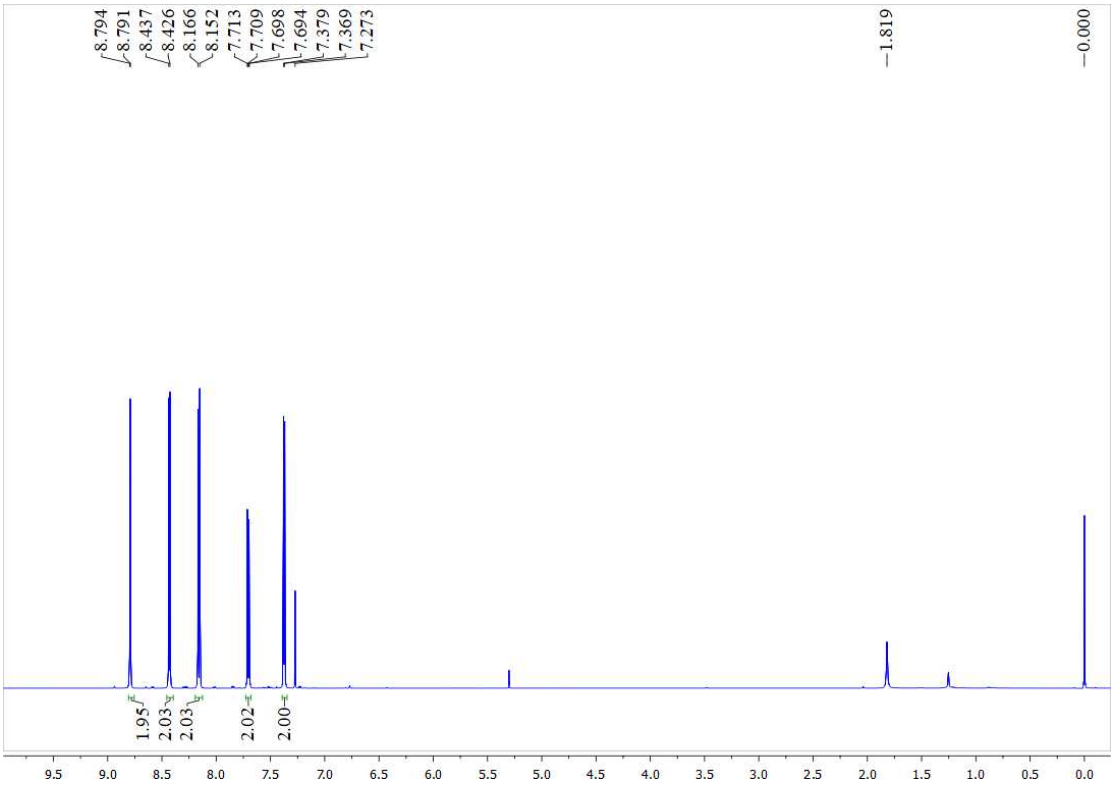

Supplementary Figure 1b: Mass spectra of DCQO

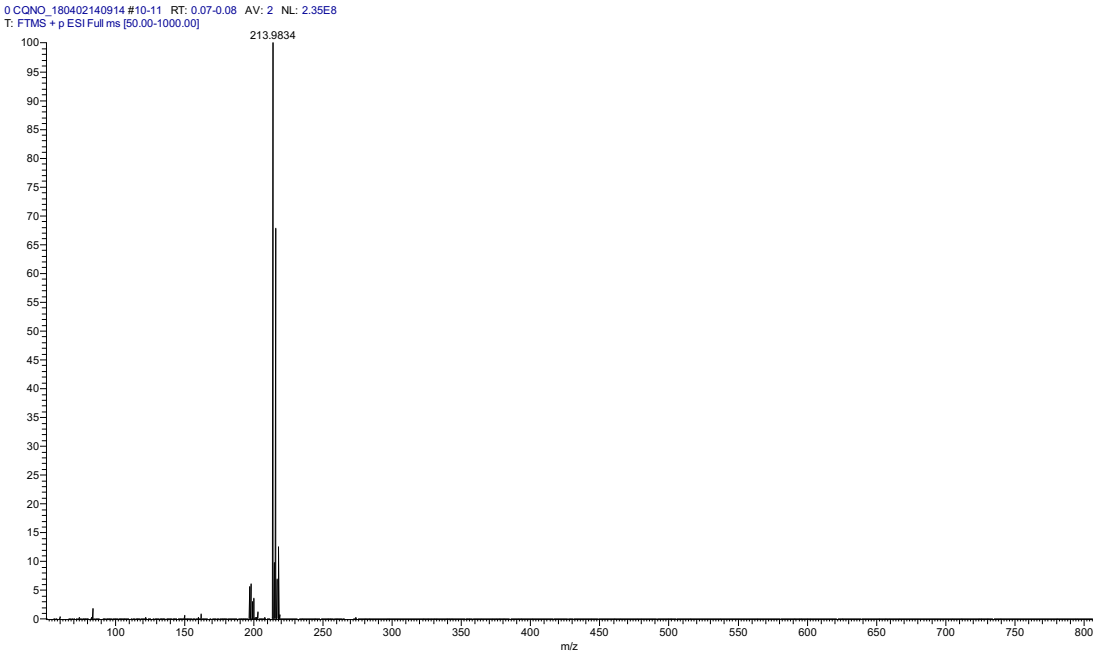

2. Synthesis of BAQO. Sodium bicarbonate (840 mg, 10 mmol) and diethylenetriamine (432 μL, 4 mmol) were added to the solution of DCQO (2.14 g, 10 mmol) in 30 mL anhydrous ethanol. The mixture was refluxed at 95 °C for 48 hr. TLC was used to indicate the generation of the target materials material (TM, the yellow spot). Ethanol was evaporated under reduced pressure and the residue was re-resuspended by 30 mL methanol, which was slowly dropped into a 300 mL beaker with the mixed solution of 100 mL hydrochloric acid (1 M) and 50 mL dichloromethane. The aqueous phase was collected, washed with dichloromethane (50 mL×2), alkalized to pH 10 using 10 M NaOH (12 mL) to generate yellow precipitation. The precipitation was collected, washed by water (30 mL×3) and dried under vacuum to afford 850 mg BAQO as yellow solid. ^{1}HNMR (600 MHz, CD_3OD) δ 8.51 (d, J=1.8 Hz, 2H), 8.35 (d, J=7.2 Hz, 2H), 8.14 (d, J=9.0 Hz, 2H), 7.55 (d, J_1=9.0 Hz, J_2=2.4 Hz, 2H), 6.63 (d, J=7.2 Hz, 2H), 3.58 (t, J=6.0 Hz, 4H), 2.94 (t, J=6.0 Hz, 4H). HRMS (ESI): m/z calculated for $C_{22}H_{22}Cl_2N_5O_2$ $[M+H]^+$ 458.1145, found 458.1126.

Supplementary Figure 1c: H^1NMR spectra of BAQO in CD_3OD

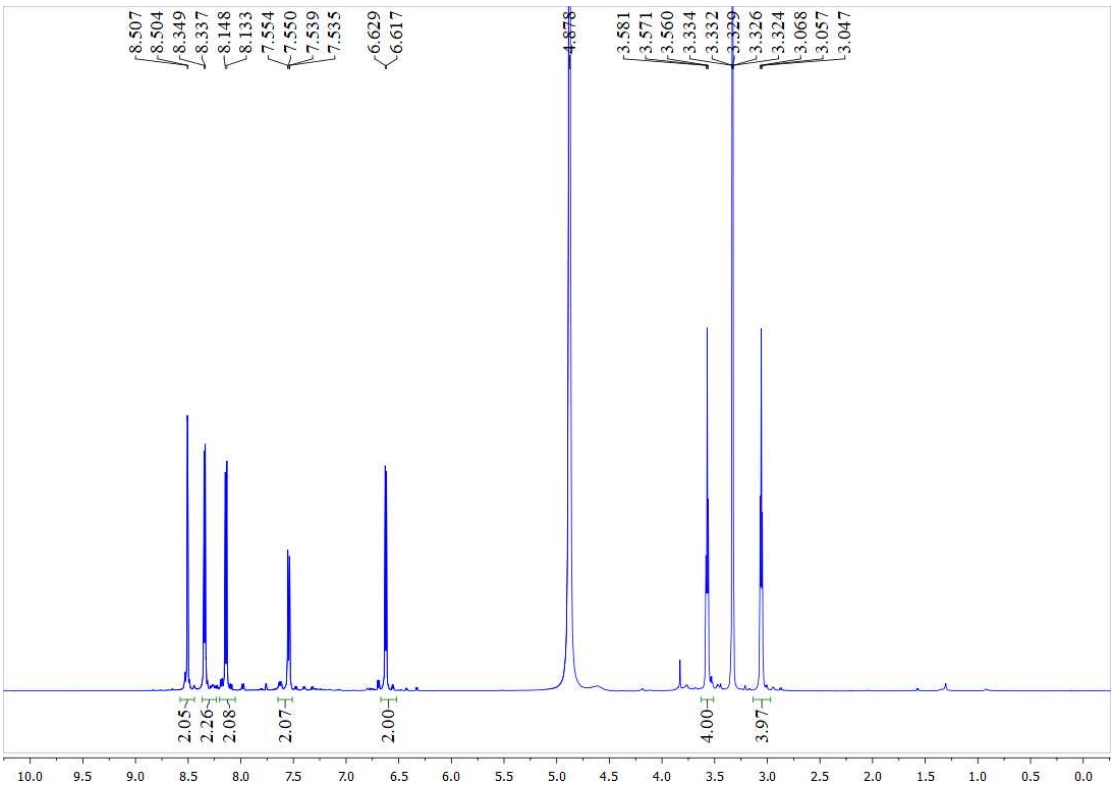

Supplementary Figure 1d: Mass spectra of BAQO

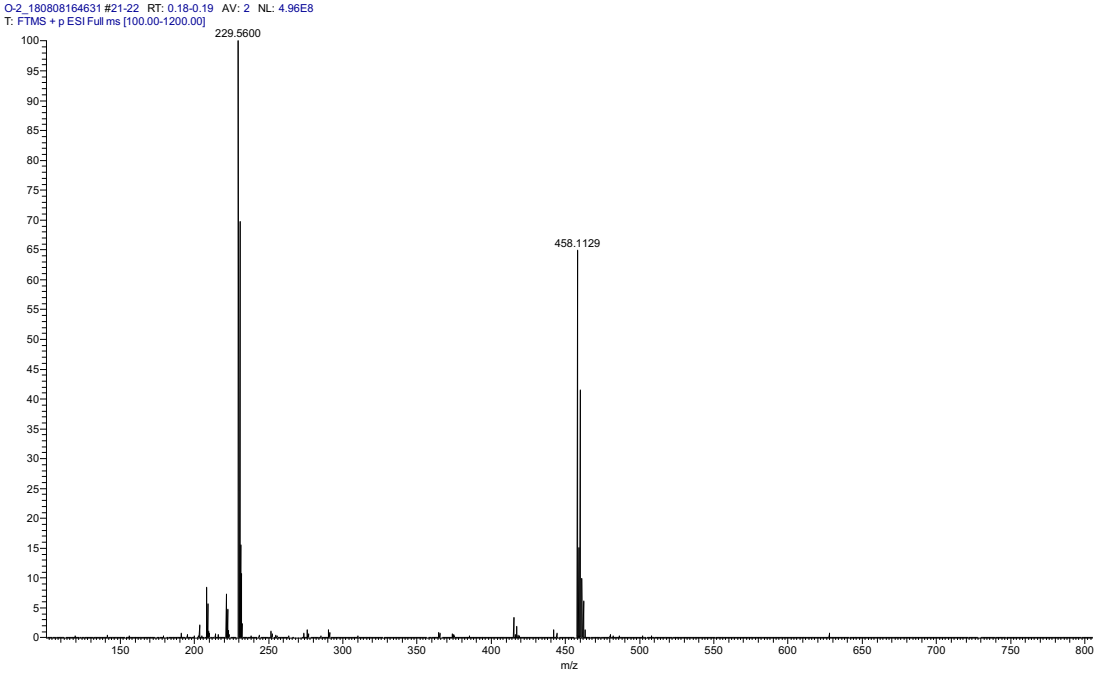

3. Synthesis of BAQ12O. The mixture of BAQO (916 mg, 2 mmol), dodecyl aldehyde (1.8 mL, 8 mmol) and acetic acid (20 μL) was vigorously stirred (500 rpm) at room temperature for 30 min. Sodium cyanoborohydride (377 mg, 6 mmol) was then added slowly. The reaction mixture was stirring at room temperature for another 12 hrs. TLC indicated the complete conversion of starting materials to one major spot. The solvent was concentrated to 25 mL and then the resulting residue was diluted in 75 ml dichloromethane). The organic phase was washed with 100 mL saturated sodium bicarbonate three times. The emulsion layer was collected, and then was filtered to provide a yellow solid, which was washed by water (30 mL ×3) and ethyl ether (30 mL ×3). The collected yellow solid was dried under vacuum to afford 1.2 g BAQ12O. ^{1}HNMR (CD3OD, 600MHz) δ 8.43 (d, *J*=1.8 Hz, 2H), 8.31 (d, *J*=7.2 Hz, 2H), 7.82 (d, *J*=9.0 Hz, 2H), 7.31 (d, J_1=9.0 Hz, J_2=2.4 Hz, 2H), 6.56 (d, *J*=7.2 Hz, 2H), 3.50 (t, *J*=6.0 Hz, 4H), 2.94 (t, *J*=6.0 Hz, 4H), 2.71 (t, *J*=7.2 Hz, 2H), 1.55 (m, 2H), 1.32 (m, 18H), 0.92 (t, J_1=6.6 Hz, 3H). CNMR (CD_3OD, 150MHz) δ 148.0, 140.1, 139.9, 138.4, 127.6, 123.9, 118.7, 117.9, 98.09, 54.9, 52.3, 41.5, 32.4, 30.2, 30.1, 30.1, 29.8, 28.1, 27.7, 23.1, 13.8. HRMS (ESI): m/z calcd for C34H46Cl2N5O2 [M+H]+ 626.3023, found 626.3060.

Supplementary Figure 1e: H^1NMR spectra of BAQ12O in CD_3OD

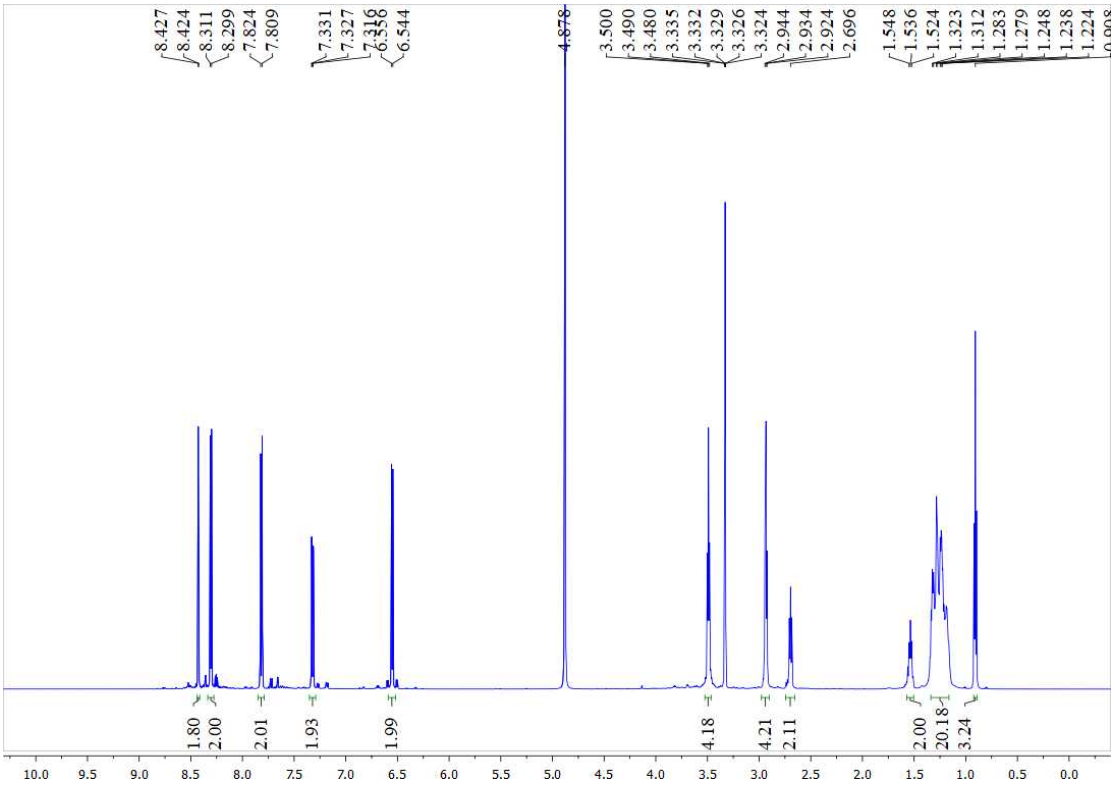

Supplementary Figure 1f: Mass Spectra of BAQ12O

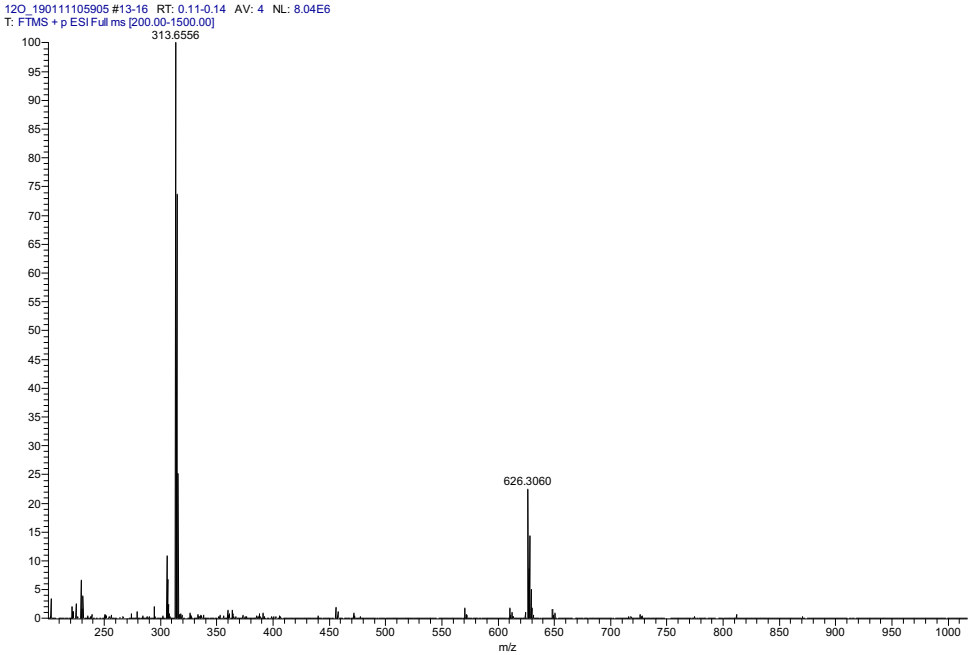

Supplementary Figure 1g: C^{13}NMR spectra of BAQ12O in CD_3OD

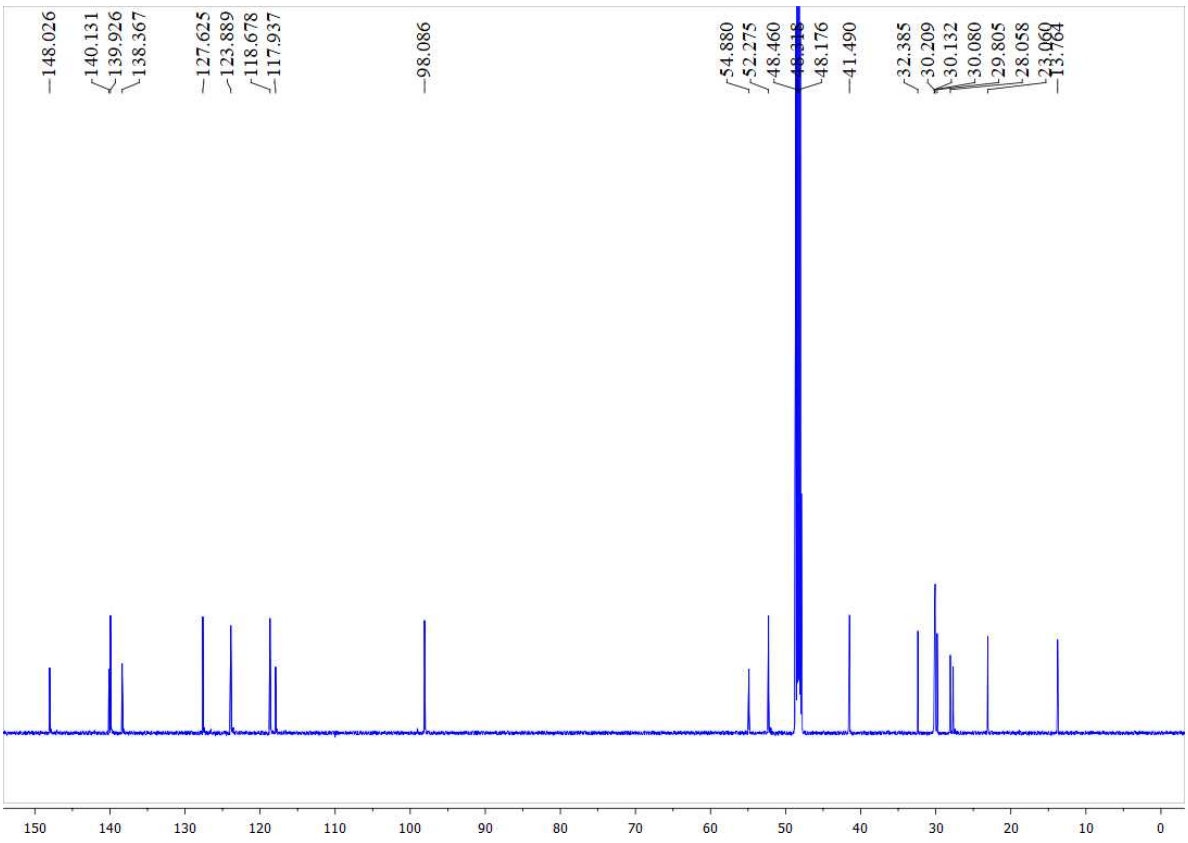

Supplementary Figure 2: 12O Toxicity

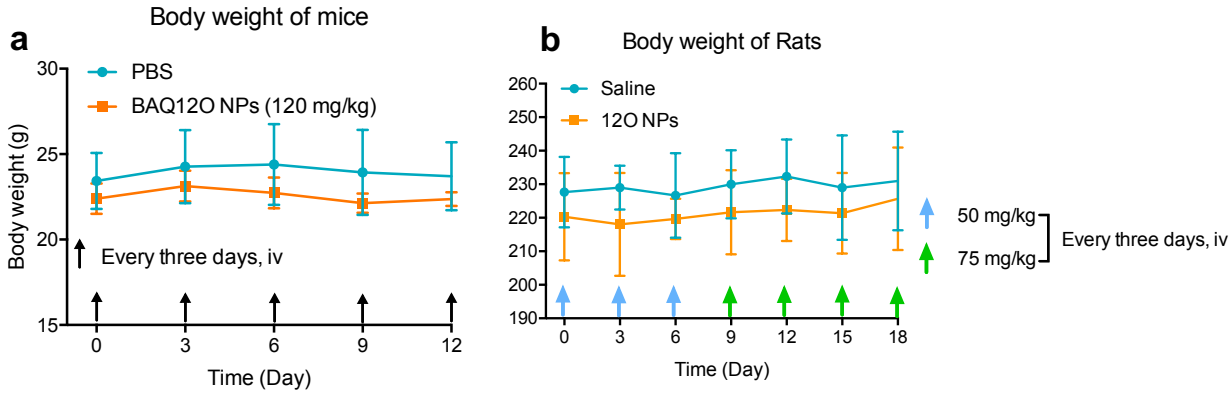

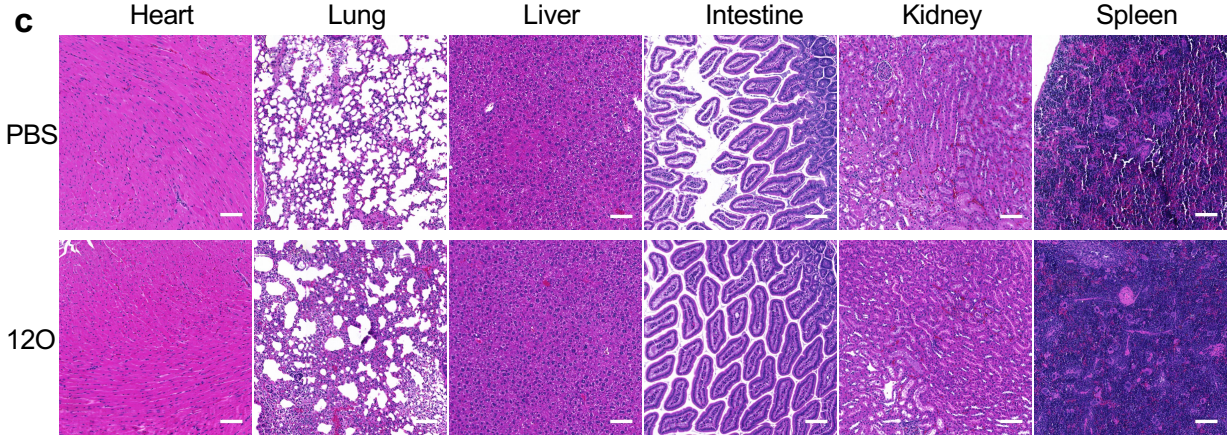

d

	RBC	WBC	Platelets	ALP	Bilirubin	BUN	Creatinine	Albumin	Glucose
Mouse-PBS	10.48±0.91	10.3±1.2	374±47	79±42	0.4±0.1	19.5±1.4	0.3±0.1	2.9±0.2	128±32
Mouse-12O	11.0±0.15	9.4±0.5	386±69	99±14	0.8±0.2	19.2±0.8	0.2±0.0	2.9±0.1	114±2

	RBC	WBC	Platelets	ALP	Bilirubin	BUN	Creatinine	Albumin	Glucose
Rat-PBS	8.25±0.91	12.6±4.9	162±73	320±91	0.4±0.4	20.1±7.3	0.4±0.1	4.5±0.2	164±107
Rat-12O	7.87±0.31	10.2±2.6	195±114	317±103	0.4±0.4	27.4±5.3	0.5±0.2	4.3±0.4	114±8

e

Cell line	NIH-3T3	human MSC
IC_{50} (μM)	13.91	11.2

Supplementary Figure 2: BAQ12O Toxicity

a-b Systemic toxicity in (a) mouse and (b) rat given BAQ12O in the listed treatment regimens. No obvious loss of body weight in either species. **c** Representative H&E images of main organs in mice. No obvious pathological toxicities. Scale bar is 100 μm. **d** Representative hematologic indexes in mouse and rat. Tissue or blood samples collected 12h after last administration. Data is shown as mean ± SD, n=3. **e** IC50 evaluated in non-cancerous cells. MSC are mesenchymal stem cells collected from 2 different donors, IC50 is average from two donors. Each value was calculated from n=3 independent experiments incubated for 48h.

Supplementary Figure 3: 12O is more potent than precursors and selective to CSCs

a

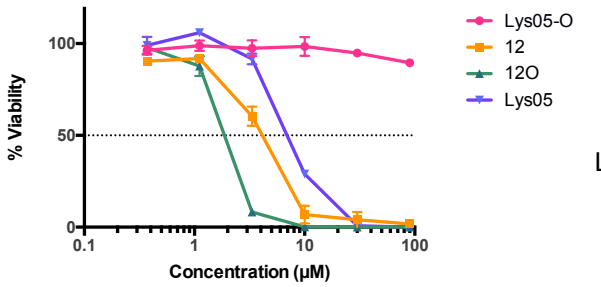

	Lys05-O	Lys05	12	12O
IC_{50} (μM)	>90	7.212	3.987	1.869

b

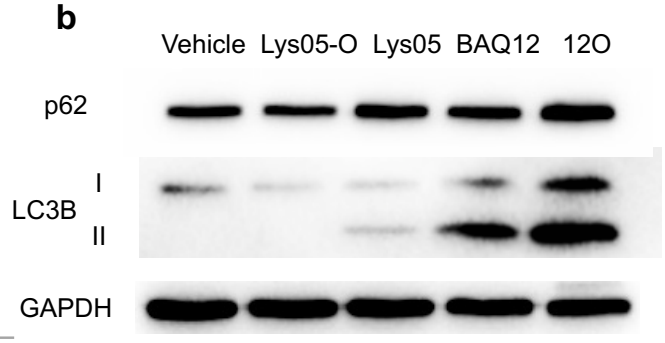

Lys05-O

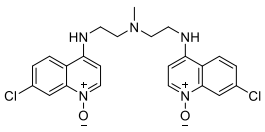

Lys05

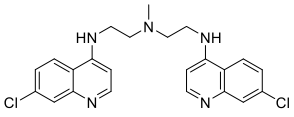

BAQ12

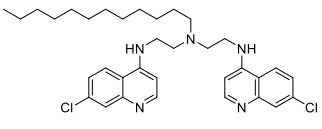

BAQ12O

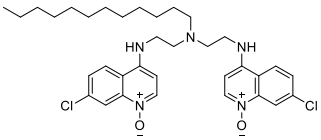

c

IC_{50} (μM)	Tumorsphere cells	Whole population
ASPC1	2.488	12.43
Panc1	6.255	25.72
BXPC3	1.399	8.496
MIA-PaCa2	2.404	15.78

Panc1 Tumorspheres before dissociation and collection

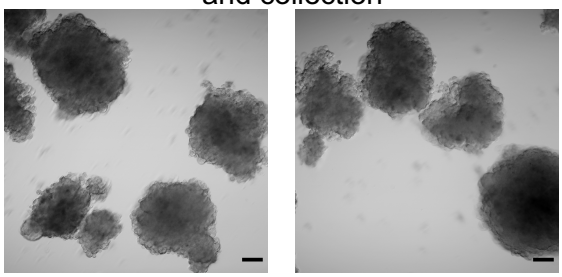

DQ-BSA | LC3B-GFP | Merged

d

MIA-PaCa2 conditions	IC_{50} (μM)
10% serum	13.36
2.5% serum	9.48
Human Serum Albumin (HSA) 2 mg/mL	10.11

e

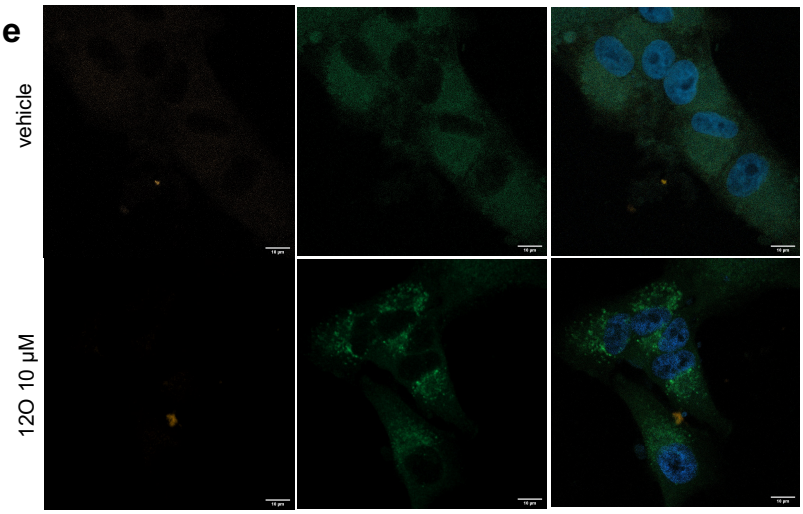

Supplementary Figure 3: BAQ12O is more potent than precursors and selective to CSCs

a BAQ12O is the most potent in the CSC cell line. Previous generation and their structures are shown below including Lys05 and its oxidized form Lys05-O, BAQ12 and BAQ12O for comparison. **b** BAQ12O is the most potent in in inhibiting autophagy compared to the precursors showing the most increase in autophagic markers p62 and LC3B in the following western blot in CSC treated lysates. **c** Screening of IC_{50} in tumorsphere cells using different pancreatic cancer cells which were cultured in sphere forming conditions and compared to their normal media and culture conditions. Shown on right is Panc1 tumorspheres before being dissociated and collected. Scale bar is 100 μm. **d** Selectivity of BAQ12O is not due to serum binding and inactivation of drug. MIA-PaCa2 cell line was cultured in the following conditions and BAQ12O was treated for 48h. Each IC_{50} is relative to untreated cells in that specific condition and n=3. **e** DQ-BSA seen clearly in CSC cells after BAQ12O treatment is not seen in A549 containing stably transduced LC3-GFP vector. BAQ12O dose was increased showing autophagy inhibition but no signal from DQ-BSA was observed.

Supplementary Figure 4: Hemolysis

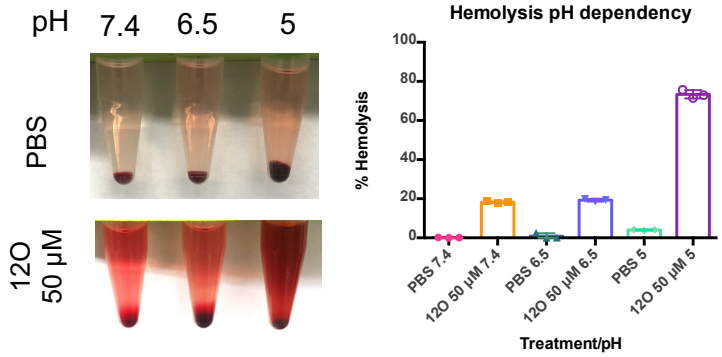

Supplementary Figure 4: Hemolysis

Hemolysis: pH dependent hemolysis. Red blood cells were treated as indicated for 4h. Representative images are shown. n=3. Hemolysis was measured by absorbance at 541 nm.

Supplementary Figure 5: Endocytosis

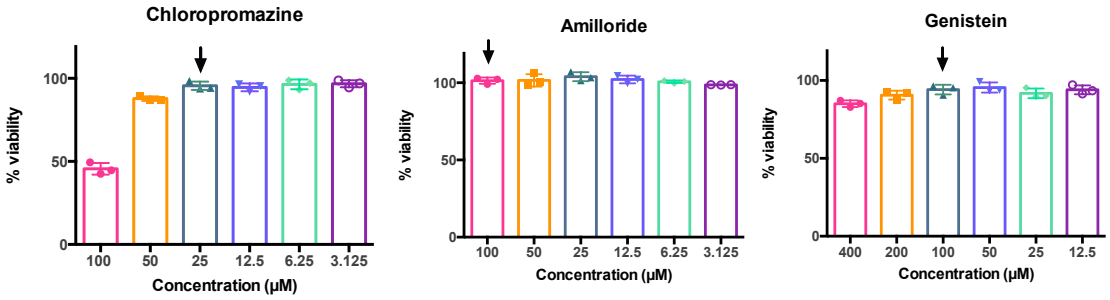

Supplementary Figure 5: Endocytosis

Endocytosis: Cytotoxicity of endocytosis inhibitors on CSC. CSCs were incubated with the inhibitors for 30 min. n=3 Arrows indicate the dose of drug used in the experiment.

Supplementary Figure 6: Death Pathways

a Apoptosis

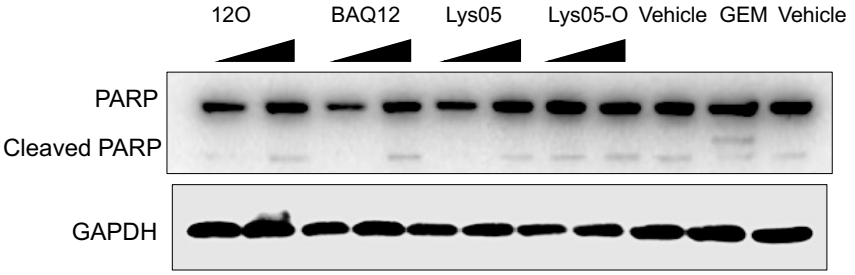

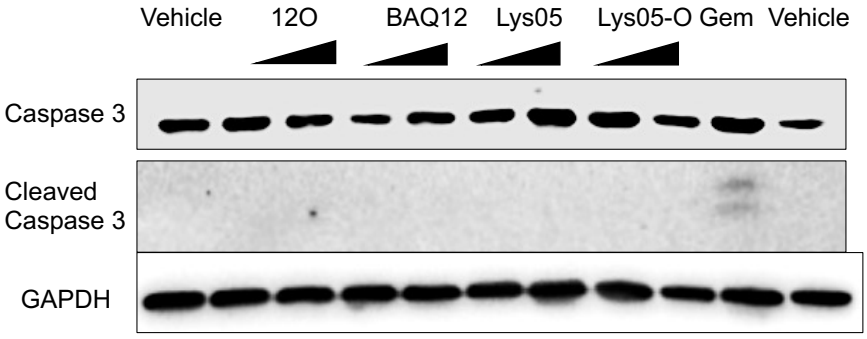

b Necrosis

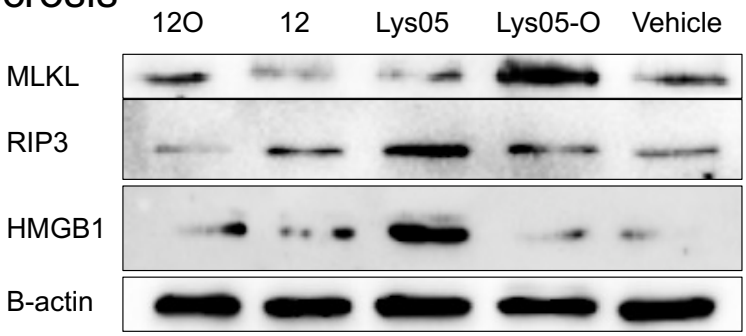

c Ferritinophagy

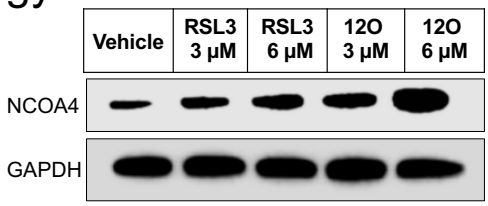

Supplementary Figure 6: Death Pathways

a-b immunoblotting for the following apoptosis and programmed necrosis proteins in CSCs. There is no significant difference with vehicle treated group at a toxic dose of BAQ12O in cleaved caspase 3, cleaved PARP, MLKL, RIP3, or HMGB1. Other precursors were included for comparison. GEM=gemcitabine as an apoptosis positive control. **c** Western blot for measuring ferritinophagy marker NCOA4 which shows increase in both RSL3 ferroptosis inducer as well as BAQ12O treated CSC lysates. Indicating that ferroptosis induction is not caused through ferritinophagy in CSCs with BAQ12O.

Supplementary Figure 7: Treatment Schedules

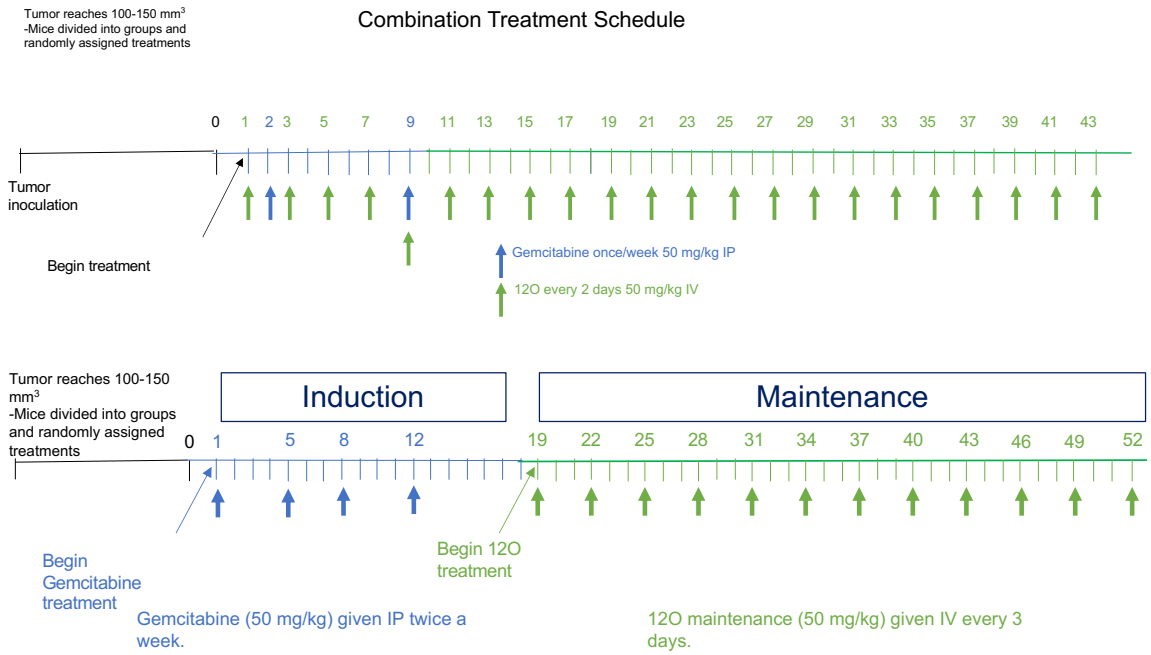

Supplementary Figure 7: The treatment schedules for the mouse efficacy studies. CSCs were engrafted in the mouse flanks and allowed to grow until the tumor reached 100-150 mm^3 upon which the following treatment regimens were started. The bottom maintenance shows the phases of treatment including the induction with no BAQ12O treatment then maintenance to prevent regrowth.

Supplementary Figure 8: RNA sequencing data ferroptosis

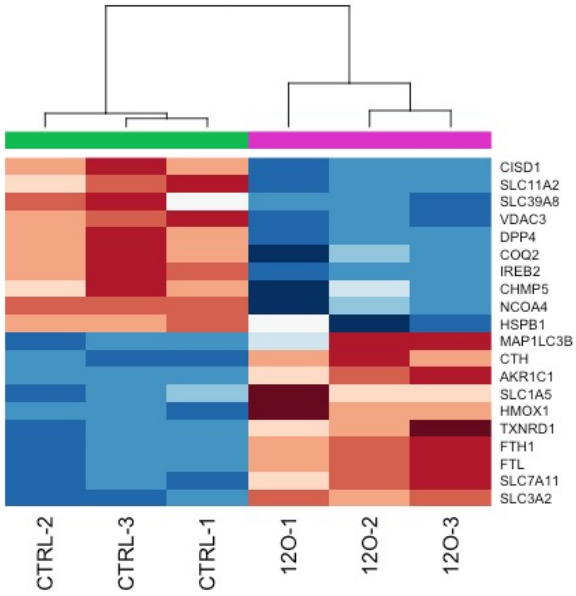

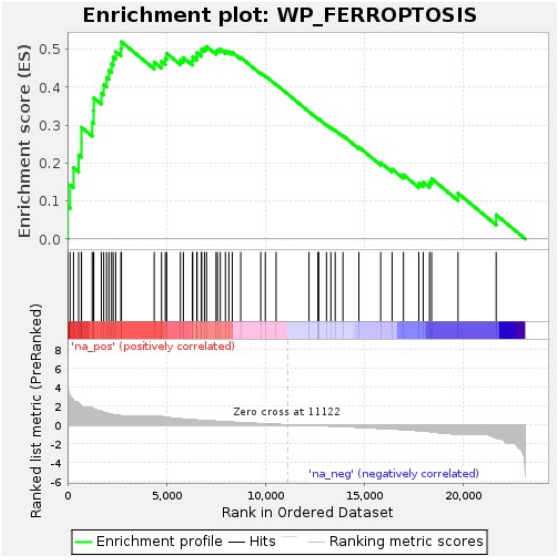

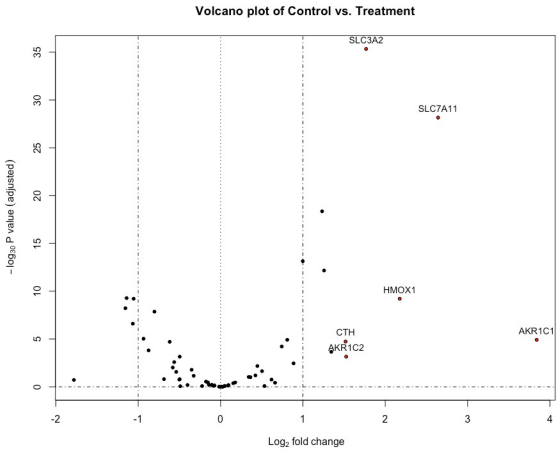

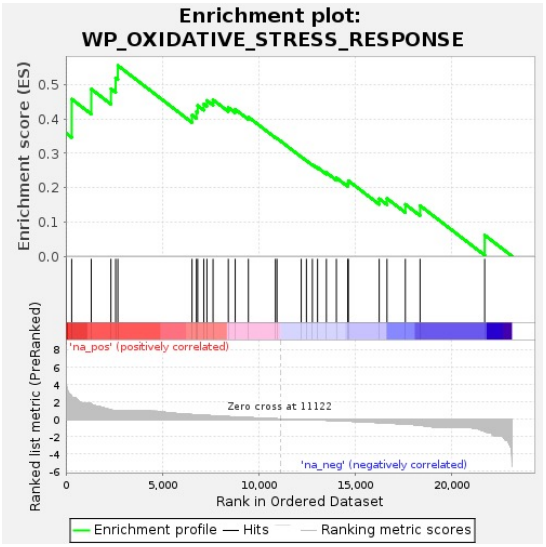

Supplementary Figure 8: RNA Sequencing data ferroptosis

Differential expression of genes obtained from RNA sequencing of CSCs treated with BAQ12O (5 μM, 24h) compared to vehicle treated CSCs. List of ferroptosis related genes was obtained from the GSEA database and analyzed using R program DESeq2. The heat map shows the top ten upregulated and downregulated statistically significant genes in the ferroptosis pathways. Volcano plot showing upregulated ferroptosis genes with a fold change of greater than log2. Gene Set Enrichment Analysis of Ferroptosis related genes and oxidative stress. Both showed positive enrichment scores.

Reference:

1. Siegel, R.L., et al., *Cancer statistics, 2022.* CA Cancer J Clin, 2022. **72**(1): p. 7-33.
2. Nazio, F., et al., *Autophagy and cancer stem cells: molecular mechanisms and therapeutic applications.* Cell Death & Differentiation, 2019. **26**(4): p. 690-702.
3. Levy, J.M.M., C.G. Towers, and A. Thorburn, *Targeting autophagy in cancer.* Nature reviews. Cancer, 2017. **17**(9): p. 528-542.
4. Yang, S., et al., *Pancreatic cancers require autophagy for tumor growth.* Genes & development, 2011. **25**(7): p. 717-729.
5. Karasic, T.B., et al., *Effect of Gemcitabine and nab-Paclitaxel With or Without Hydroxychloroquine on Patients With Advanced Pancreatic Cancer: A Phase 2 Randomized Clinical Trial.* JAMA Oncology, 2019. **5**(7): p. 993-998.
6. Boone, B.A., et al., *Safety and Biologic Response of Pre-operative Autophagy Inhibition in Combination with Gemcitabine in Patients with Pancreatic Adenocarcinoma.* Annals of surgical oncology, 2015. **22**(13): p. 4402-4410.
7. McAfee, Q., et al., *Autophagy inhibitor Lys05 has single-agent antitumor activity and reproduces the phenotype of a genetic autophagy deficiency.* Proceedings of the National Academy of Sciences of the United States of America, 2012. **109**(21): p. 8253-8258.
8. Ma, Z., et al., *Pharmacophore hybridisation and nanoscale assembly to discover self-delivering lysosomotropic new-chemical entities for cancer therapy.* Nat Commun, 2020. **11**(1): p. 4615.

9. Ma, Z., et al., *A pH-Driven Small-Molecule Nanotransformer Hijacks Lysosomes and Overcomes Autophagy-Induced Resistance in Cancer.* Angew Chem Int Ed Engl, 2022.

10. Lin, K., et al., *Single Small Molecule-Assembled Mitochondria Targeting Nanofibers for Enhanced Photodynamic Cancer Therapy In Vivo.* Advanced Functional Materials, 2021. **31**(10): p. 2008460.

11. Tang, M., et al., *A mitochondria-targeting lipid-small molecule hybrid nanoparticle for imaging and therapy in an orthotopic glioma model.* Acta Pharm Sin B, 2022. **12**(6): p. 2672-2682.

12. Silindir-Gunay, M. and A.Y. Ozer, *Chapter 8 - Liposomes and micelles as nanocarriers for diagnostic and imaging purposes*, in *Design of Nanostructures for Theranostics Applications*, A.M. Grumezescu, Editor. 2018, William Andrew Publishing. p. 305-340.

13. Li, C., et al., *Identification of Pancreatic Cancer Stem Cells.* Cancer Research, 2007. **67**(3): p. 1030-1037.

14. Dixon, S.J., et al., *Ferroptosis: an iron-dependent form of nonapoptotic cell death.* Cell, 2012. **149**(5): p. 1060-72.

15. Mancias, J.D., et al., *Quantitative proteomics identifies NCOA4 as the cargo receptor mediating ferritinophagy.* Nature, 2014. **509**(7498): p. 105-109.

16. Elgendy, S.M., et al., *Ferroptosis: An emerging approach for targeting cancer stem cells and drug resistance.* Crit Rev Oncol Hematol, 2020. **155**: p. 103095.

17. Fam, S.Y., et al., *Stealth Coating of Nanoparticles in Drug-Delivery Systems.* Nanomaterials (Basel), 2020. **10**(4).

18. Ma, Z., et al., *Heterocyclic N-Oxides as Small-Molecule Fluorogenic Scaffolds: Rational Design and Applications of Their "On-Off" Fluorescence.* Anal Chem, 2020. **92**(18): p. 12282-12289.

19. Huang, L., et al., *IQGAP1 Is Involved in Enhanced Aggressive Behavior of Epithelial Ovarian Cancer Stem Cell-Like Cells During Differentiation.* Int J Gynecol Cancer, 2015. **25**(4): p. 559-65.

20. Rao, W., et al., *Chitosan-Decorated Doxorubicin-Encapsulated Nanoparticle Targets and Eliminates Tumor Reinitiating Cancer Stem-like Cells.* ACS Nano, 2015. **9**(6): p. 5725-40.

21. Eng, J.W.L., et al., *Pancreatic cancer stem cells in patient pancreatic xenografts are sensitive to drozitumab, an agonistic antibody against DR5.* Journal for ImmunoTherapy of Cancer, 2016. **4**(1): p. 33.

22. Greenow, K. and A.R. Clarke, *Controlling the Stem Cell Compartment and Regeneration In Vivo: The Role of Pluripotency Pathways.* Physiological Reviews, 2012. **92**(1): p. 75-99.

23. Kinnear, C., et al., *Form Follows Function: Nanoparticle Shape and Its Implications for Nanomedicine.* Chemical Reviews, 2017. **117**(17): p. 11476-11521.

24. Klionsky, D.J., et al., *Guidelines for the use and interpretation of assays for monitoring autophagy (4th edition)(1).* Autophagy, 2021. **17**(1): p. 1-382.

25. Zhou, Y., et al., *Metascape provides a biologist-oriented resource for the analysis of systems-level datasets.* Nature Communications, 2019. **10**(1).

26. Hamad, M., et al., *Heme Oxygenase-1 (HMOX-1) and inhibitor of differentiation proteins (ID1, ID3) are key response mechanisms against iron-overload in pancreatic β-cells.* Mol Cell Endocrinol, 2021. **538**: p. 111462.

27. Li, Y., K. Atkinson, and T. Zhang, *Combination of chemotherapy and cancer stem cell targeting agents: Preclinical and clinical studies.* Cancer Letters, 2017. **396**: p. 103-109.

28. Hammel, P., et al., *Effect of Chemoradiotherapy vs Chemotherapy on Survival in Patients With Locally Advanced Pancreatic Cancer Controlled After 4 Months of Gemcitabine With or Without Erlotinib: The LAP07 Randomized Clinical Trial.* Jama, 2016. **315**(17): p. 1844-53.

29. Hann, A., et al., *Feasibility of alternating induction and maintenance chemotherapy in pancreatic cancer.* Scientific reports, 2017. **7**: p. 41549-41549.

30. Kasi, P.M. and A. Grothey, *Chemotherapy Maintenance.* Cancer J, 2016. **22**(3): p. 199-204.

31. Gryzik, M., et al., *NCOA4-mediated ferritinophagy promotes ferroptosis induced by erastin, but not by RSL3 in HeLa cells.* Biochim Biophys Acta Mol Cell Res, 2021. **1868**(2): p. 118913.

32. Yamamoto, K., et al., *Autophagy promotes immune evasion of pancreatic cancer by degrading MHC-I.* Nature, 2020. **581**(7806): p. 100-105.

CONCLUSION

Here we have summarized the current state of pancreatic cancer including what is known about disease progression and current chemotherapies. First, the most common subtype of pancreatic cancer is pancreatic ductal adenocarcinoma (PDAC) accounting for the vast majority of pancreatic cancer occurrences and deaths.[1] The current first in line treatments including gemcitabine and the FOLFIRNOX composed of fluoruracil, luecovorin, irinotecan, and oxaliplatin, are not enough to address the high mortality rate associated with pancreatic cancer. Additionally, chemotherapies are particularly important for pancreatic cancer treatment which in many patient cases have already metastasized upon detection (52% of new cases) and patients are unable to undergo surgical resection.[2] New treatment modalities are urgently needed to improve this lethal cancer subtype.

One new targeting approach discussed extensively in this dissertation is to develop lysosome targeting drugs that modulate autophagy. Autophagy is the process of degrading macromolecules, including proteins, lipids, and cell organelles, in the lysosome. A general overview of the process begins with an initiation and nucleation of a phagophore to begin enveloping the targeted cargo marked for degradation, followed by maturation of the membrane to form a vesicle around the cargo known as the autophagosome, and then finally degradation in which the autophagosome and lysosome fuse to full degrade the cargo.[3] Autophagy is widely given the term “double-edged sword” because the context of the cell is highly important as to whether autophagy inhibition or induction leads to cell death.[3] In relation to many cancer subtypes, autophagy is initially used to inhibit tumor formation and growth and after

tumor establishment, autophagy is hijacked to sustain tumor growth and maintenance.[3] However, in pancreatic cancer the level of basal autophagic flux is already high and many have proven that autophagy is required in PDAC for growth and maintenance.[4]

Within the heterogenous tumor population, there is a subset of cells that display marked autophagy dysfunction.[5] Cancer stem cells (CSCs) are a rarer type of cell in the tumor that possess, as their name suggests, stem cell-like properties. They can self-renew, differentiate into other types of cells, cause tumor recurrence and metastasis as well as avoid many chemotherapies that target actively replicating cells, due to their often-quiescent state.[5] CSCs use autophagy to regulate many of their functions including pluripotency, differentiation, migration/invasion, and for their own homeostasis.[5] Targeting this process particularly for eliminating CSCs provides a viable strategy for the highly lethal pancreatic tumor. The current autophagy inhibitors, chloroquine (CQ) and its safer, more widely used derivative, hydroxychloroquine (HCQ) are the main drugs chosen for autophagy inhibitors in clinical trials for PDAC and several other cancer types. Unfortunately, the concentration of drug needed for sufficient autophagy inhibition using HCQ and CQ is not clinically relevant.[3] More potent autophagy inhibitors are needed for clinical translation. This seems to be in part the reason why a study done by Balic et.al. using CQ to treat pancreatic cancer stem cells used another mechanism apart from autophagy.[6]

In order to produce a more potent autophagy inhibitor, nanomedicine provided an innovative approach for ease of functionalization and favorable drug delivery properties. This dissertation reviewed strategies to design nanomaterials to optimize

drug delivery to the target tumor. To bypass the many biological barriers from drug administration to the target, the nanoparticle must first remain stable in blood circulation including avoid shear stress and premature clearance to reach the target location and stable enough to prevent any type of drug release. After passing blood circulation, the nanoparticle should be able to penetrate the tumor and still be able to be internalized by the cell in the often-harsh tumor microenvironment. Particularly in PDAC, there is dense fibrosis making tumor penetration challenging in this subtext. Finally, the drug should have tumor retention along with a timely clearance to prevent excessive toxicity.

We used this targeting strategy and the properties of both small molecules and nanomedicine to develop the bisaminoquinolone derivative N-oxide, BAQ 12O. BAQ BAQ12O was in the second generation of the series of compounds we previously described in the one-component new-chemical-entity nanomedicines which comprise of small molecules that can self-assemble and target the lysosome. These derivatives began with the divalent CQ derivative, Lys05,[7] and resulted in potent autophagy inhibition. BAQ 12O showed similar autophagy inhibition, however in comparison to the previous generation BAQ12, there was selectivity for pancreatic CSCs. BAQ 12O formed a micelle which we further PEGylated with DSPE-PEG_{2000} to promote nanoparticle stability and confer the benefits of PEG, a polymer known to promote stability in blood circulation.[8] BAQ12O not only inhibited autophagy in the CSCs but after proteomic analysis and RNA sequencing we identified that BAQ12O induced ferroptosis in the CSC population. Ferroptosis is the iron-mediated oxidative death pathway discovered by Dixon et. al in 2012 that is canonically different from deaths induced by apoptosis, necrosis, and autophagy.[9] Treatment with BAQ12O resulted in

notable lipid peroxidation along with lower glutathione levels, high reactive oxygen species (ROS), and high labile Fe^{2+} ions. We saw this phenomenon both in CSCs *in vitro* as well as *in vivo* from tumor tissues collected from BAQ12O efficacy studies in mice. BAQ12O showed potent tumor efficacy in mouse engrafted with CSCs and particularly in combination with standard of care, gemcitabine, making it a promising translational drug candidate. Future studies need to be completed in order to further characterize the efficacy of BAQ12O in more preclinical models as well as elucidate the lysosome targeting mechanism of the compound. In this work, we have provided the basis for future studies in this area of CSC targeting nanomaterials and the role of autophagy and ferroptosis in pancreatic CSCs.

Reference:

1. Torphy, R.J., Y. Fujiwara, and R.D. Schulick, *Pancreatic cancer treatment: better, but a long way to go.* Surg Today, 2020. **50**(10): p. 1117-1125.
2. Siegel, R.L., et al., *Cancer statistics, 2022.* CA Cancer J Clin, 2022. **72**(1): p. 7-33.
3. Amaravadi, R.K., A.C. Kimmelman, and J. Debnath, *Targeting Autophagy in Cancer: Recent Advances and Future Directions.* Cancer Discov, 2019. **9**(9): p. 1167-1181.
4. Yang, S., et al., *Pancreatic cancers require autophagy for tumor growth.* Genes & development, 2011. **25**(7): p. 717-729.
5. Nazio, F., et al., *Autophagy and cancer stem cells: molecular mechanisms and therapeutic applications.* Cell Death & Differentiation, 2019. **26**(4): p. 690-702.
6. Balic, A., et al., *Chloroquine Targets Pancreatic Cancer Stem Cells via Inhibition of CXCR4 and Hedgehog Signaling.* Molecular Cancer Therapeutics, 2014. **13**(7): p. 1758-1771.
7. McAfee, Q., et al., *Autophagy inhibitor Lys05 has single-agent antitumor activity and reproduces the phenotype of a genetic autophagy deficiency.* Proceedings of the National Academy of Sciences of the United States of America, 2012. **109**(21): p. 8253-8258.
8. Fam, S.Y., et al., *Stealth Coating of Nanoparticles in Drug-Delivery Systems.* Nanomaterials (Basel), 2020. **10**(4).
9. Dixon, S.J., et al., *Ferroptosis: an iron-dependent form of nonapoptotic cell death.* Cell, 2012. **149**(5): p. 1060-72.

ACKNOWLEDGEMENTS

I would like to first thank my advisor, Professor Yuanpei Li for supporting me during this degree since joining his lab. Dr. Zhao Ma was another invaluable source of help who completed all the chemistry related data in this dissertation. Thanks to my current and previous lab members who contributed and advised me on the project including, Dr. Cindy Lin, Dr. Kai Lin, Menghuan Tang, Dr. Marina Ricci, Dr. Ruonan Bo, Dr. Yaping Shiau, Longmeng Li, Dr. Haijing Qu, and many, many more. Thanks to several of the UC Davis Cores including Stephenie Liu, Ryan Davis and Dr. Cliff Tepper in the Bioinformatics core, Dr. Gabriella Grigorean in the Proteomics Core, Dr. Qian/Jane Chen in the Pathology Core, and finally Jonathan Van Dyke and Bridget McLaughlin from the Flow Cytometry Core.

Thank you to my committee members, Professor Kit Lam and Professor Kermit Caraway for their help and advice. I am not only grateful for their advice but have the pleasure of collaborating with their lab members during my degree which was a great experience. Thanks also to Professors Ping Zhou and Priya Shah whose labs provided some of the cell lines used in the data shown.

Thanks finally to my friends and family who supported me during this endeavor without whom I could not have managed.